Backman, J., Duncan, R. A., et al., 1988
Proceedings of the Ocean Drilling Program, Initial Reports, Vol. 115

12. SITE 715[1]

Shipboard Scientific Party[2]

HOLE 715A

Date occupied: 2245 L, 24 June 1987

Date departed: 2300 L, 26 June 1987

Time on hole: 48 hr, 15 min

Position: 05°04.89′N, 73°49.88′E

Water depth (sea level; corrected m, echo-sounding): 2266.3

Water depth (rig floor; corrected m, echo-sounding): 2276.8

Bottom felt (m, drill pipe): 2272.8

Penetration (m): 287.8

Number of cores: 31

Total length of cored section (m): 287.8

Total core recovered (m): 137.6

Core recovery (%): 47.8

Oldest sediment cored:
Depth (mbsf): 211.3
Nature: shallow-water (reef) limestone
Age: early Eocene
Measured velocity (km/s): ~3.4–5.1

Basement rocks:
Depth (mbsf): 211.3 to 287.8
Nature: olivine basalts
Age: early Eocene (?)
Measured velocity (km/s): ~3.2–6.3

Principal results: Site 715 is located on the eastern margin of the Maldives Ridge, at 5°04.89′N and 73°49.88′E, in water depths of 2262.3 m. Our main objective for drilling at this site was to penetrate the supposed basaltic basement underlying the carbonate bank deposits which form the Maldive Islands. This site lies on the Chagos-Maldive-Laccadive Ridge, roughly midway between Site 713 on the Chagos Bank and the southern limit of the Deccan flood basalts of western India (Fig. 1). According to the model which attributes this volcanic lineament to India's northward motion over the Réunion hotspot (Morgan, 1981), we expected to find a basalt age of about 55 Ma (Duncan, 1981; Emerick, 1985). We hoped that the composition of the basalts would also reveal the relative contributions of mantle melts from the hotspot and asthenosphere mid-ocean ridge basalt (MORB) sources.

The specific position for this site was guided by previous seismic reflection surveys through the region and chosen from the final *JOIDES Resolution* profiles (see "Seismic Stratigraphy" section, this chapter). The best opportunity for drilling to basement appeared to lie at the base of the eastern slope of a narrow peripheral ridge which connects with the main shallow carbonate bank to the west. To the east, the ocean floor drops away to a 2600-m-deep plain containing more than 1 km of sediment, mostly hemipelagic deposits derived from the Indian subcontinent (Sclater et al., 1977).

At this site one hole was drilled which penetrated basalt at 211.3 m and continued a further 76.6 m into basement. Above the basalt was 100 m of lower Eocene shallow-water limestone. Pelagic nannofossil oozes of Pleistocene to Miocene age lie above the limestone. Some 31 cores were taken by rotary drilling, with 47.8% recovery of the total 287.8 m cored. Very low recovery (7.7%) resulted from drilling through the limestone section, probably because of the brittle and inhomogeneous character of the reef carbonate. Basement recovery was good (49.6%), except that we recovered nothing from two cores due to an obstruction in the bit.

The major lithologies identified at Site 715 correspond to the following subdivisions:

1. From 0 to 104.6 mbsf: Clay-bearing to foraminifer-bearing nannofossil oozes and chalks. This rather homogeneous sequence can be divided further on the basis of color and age into an upper greenish gray unit of late Pleistocene age separated by hiatus from pale white nannofossil ooze and chalk of middle to early Miocene age.
2. From 104.6 to 211.3 mbsf: This interval contains a shallow-water carbonate sequence of Eocene age, progressing downhole from (1) wackestone, composed of benthic foraminifers, fragments of bivalves, brachiopods, pelecypods, minor hardgrounds, and glauco-

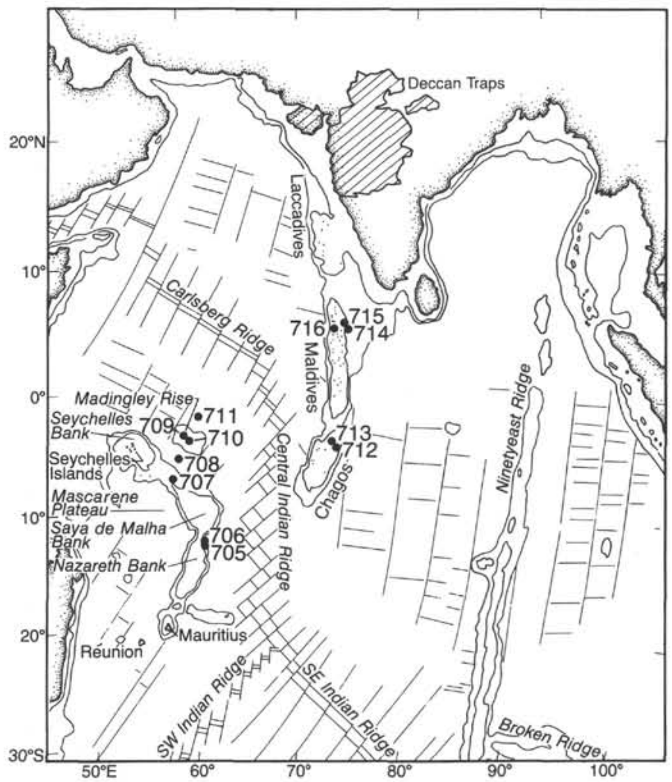

Figure 1. Bathymetry and location of Site 715, eastern Maldives Ridge, central Indian Ocean. Drilling on this elevated ridge recovered subaerially erupted, basaltic lava flows at a point midway between the Chagos Bank (Site 713) and the Deccan flood basalts of western India.

[1] Backman, J., Duncan, R. A., et al., 1988. *Proc. ODP, Init. Repts.*, 115: College Station, TX (Ocean Drilling Program).
[2] Shipboard Scientific Party is as given in the list of Participants preceding the contents, with the addition of Isabella Premoli Silva and Alde Nicora, Dipartimento di Scienze della Terra, Universitá di Milano, Via Mangiagalli 34, I-20129 Milano, Italy.

nite, interpreted to be slope deposits; (2) packstone with large intact benthic foraminifers, bryozoans, gastropods, and molluscs, indicating shallower-water deposition; and (3) grainstone with solitary and colonial coral fragments and bryozoans, indicating very shallow water and high energy conditions of deposition.

3. From 211.3 to 287.8 mbsf: Subaerially erupted lava flows of olivine basalt composition, fine grained, plagioclase-phyric, slightly to moderately altered. Flows are 1-5 m thick with one limestone interbed (0.5 m thick) and several baked laterite contacts. Overlain by very shallow-water reef limestones of early Eocene age.

Figure 2 summarizes the biostratigraphic and lithostratigraphic data in a geological column.

The uppermost pelagic ooze section was similar to that cored at Site 714 only 3 nmi to the west. A major hiatus of about 14 m.y. exists between Pleistocene and middle Miocene nannofossil oozes. The next unit down gives a fascinating look at the early stages of reef building and subsidence of the volcanic edifice in Eocene/Paleocene time. Unfortunately, the hard, partially recrystallized carbonate broke into fragments which did not end up in the core barrel; recovery, therefore, was very low. Enough material was recovered, however, to conclude that these deposits record a progressive deepening of the site from littoral to bank to slope conditions.

In the basaltic section, we see the dying activity of an oceanic island in early Tertiary time. Subaerially erupted olivine basalts are overlain by a coarse volcanic sandstone of angular and rounded fragments in a carbonate cement, interpreted as a beach deposit. A later flow followed, and this is succeeded by a section of intertidal to shallow-water coral reef limestones. Hence, we have a record of the initial stages of subsidence of the volcano. We also distinguished 21 separate flow units in the recovered section and identified 2 distinct magma types. The upper type is a plagioclase-phyric basalt, while the lower type is a mafic, olivine-rich basalt with a slight alkaline character. Flows are vesicular toward the margins and vary from 1 to 5 m in thickness.

We can use seafloor subsidence curves for the Indian Ocean (Sclater et al., 1977) to date the volcanic rocks (Fig. 3) indirectly. We know that the basalts were erupted above sea level and that they are now at about 2500 mbsl. Thermal subsidence is most rapid for volcanoes built on young oceanic lithosphere (i.e., near spreading ridges) and less rapid for volcanoes erupted in the interior of old, thick oceanic plates (Crough, 1978). Using the young lithosphere end-member, 2500 m of subsidence would have taken a minimum of about 47 m.y., and a more average range is 55-60 m.y. These age estimates, while imprecise, are consistent with the tentative shipboard biostratigraphic age for the shallow-water limestone. We expect considerable age refinement from shore-based biostratigraphic studies and radiometric analyses of the fresher basalts.

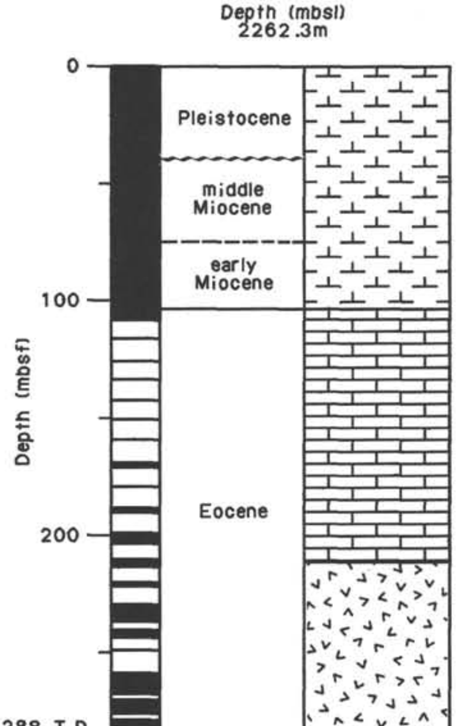

Figure 2. Geologic column for Site 715 constructed from analysis of cored material.

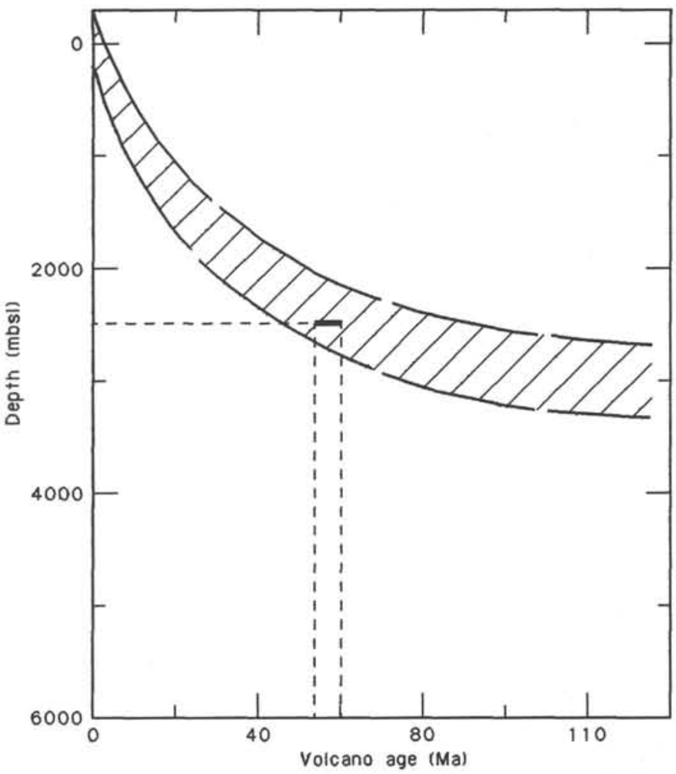

Figure 3. Hypothetical thermal subsidence curve for Site 715. The site was at or above sea level at the time of volcanism and has subsided 2500 m. The estimated basement age is thus 55-60 Ma, which is consistent with our early Paleogene biostratigraphic age estimate and the hotspot-predicted age of 55 Ma.

Paleomagnetic measurements of the basalts from Site 715 show two polarities. The uppermost flow shows normal polarity, and the remainder of the sequence is reversed. The magnetic directions are stable, and the site paleolatitude calculated from minicore measurements is 25° ± 5°S. This result is consistent with the paleolatitude estimates for Site 707 and the Deccan flood basalts (Courtillot et al., 1986). The measured Site 713 paleolatitude is significantly further north, which may be due to postcrystallization tectonic movements. We conclude from the paleolatitude study of the basement sites that there has been a significant true polar wander of about 8° in the northward motion of the Réunion hotspot with respect to the geomagnetic pole (= spin axis) since 67 Ma (Fig. 4). We cannot resolve from these data whether this motion occurred steadily over Tertiary time or in one or more rapid episodes. The sense of motion, however, agrees with measurements from the Pacific Ocean basin (Gordon and Cope, 1981).

BACKGROUND AND OBJECTIVES

The Chagos-Maldives-Laccadive Ridge stretches nearly 3000 km, nearly due north, along the 73° meridian (Fig. 5). At its northern end, where it intersects the Indian subcontinent, are the Deccan Traps, massive accumulations of flood basalts which erupted at about the time of the Cretaceous-Tertiary boundary (ca. 67 Ma). Its southern end was once joined to the Mascarene Plateau at the northern edge of the Nazareth Bank, but this

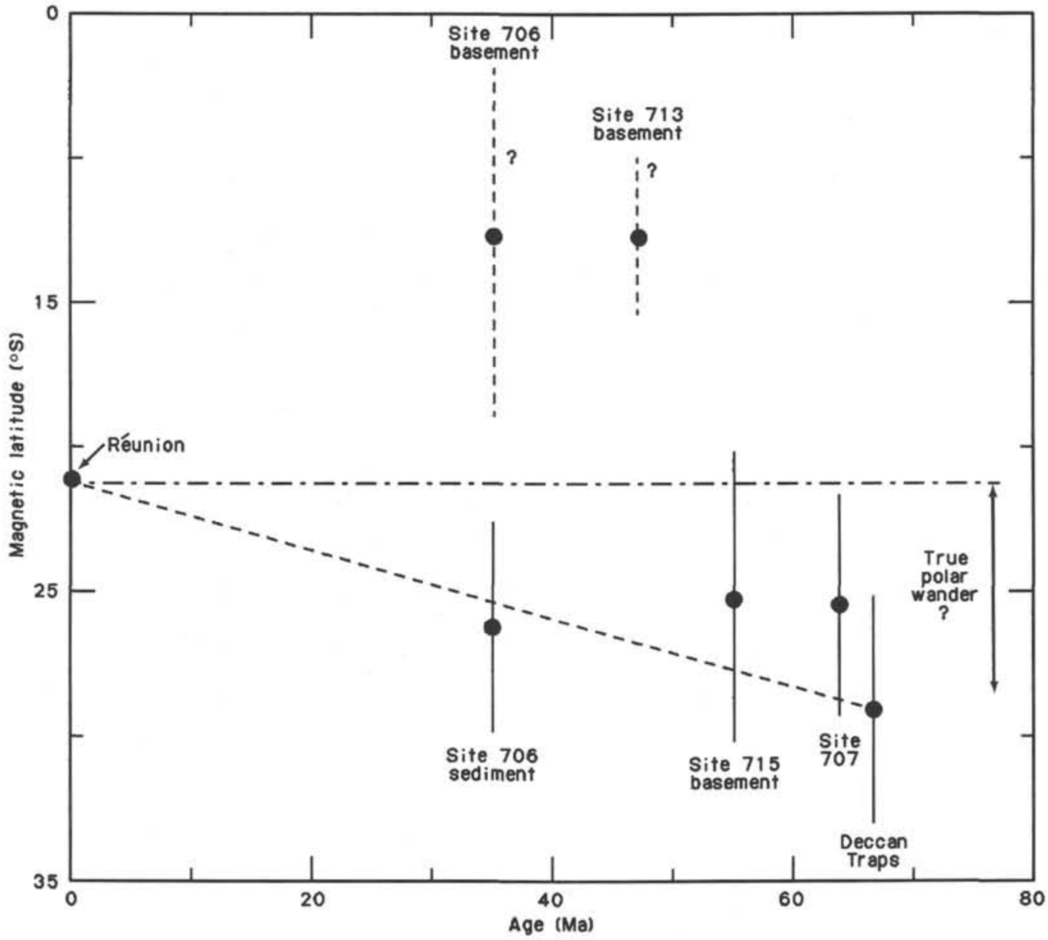

Figure 4. Paleolatitudes of sites along the Réunion hotspot track. The dash-dot line shows the expected paleolatitudes if the hotspot has not moved in relation to the earth's spin axis. The hotspot has moved about 8° north with respect to the geomagnetic axis, however, between 67 Ma and the present, an effect referred to as true polar wander. The sloping dashed line shows the possible motion of the Réunion hotspot relative to the geomagnetic axis. (Sites 713 and 706 basalts are anomalous and may have experienced postcrystallization tectonic rotation).

connection was severed by seafloor spreading on the central Indian Ridge, beginning at 36 Ma (McKenzie and Sclater, 1971). Together with the Mascarene Plateau, the volcanic islands of Réunion and Mauritius, and the Deccan Traps, the Chagos-Maldive-Laccadive Ridge manifests the motion of the Indian plate over the Réunion hotspot through Cenozoic time. The Ninetyeast Ridge to the east is a parallel volcanic ridge which is the trace of the Kerguelen hotspot (Duncan, 1978; Morgan, 1981).

Drilling on the Maldives Ridge is part of our overall program of sampling different times of hotspot activity during the construction of this ridge. This is the northernmost basement site attempted and is located roughly midway between the Chagos Bank (Site 713) and the southernmost Deccan basalts. Our first objective was to determine the age of the basaltic volcanism at this location. By knowing ages at a number of well-spaced positions along these lineaments, it is possible to calculate poles of rotation for motion of the Indian plate over the mantle during Cenozoic time. We can then make accurate plate reconstructions that will predict, for example, the paleolatitude of drilling sites, the geometry of basins which control deep-water circulation, and the timing of the India-Asia collision and the rise of the Himalayas. From dated hotspot traces on the African plate and locations along the Ninetyeast Ridge, we predict that the volcanic activity at Site 715 occurred about 55 Ma (Emerick, 1985).

An additional subject of much current interest is the scale and degree of mixing of distinct mantle source compositions which contribute to basaltic volcanism. The mantle hotspot composition is most clearly exhibited at Réunion and Mauritius, both intraplate volcanic islands. At the northern end, over 1.5 million km^3 were erupted from a combination of subcontinental, hotspot, and spreading-ridge mantle sources. At Site 715 we expected to recover basalts erupted when the hotspot lay to the north of the spreading ridge separating India and Africa (Fig. 6). Thus, compositions should reflect magmas from the hotspot mantle source, with perhaps some contribution from the MORB mantle source. Studies of basalt compositions from Sites 706, 713, and 715 will be integrated with the plate reconstructions to evaluate the significance of hotspot-spreading ridge geometry to basalt geochemistry along this volcanic trace.

The phenomenon of true polar wander will also be investigated at Site 715. If the position of the earth's spin axis changes (due, say, to mass redistributions), then the hotspot reference frame will appear to move with respect to the geomagnetic pole (aligned with the spin axis). Thus, a straightforward test is to determine the paleomagnetic latitude of sites along the hotspot track. If the hotspot has not moved with respect to the spin axis, then all sites should exhibit the same paleolatitude. Systematic departures indicate true polar wander. This is a particularly good hotspot lineament for such a test because plate motion through Tertiary time has been fast and virtually due north, the

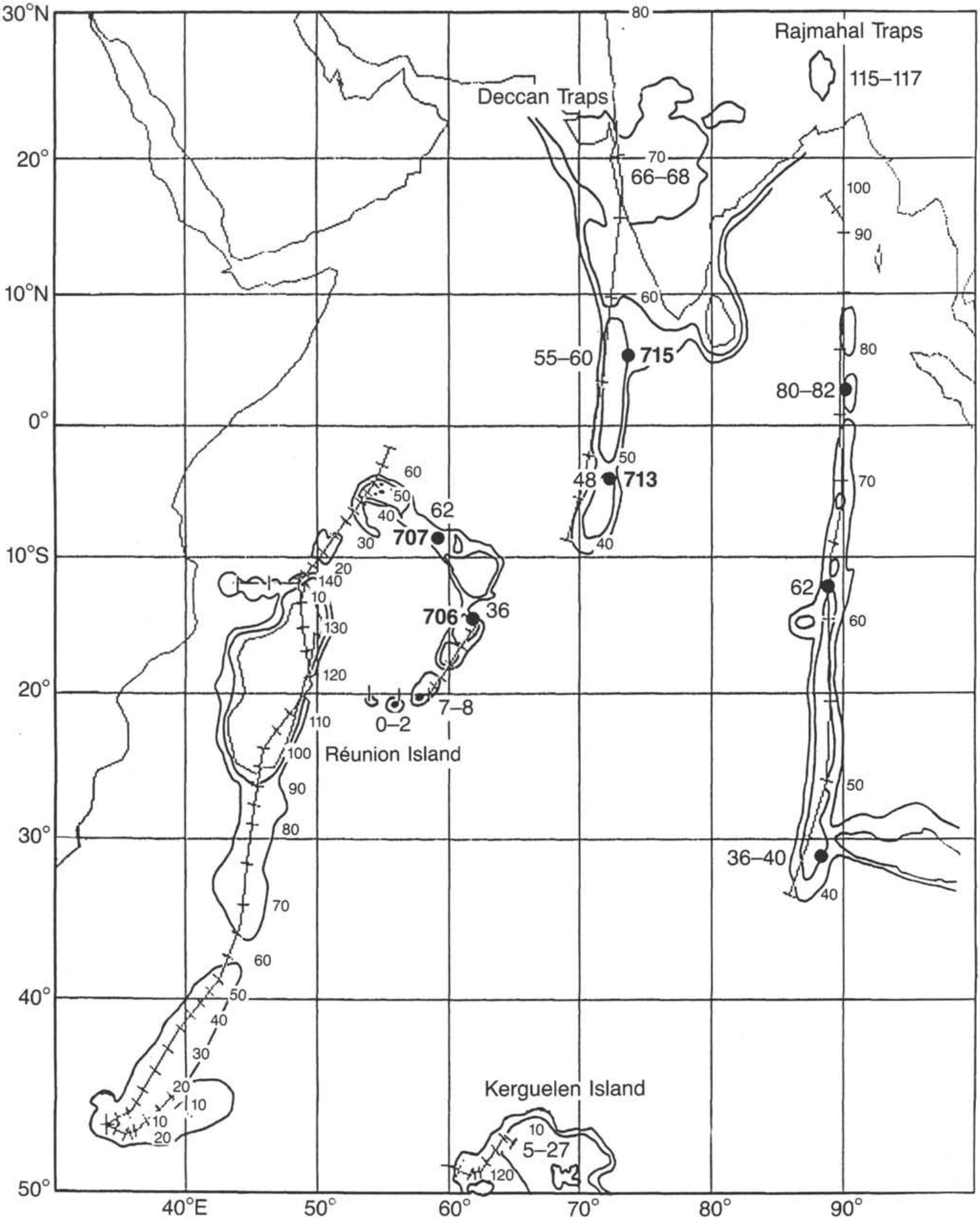

Figure 5. The location of Site 715, Maldives Ridge, central Indian Ocean. Computer-modeled hotspot tracks are calculated assuming hotspots are stationary. The predicted tracks are determined from African plate motion over South Atlantic hotspots and relative motion between the Indian and African plates (following Morgan, 1981, and Emerick, 1985). These compare well with the actual lineaments and measured ages (Ma) of volcanic activity along the Réunion hotspot (McDougall, 1971; Courtillot et al., 1986) and Kerguelen hotspot (Duncan, 1978) tracks.

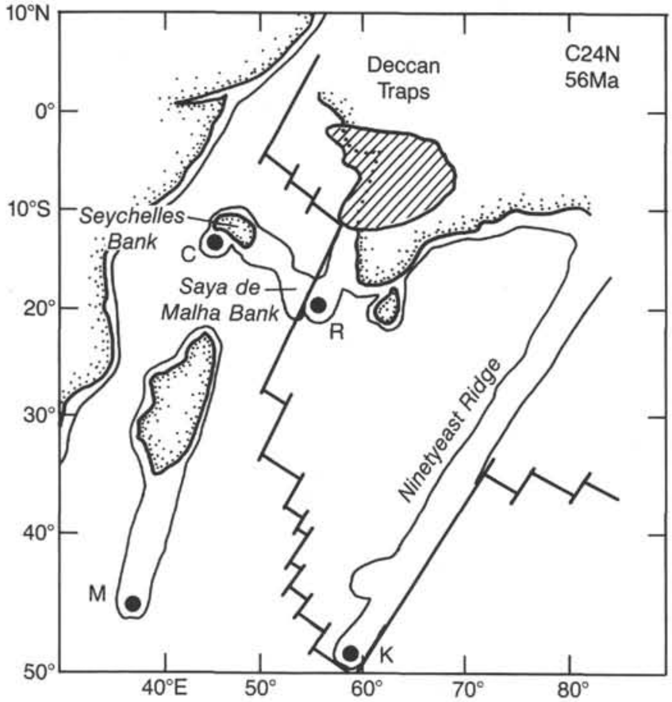

Figure 6. Reconstruction of the western Indian Ocean for 56 Ma, the predicted age of volcanism at Site 715, in the hotspot reference frame. The hotspot lies under the Indian plate and just to the north of a spreading ridge. A major transform fault lies to the west of the hotspot. Hotspots are Réunion (R), Comores (C), Marion (M), and Kerguelen (K).

direction which best resolves latitudinal differences. We know that the Deccan flood basalts yield a paleolatitude of about 29°S (Courtillot et al., 1986), or 8° south of Réunion. Thus, there has been 8° of true polar wander since about 67 Ma. Paleolatitudes from additional sites along this lineament will allow us to determine when the true polar wander occurred.

The seismic reflection profile over the chosen site suggested not only that the sediment cover was sufficiently thick to provide the necessary support for the drill string during basement coring, but also that these sediments would hardly yield suitable material for paleoceanographic work. Our major sediment objective was, therefore, to use the microfossil content for dating of the sediment/basement contact.

OPERATIONS

Site 714 to Site 715 (MLD-4)

Once the mud line was cleared at Hole 714B, the ship was moved in the dynamic positioning (DP) mode 3 nmi north to Site MLD-4, while the drill string was being tripped out. Drilling plans called for the penetration of basement rocks at Site MLD-4, so the drill string had to be tripped to change the bottom hole assembly (BHA). A beacon was dropped at 1600 hr, 24 June 1987, to establish Site 715.

Hole 715A

The rotary core barrel (RCB) BHA was lowered to the seafloor, and a water core was brought up in the first attempt to establish the mud line. At 2245 hr, the mud line was established on the second attempt at 2262.3 m and coring continued. The first 11 RCB cores recovered nearly 100%, but recovery then fell off drastically after penetration of a hard brittle reef limestone first encountered in Core 115-715A-12R. Basalt was encountered at 210 mbsf (2472.3 m). At 230 mbsf (2492.3 m) problems were encountered again and the hole was swept with 20 bbl of mud after each core. Total penetration was 287.8 mbsf to 2550.1 m, with 137.6 m of core recovered for a recovery rate of 47.8% (Table 1). The BHA was pulled to 70 mbsf, and the Schlumberger line was rigged over the crown to begin logging.

The first suite of logging tools consisted of DIL-SONIC-GR-CAL. The second suite of logging tools consisted of GST-ALT-NGT. The third logging tool was an LTD. All three logging runs were to 2545 m, and the hole was logged up to the BHA. All three suites of logging tools functioned properly. The logging equipment was rigged down at 0300 hr, 28 June 1987, and the drill string was tripped out.

Site 715 to Site 716 (MLD-1)

With the drill floor secured and thrusters raised, the ship was under way for the 30 nmi west-southwest transit to Site MLD-1 at 0745 hr, 28 June 1987.

LITHOSTRATIGRAPHY

Site 715 is located on the eastern shoulder of the Maldives Ridge at a water depth of 2262.3 m. Because the primary objective of this site was to sample basement rock, the sediments were rotary drilled. As a result, the recovered sediments are quite badly disturbed and original sedimentary fabrics are very difficult to deduce. Approximately 105 m of soft sediment was cored with about 103 m recovered (98%), whereas 106 m of well-consolidated limestone was cored with only about 7 m (6%) recovered. Recovery was actually better in basement basalts.

We divided the sedimentary section at Site 715 into three units. In addition, there is a very thin interval of limestone interbedded with basement rocks. We will not discuss this limestone in this section, but a description of it can be found in the "Basement Rocks" section, this chapter.

Table 1. Coring summary, Site 715.

Core no.	Date (June 1987)	Time (Local)	Depth (mbsf)	Cored (m)	Recovered (m)	Recovery (%)
115-715A-						
1R	24	2300	0–8.1	8.1	8.15	100.0
2R	24	2345	8.1–17.8	9.7	9.33	96.2
3R	25	0015	17.8–27.5	9.7	9.49	97.8
4R	25	0045	27.5–37.1	9.6	9.49	98.8
5R	25	0115	37.1–46.8	9.7	9.37	96.6
6R	25	0145	46.8–56.5	9.7	9.60	98.9
7R	25	0215	56.5–66.1	9.6	9.50	98.9
8R	25	0245	66.1–75.7	9.6	9.12	95.0
9R	25	0315	75.7–85.3	9.6	9.63	100.0
10R	25	0345	85.3–94.9	9.6	9.53	99.3
11R	25	0415	94.9–104.6	9.7	9.50	97.9
12R	25	0530	104.6–114.3	9.7	1.48	15.2
13R	25	0715	114.3–123.9	9.6	0.24	2.5
14R	25	0815	123.9–133.5	9.6	0.34	3.5
15R	25	1030	133.5–143.2	9.7	0.77	7.9
16R	25	1145	143.2–152.9	9.7	0.31	3.2
17R	25	1245	152.9–162.6	9.7	0.28	2.9
18R	25	1345	162.6–172.2	9.6	0.79	8.2
19R	25	1500	172.2–181.8	9.6	0.69	7.2
20R	25	1615	181.8–191.4	9.6	0.18	1.9
21R	25	1900	191.4–201.1	9.7	0.72	7.4
22R	25	2100	201.1–210.8	9.7	0.94	9.7
23R	25	2345	210.8–220.5	9.7	3.73	38.4
24R	26	0600	220.5–230.0	9.5	2.29	24.1
25R	26	0830	230.0–239.5	9.5	6.73	70.8
26R	26	1100	239.5–248.9	9.4	3.38	35.9
27R	26	1300	248.9–258.3	9.4	0.05	0.5
28R	26	1600	258.3–267.7	9.4	0	0
29R	26	1915	267.7–270.7	3.0	2.55	85.0
30R	26	2230	270.7–278.2	7.5	5.82	77.6
31R	27	0330	278.2–287.8	9.6	3.62	37.7

Unit I: Cores 115-715A-1R through -5R, 0–46.8 mbsf; Age: Pleistocene.

Sediments of Unit I consist entirely of clay-bearing nannofossil ooze, except for Core 115-715A-1R which contains enough foraminifers to be designated a foraminifer-bearing, clay-bearing nannofossil ooze. The average calcium carbonate content of these sediments is about 70 wt%. Foraminifers range from 2% to 20% of the sediments and average about 5%. Biogenic silica is rare; there are almost no diatoms, and radiolarians typically comprise less than 5% of the sediment.

Unit I sediments at Site 715 accumulated at about twice the rate of the correlative section at nearby Site 714. We tentatively explained this phenomenon as being the result of resedimentation (see "Geochemistry" section, this chapter), an explanation which was not substantiated by shipboard sedimentological observations, possibly due to core disturbance.

Unit I is most easily distinguished from the underlying sediments on the basis of its color, which ranges from light gray (5Y 7/1), light greenish gray (5GY 7/1), light yellowish gray (5Y 7/2), yellowish gray (5Y 6/2), greenish gray (5GY 5/1, 6/1), and gray (5Y 5/1, 6/1) to dark greenish gray (5GY 4/1). Slight variations in color are probably caused by fluctuations in the carbonate content related to Pleistocene climatic changes or sea level excursions. Unit I averages 1.6 color changes per meter of core.

Unit II: Cores 115-715A-6R through -11R, 46.8–104.6 mbsf; Age: middle to early Miocene.

A paleontologically recognized hiatus occurs between Cores 115-715A-5R and -6R. No hiatus was evident in the sediments themselves, so it is assumed that the hiatus must have occurred over a missing interval between the two cores. This hiatus represents about 14 m.y. at Site 715 but only about 8 m.y. at Site 714, so all of the upper Miocene and much of the middle Miocene section present at Site 714 is absent from Site 715.

As noted above, sediments of Unit II are readily distinguished from those of Unit I on the basis of color. Unit II sediments are almost entirely white (5G 8/1, 10Y 8/1), although some gray pyritic staining occurs in them, an indication that the sediments have undergone some microbial sulfate reduction. There are no color cycles observed in Unit II. The calcium carbonate content of Unit II sediments averages about 84%.

Sediments of Unit II consist of foraminifer-bearing nannofossil oozes and chalks (Cores 115-715A-6R through -9R), with lesser amounts of foraminifer-nannofossil ooze and chalk (Cores 115-715A-10R and -11R). A similar change, that is, from foraminifer-bearing nannofossil ooze to foraminifer-nannofossil chalk, was noted at Site 714. At that site, the change was recognized at about 120 mbsf in slightly younger sediments. The estimated foraminifer content of Unit II at Site 715 varies from 12% to 30%. Biogenic silica is even more scarce than in Unit I; no diatoms are observed in smear slides, and only trace amounts of radiolarians and siliceous sponge spicules were observed.

The first occurrence of indurated, chalky lumps occurs in Section 115-715A-8R-2 (68 mbsf). The ooze/chalk boundary was identified in Core 115-715A-10R around 90 mbsf.

Unit III: Cores 115-715A-12R through -23R, 104.6–211.3 mbsf; Age: Eocene.

Unit III is composed of numerous 1–20-cm-diameter chunks of very well-consolidated, shallow-water limestones of probable Eocene age (see "Biostratigraphy" section, this chapter). These limestones have thus far only been described on the basis of hand specimens. They have been designated as wackestones (Core 115-715A-12R), packstones (Cores 115-715A-13R to -21R and 115-715A-23R), and grainstones (115-715A-16R to -22R).

Core 115-715A-12R contains a unique type of limestone, a wackestone containing about 15% grains with the remainder being micrite. The only recognizable grains in hand specimens are large, shallow-water benthic foraminifers; a few small, thin bivalve fragments; a brachiopod; and a pelecypod. The grains are all aligned parallel to bedding (or possibly cross-bedding). The limestones have abundant grain-moldic porosity. A few of the fragments show cross-cutting, glauconitized hardgrounds. We tentatively identified these limestones as having originated on a carbonate slope in front of a shallow-water bank.

Core 115-715A-13R contains mostly white (10YR 8/2) or very pale brown (10YR 7/3) packstone. Most of the recognizable grains are benthic foraminifers. This core also contains one fragment of black, highly porous packstone, probably stained with manganese oxide.

Cores 115-715A-14R through -23R contain shelly packstones and grainstones. Recognizable grains in these rocks include calcareous algae, shallow-water benthic foraminifers, solitary and colonial corals, bryozoans, gastropods, boring clams, and skeletal debris of all of these organisms. Most samples have abundant moldic porosity. Occasional samples have a bulbous pisolitic type of texture. Quite a few samples are highly recrystallized. There is one fragment of chert. All of these limestones are definitely of a reefal origin. Most reasonably they can be interpreted as very shallow-water (less than 100 m) deposits.

BIOSTRATIGRAPHY

Introduction

The 211-m-thick sedimentary sequence recovered in the single hole at Site 715 consists, from top to bottom, of (1) 47 m of upper Pleistocene nannofossil ooze, (2) a major unconformity spanning a time interval of approximately 14 m.y., (3) a 58-m-thick middle to lower Miocene sequence of nannofossil ooze and chalk, and (4) a 106-m-thick section of shallow-water limestone overlying basement. A major hiatus spans the entire Oligocene, but a short, very condensed upper to middle Eocene interval, dated by nannofossils, appears to occur between the Neogene calcareous ooze and the lower Eocene limestone.

Calcareous nannofossils are abundant in the Neogene, well preserved in the Pleistocene, and moderately well to well preserved in the Miocene. They are very rare in the upper to middle Eocene interval with moderately poor preservation. The shallow-water limestones, as well as the limestone interbedded in the basalt, are barren of calcareous nannofossils.

Planktonic foraminifers, abundant throughout the Neogene sequence, are well preserved in the Pleistocene and moderately well to well preserved in the Miocene. A few age-diagnostic forms are present in the lower Eocene limestone. Well-preserved benthic foraminifers are common through the Neogene, consisting of lower intermediate-water assemblages. Age-diagnostic larger benthic foraminifers are common in the lower Eocene reefal limestone.

Radiolarians are common and well preserved in the Pleistocene interval, and rare and moderately well preserved in the middle Miocene. They are absent in the remainder of the section. Diatoms are present only in the Pleistocene, where they are rare and poorly preserved at best.

A biostratigraphic summary for Site 715 is presented in Figure 7.

Calcareous Nannofossils

Late Pleistocene and middle Miocene through late Oligocene assemblages of calcareous nannofossils were recovered from Hole

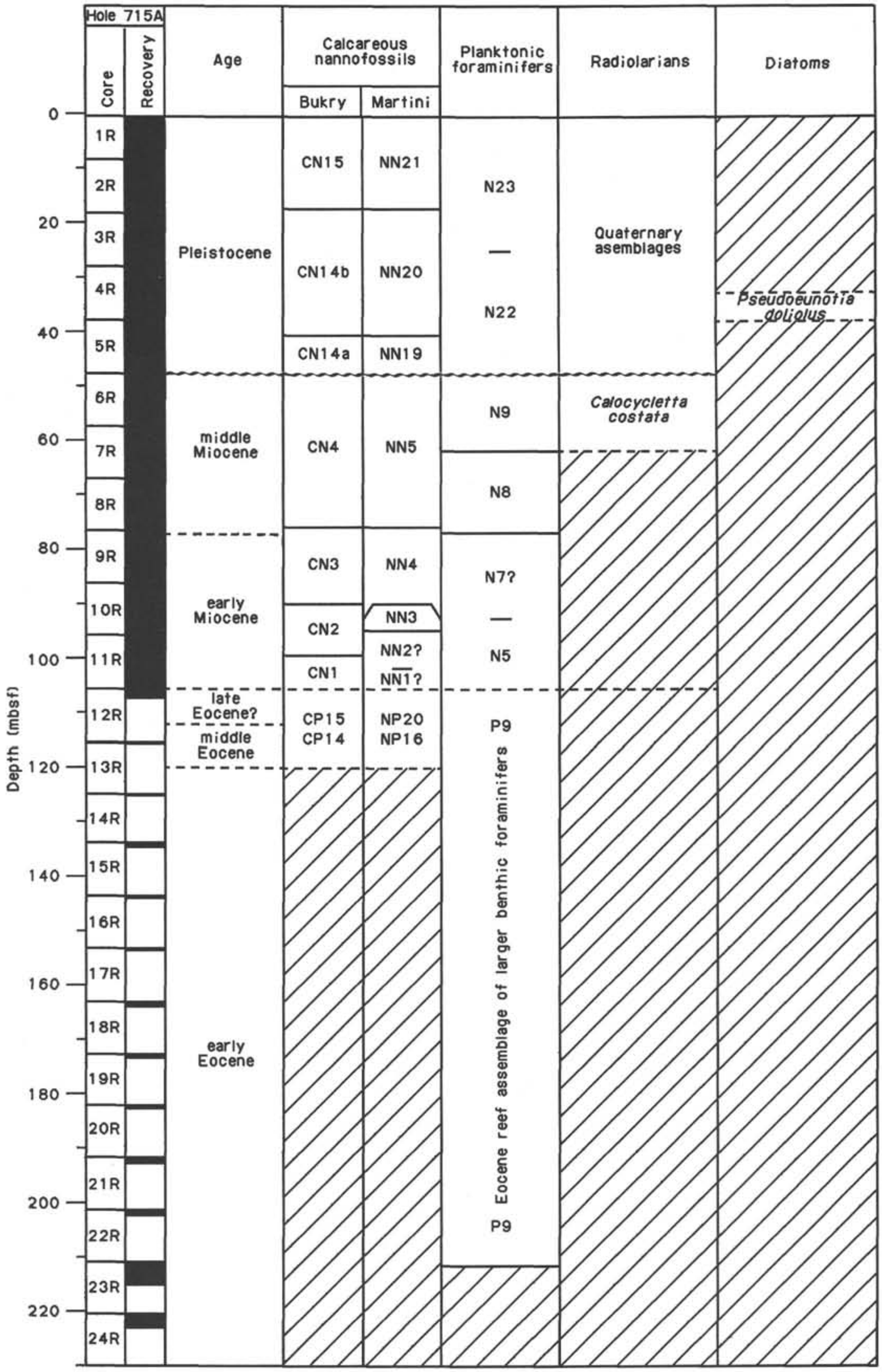

Figure 7. Biostratigraphic summary of Site 715. Recovery in Hole 715A is indicated by black bars.

715A. The Pleistocene sequence is rich in well-preserved nannofossils and is characterized by high sedimentation rates (86.5 m/m.y.). Nannofossils are moderately well preserved in the Miocene sequence with slight to moderate overgrowth, especially on discoasters.

Pleistocene

Cores 115-715A-1R through -5R recovered late Pleistocene sediments. Because of the heavy disturbance caused by rotary drilling, this sequence is not suitable for high-resolution study despite the very high sedimentation rate and good fossil preservation.

We placed the first occurrence (FO) of *Emiliania huxleyi* (base of Zone CN15) between Sample 115-715A-2R-6, 44–45 cm, and Section 115-715A-2R, CC. Because of frequent occurrences of reworked forms in some samples, the last occurrence (LO) of *Pseudoemiliania lacunosa* (base of Subzone CN14b) is difficult to identify with confidence. Reworked *P. lacunosa* are common in many section samples of Core 115-715A-4R, but they are completely absent from the upper two sections of the underlying core. This species is also abundant in the middle sections of Core 115-715A-5R; it decreases in abundance, however, in the lower part of the core. We have tentatively placed the LO of *P. lacunosa* between Samples 115-715A-5R-2, 44–45 cm, and 115-715A-5R-3, 44–45 cm. The lowermost Pleistocene sediment recovered directly above the hiatus was, therefore, referred to the top part of Subzone CN14a.

Miocene

The top of Core 115-715A-6R yielded a middle Miocene assemblage assigned to Zone CN4. The hiatus located between this core and the overlying Core 115-715A-5R is estimated to represent approximately 14 m.y.

Fine-rayed discoasters such as *Discoaster exilis* and *Discoaster variabilis* become more abundant than the thick-rayed *Discoaster deflandrei* at Sample 115-715A-7R-2, 40–41 cm, and above. The LO of *Helicosphaera ampliaperta*, defining the boundary between Zones NN4 and NN5, occurs in Section 115-715A-8R, CC.

The FO of *Sphenolithus heteromorphus* (base of Zone CN3) was observed in Sample 115-715A-10R-3, 40–41 cm, and the LO of *Sphenolithus belemnos* (base of Zone NN4) was also identified in this sample. The latter event is supposed to precede the former event by 0.3 m.y., and these two species are not known to coexist (Berggren et al., 1985). We have obtained ideal materials to study the succession of evolutionary events through the Miocene, and this matter will be studied in detail. The LO of *Triquetrorhabdulus carinatus* (NN2–NN3 boundary) occurs in Sample 115-715A-10R-6, 130 cm. The FO of *S. belemnos* (base of CN2) occurs in Sample 115-715A-11R-2, 130 cm.

The interval between Sample 115-715A-11R-3, 40–41 cm, and Section 115-715A-11R, CC, is assigned to the early Miocene Zone CN1. Reworked forms are scarce in this sequence, and only a single specimen of *Sphenolithus predistentus* was identified as a reworked Oligocene form.

Eocene

Core 115-715A-12R recovered 1.5 m of limestone. Section 115-715A-12R, CC, yielded very rare nannofossils, but we did identify *Cyclicargolithus floridanus*, *Dictyococcites* sp., and *Sphenolithus moriformis*.

A limestone pebble recovered in Section 115-715A-13R-1 contains an assemblage referable to the upper or upper middle Eocene. Nannofossils are few and moderately overgrown in this sample, with *C. floridanus* dominating the flora. Other species observed here include *Coccolithus pelagicus*, *Dictyococcites bisectus*, *Discoaster barbadiensis*, *Ericsonia obruta*, *Helicosphaera euphratis*, *Sphenolithus moriformis*, and *S. predistentus*. This assemblage has been tentatively assigned to Zones CP15 and CP14.

Cores 115-715A-14R through -22R recovered apparent shallow-water limestones, and these materials proved to be barren of calcareous nannofossils. Cores 115-715A-23R through -25R retrieved an intercalated sequence of limestones and basalts. These limestones were also barren of nannofossils.

Planktonic Foraminifers

Neogene

The planktonic foraminiferal biostratigraphy of Hole 715A is based on data from core catchers. Planktonic foraminifers are abundant throughout the Neogene sequence, being very well preserved in the uppermost two cores, well preserved in the remainder of the Pleistocene, and moderately well preserved in the Miocene.

Sections 115-715A-1R, CC, through 115-715A-5R, CC, belong to the Pleistocene zonal interval N23–N22 based on the presence of rare *Globorotalia truncatulinoides*. The assemblages, typical of tropical water, contain common *Globigerinoides sacculifer*, *G. ruber*, *Neogloboquadrina dutertrei*, and *Pulleniatina obliquiloculata*. *Globorotalia menardii* specimens are common in Sections 115-715A-1R, CC, and 115-715A-2R, CC, and less common in Sections 115-715A-3R, CC, through 115-715A-5R, CC. *Globorotalia tumida*, on the other hand, show a reversed trend, being rare in Sections 115-715A-1R, CC, and 115-715A-2R, CC, and common in Sections 115-715A-3R, CC, through 115-715A-5R, CC.

Section 115-715A-6R, CC, assigned to the middle Miocene Zone N9, contains common *Globorotalia siakensis*, *G. mayeri*, *Globoquadrina altispira*, and rare *Orbulina*. The latter species was not found below this level. Sections 115-715A-7R, CC, and 115-715A-8R, CC, which contain *Globigerinoides sicanus*, are assigned to Zone N8. Sections 115-715A-9R, CC, through 115-715A-11R, CC, are dominated by a small-sized fauna assigned to the zonal interval N7–N5.

Paleogene

Paleogene planktonic foraminifers were recovered within the shallow-water limestones drilled in Hole 715A. In Sections 115-715A-12R-1 to 115-715A-13R-1, the presence of *Planorotalites palmerae*, *P. pseudoscitula*, *Globigerinatheka senni*, *Subbotina yeguaensis*, *Acarinina pentacamerata*, *A. rohri*, and *A. pseudotopilensis* associated with rare *Morozovella aragonensis* indicates a later early Eocene age, probably Zone P9.

Benthic Foraminifers

We recovered well-preserved benthic foraminifers from all Pleistocene and early Miocene cores recovered at Site 715. All foraminifers appeared to be in place and were consistent with deposition in a lower intermediate water. Faunal composition suggests low oxygen conditions at the bottom in the early Miocene, so that a moderately low-oxygen, intermediate water extending at least from 1,000 to 2,200 m is indicated in this area of the Indian Ocean through much of the Neogene. The benthic fauna just above the limestone in Core 115-715A-12R contains species indicative still of lower intermediate depths.

Pleistocene

In Pleistocene sediments at Site 715 (Cores 115-715A-1R through -5R), benthic foraminifers are uncommon to rare, although they do increase in number as carbonate dissolution increases below Core 115-715A-2R. Faunas contain elements of the upper intermediate fauna found at Site 714, but lack several of the genera usually restricted to upper intermediate depths.

Episodically, they contain a high number of deep-water immigrants, presumably during glacial cycles.

The *Ceratobulimina pacifica–Bulimina aculeata* association contains *Bulimina aculeata* (not found at Leg 115 sites to the west), *Cassidulina carinata, Bolivinitella olssoni, Uvigerina proboscidea, U. auberiana, Bulimina alazanensis, Brizalina subaenariensis*, and *Hoeglundina elegans*. An alternating assemblage (e.g., Sample 115-715A-3R-2, 120 cm), the *Cibicidoides kullenbergi–Nuttalides umbonifera* association, contains other deeper-water forms such as *Melonis pompilioides* and large *Uvigerina hispidocostata*. This latter association suggests upward migration of deeper-water faunas, possibly during glacial episodes.

Lacking from this site are the tropical intermediate-water Car Nicobar species, particularly the large nodosariids and all osangularids. Bolivinids are more common than at any of the western sites on Leg 115, but are much less common than in faunas at nearby Site 714.

Early Miocene

As at other sites, the early Miocene benthic foraminiferal fauna is limited in number, benthic foraminifers are rare and not well preserved, and individuals are often small in size even in samples which are moderately well preserved. Faunas are composed of generalists and solution-resistant species such as *Globocassidulina subglobosa*. Unlike in the Pleistocene, a few reworked late Oligocene, upper-intermediate depth markers are present, and the deeper-water element contains *Cibicidoides kullenbergi*, but no typically abyssal species.

Faunas are dominated by the ornamented brizalinids, including *Brizalina reticulata, B. tectiformis*, and *Bolivinitella olssoni. Osangularia mexicana*, but not the large planulinids, occurs in several samples. Preservation improves temporarily in the *Paragloborotalia kugleri* Zone (Section 115-715A-11R, CC). The more diverse benthic samples include the typical late Paleogene species *Bulimina tuxpamensis, B. impendens*, and *Rectuvigerina multicostata*, along with *Globocassidulina subglobosa* and *Cibicidoides kullenbergi*. This fauna suggests deposition at intermediate depths at the beginning of the Miocene, just above the limestone sequence.

Larger Benthic Foraminifers

The limestones from Cores 115-715A-12R to -22R were studied in thin section. They contain a typical shallow-water reefal assemblage rich in age-diagnostic larger benthic foraminifers. In the upper cores, we also identified planktonic foraminifers (see above). Larger benthic foraminifers at the top (between Samples 115-715A-12R-1, 44 cm, and 115-715A-13R-1, 14 cm) associated with *Melobesiae* and rare bryozoans, included *Nummulites pratti, N. caupennensis, Discocyclina sella, D. douvillei, Asterocyclina* spp., and *Operculina*. This assemblage is indicative of a late Cuisian age, late early Eocene.

Cores 115-715A-13R and -14R also can be assigned to the late Cuisian on the basis of several transition forms of *Fasciolites dainellii* to *F. palermitana*, together with the *Nummulites burdigalensis* group and *Rotalia viennoti*. The assemblages also contain miliolids, several dasycladacean and melobesian algae, rare gastropods, corals, and possibly hydrozoans. The bottom cores (115-715A-15R to -21R) contain the same species of *Fasciolites*, together with the granulated *Nummulites campesinus*. The presence of this species places the bottom core in the late early Eocene *Fasciolites dainellii* Biozone, according to the alveolinid zonal scheme of Hottinger (1960).

A paleoenvironmental assessment of these faunas suggests the younger to older evolution from a diversified carbonate platform facies in an open marine environment, indicated by the lack of alveolinids and the presence of planktonic foraminifers, to a back reef area characterized by abundant miliolids near the bottom of the sequence.

Radiolarians

Quaternary radiolarians are present in Sections 115-715A-1R, CC, through 115-715A-5R, CC (8.1–46.8 mbsf). Diagnostic species include *Didymocyrtis tetrathalamus, Spongaster tetras, Theocorythium trachelium, Amphirhopalum ypsilon*, and *Anthocyrtidium nigriniae*. We made no attempt to subdivide the Quaternary into zones, although the marker species for the uppermost Quaternary (*Buccinosphaera invaginata* and *Collosphaera tuberosa*) are clearly present in the uppermost core. Radiolarians are common throughout the Quaternary interval. Preservation is good at the top of the interval and moderate toward the base.

An unconformity is present within Core 115-715A-6R. Section 115-715A-6R, CC, is of middle Miocene age and is assigned to the *Calocycletta costata* Zone. Radiolarians are few and moderately well preserved. Diagnostic taxa include *Stichocorys delmontensis, S. wolffii*, and *Calocycletta costata*.

Radiolarians are absent in all cores below Core 115-715A-6R (56.5 mbsf).

Diatoms

The occurrence of diatoms at Site 715 is restricted to one Pleistocene core-catcher sample (Section 115-715A-4R, CC). This sample provides a moderately to poorly preserved assemblage, which includes such age-diagnostic species as *Pseudoeunotia doliolus, Thalassiosira oestrupii*, and *Nitzschia marina*. The lack of *Rhizosolenia praebergonii* and *Nitzschia reinholdii* places the sample in the youngest of the Quaternary diatom zones, the *P. doliolus* Zone.

Diatoms are absent in all core-catcher samples below Core 115-715A-4R.

PALEOMAGNETICS

Introduction

The rotary-drilled sediments recovered at Site 715 proved difficult to study effectively: most sediments showed only weak magnetic intensity and, in the more lithified portions, recovery was poor with most pieces broken and disoriented. The preservational state of the basement rocks varies considerably. The recovered basalt includes small weathered pieces as well as longer segments of fresh rock. Despite the relatively poor preservation of these rocks, the basalts provide the only meaningful magnetic measurements made at this site.

Results

Pass-through magnetometer measurements of sediment cores were performed on one section per core (through Core 115-715A-11R); however, little information of value was obtained. Aside from the disturbance involved in rotary drilling, paleomagnetic measurements were difficult because the magnetic intensity of these sediments is smaller than 10^{-7} emu/cm^3. Presumably the measurement of discrete samples (with the much smaller effective volume) will be even more difficult. The bottom-most reef carbonate sediments present another problem: the lithified sediments are sufficiently fragile so that they were brecciated by drilling. The small size of the resulting pieces makes it impossible to orient them for paleomagnetic analysis.

Preservation of the basalt from Site 715 varies dramatically, with rust-colored weathering alternating with completely fresh sequences. We sampled 12 of the 21 identified petrologic units and measured 1–3 minicores from each. These generally yielded good results. Measurement with the spinner magnetometer using alternating-field (AF) treatment shows that, after 5–10 mT, the magnetization decays straight to the origin (Fig. 8). The polarity in the samples measured is presumed to be normal, except in 2 of the minicores where measurements revealed positive in-

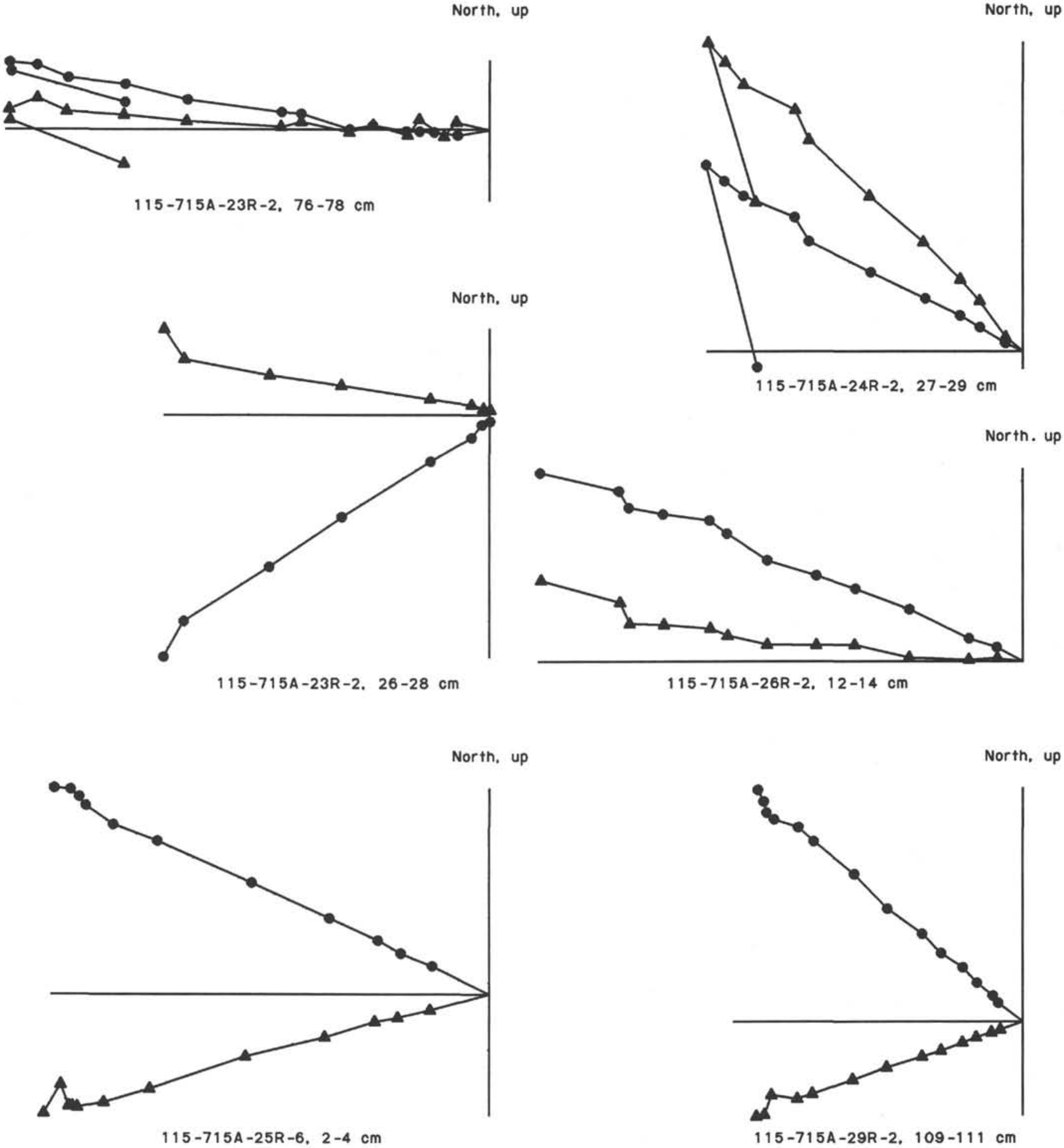

Figure 8. Zijderveld diagrams for six basalt samples showing behavior representative of the samples examined. All demagnetization is by alternating-field (AF) treatment. Dots represent projection onto the vertical plane, triangles represent projection onto the horizontal plane.

clinations (i.e., reversed polarity). The results of principal component analysis are given in Table 2.

Discussion

The presence of two polarity states within the basalt sequence suggests that an appreciable amount of time has been sampled by these rock units. Some caution is advised, however, as the misorientation of a single sample is distinctly possible. This possibly explains the positive inclination (apparently reversed polarity) found in one sample from Unit 9 (Sample 115-715A-25R-2, 83-86 cm). The natural remanent magnetization (NRM) of all other samples from Unit 9 (both above and below) as well as demagnetization results from one of these (Sample 115-715A-25R-3, 83-86 cm) consistently show negative inclinations (normal polarity).

Table 2. Directions of primary component of magnetization in basalt samples from Site 715 as determined with principal component analysis.

Sample interval (cm)	Number of samples	MAD	Declination (degrees)	Inclination (degrees)	Hard rock unit
115-715A-					
23R-2, 26–28 (Piece 2A)	5	1.7	43.7	3.957	4
23R-2, 76–78 (Piece 5)	12	3.8	−12.9	0.215	5
23R-3, 104–106 (Piece 14B)	7	1.2	−22.6	2.826	7
24R-1, 109–111 (Piece 12)	7	1.1	−26.5	1.835	7
24R-2, 27–30 (Piece 3)	6	1.9	−23.2	1.132	7
25R-2, 83–86 (Piece 3C)	5	4.5	34.6	1.747	9
25R-3, 83–86 (Piece 2)	5	1.8	−31.3	1.729	9
25R-6, 2–5 (Piece 1)	6	1.5	−31.8	1.085	10
26R-2, 12–15 (Piece 1A)	3	2.9	−33.4	0.715	10
29R-1, 28–31 (Piece 2A)	5	1.5	−44.9	1.278	12
29R-1, 55–58 (Piece 2B)	10	1.8	−48.1	1.579	12
29R-1, 124–127 (Piece 4B)	5	0.8	−49.7	1.381	13
29R-2, 109–112 (Piece 1E)	10	0.8	−49.2	0.706	13
30R-1, 65–68 (Piece 2B)	6	1.9	−47.5	0.446	15
30R-2, 87–89 (Piece 1)	6	1.6	−48.4	1.569	15
30R-3, 107–109 (Piece 2A)	7	0.9	−51.5	5.197	16
30R-4, 45–47 (Piece 1B)	7	2.2	−47.8	2.033	16
30R-4, 108–110 (Piece 6)	7	1.5	−43.4	1.589	17
30R-5, 130–132 (Piece 11)	5	0.9	−50.7	0.495	20
30R-6, 16–18 (Piece 1C)	8	2.9	−50.8	2.092	20
31R-1, 116–118 (Piece 9A)	3	0.5	−44.6	0.514	21
31R-2, 107–109 (Piece 6B)	9	7.6	−44.6	0.510	21
31R-3, 14–16 (Piece 1A)	5	1.3	−47.3	1.470	21

Note: MAD = mean angular deviation of fit.

Demagnetization of one sample, however, from Unit 4 (Sample 115-715A-23R-2, 26–28 cm) shows a positive inclination which is not so easily dismissed. In the collection studied, Unit 4 is represented by this single sample, and the overlying units (1, 2, and 3) of basalt breccia cannot be oriented reliably. Thus, it is difficult to check this single reversed polarity result. We tentatively consider Unit 4 to be of reversed polarity and interpret the results from the basalt sequence as recording a normal to reverse polarity transition.

Unfortunately, we are not able to compare the basalt results with any significant data from the overlying sediments. Besides allowing a general consistency check, analysis of the sediments might reveal whether the basalts do in fact record a normal to reversed transition. Indeed, the basalt directions (listed in Table 2) show evidence for this: immediately below the supposed reversed polarity Unit 4, the measured inclination takes on intermediate values and the NRM intensity is anomalously low. These observations would suggest that some of the units may record a transitional field.

The maximum likelihood mean of all the lithologic unit inclinations is −41.1° (N = 12, kappa = 23.4, alpha 95 = 8.8°). This corresponds to a paleolatitude of 23.6° ± 6.5°. However, if Unit 5 is considered as transitional and excluded from the analysis, one obtains a mean inclination of 43.0° degrees (N = 11, kappa = 43.8, alpha 95 = 6.7°) and a paleolatitude of 25.0° ± 5.1°. The difference in the mean is not great, but the exclusion does reduce the confidence limits. Moreover, both alternatives are in good agreement with the hotspot model as discussed below.

Leg 115 Paleomagnetic Results and the Hotspot Model

The hotspot model (Duncan, 1981; Morgan, 1981) would predict that progressive paleolatitudes should be obtained along the Maldive-Laccadive-Chagos-Mascarene Ridge system. The paleolatitude would vary between the Deccan value (29° ± 4°; Courtillot et al., 1986) and the present-day Réunion latitude (21°).

During Leg 115, basement was drilled four times: on the Mascarene Plateau (Site 706), in the Seychelles Plateau (Site 707), in the Chagos Archipelago (Site 713), and in the Maldive Archipelago (this site). In addition, sediments overlying the basement were measured at Sites 706 and 713. Paleomagnetic results from these sites are summarized in Table 3.

Two criteria may be used to assess the reliability of the paleomagnetic data obtained from these various sites. One can judge the sediment results simply by the consistency of the inclinations, while for the basement results the reliability of the average depends on whether an appropriate amount of secular variation is displayed.

Site 706 sediments show consistent directions and thus probably give a reliable result; however, Site 713 sediments do not yield consistent inclinations. Of the basement sites, Site 707 results show small scatter and may not be reliable if they incompletely record geomagnetic secular variation. Site 713 inclination values show an excessively large amount of scatter, and these too may be unreliable. Site 706 and Site 715 basalt results show adequate secular variation and so would appear to be reliable.

Thus, there are three relevant inclination averages: the Site 706 sediment result, the Site 706 basalt result, and the Site 715 basalt result. Two of these (Site 706 basement and sediment) disagree distinctly, however. The sediments show an average inclination of 44° (paleolatitude = 26°), while the basement rocks give an average inclination of −14° (paleolatitude = 13°). To reconcile these results, we may suppose that the basement has been tilted; if so, the sediments would provide the better paleolatitude value to test the hotspot model. In addition, the basalt results from Site 715 give, as discussed above, an average inclination of −43° (paleolatitude = 25°) and provide a second test of the hotspot model.

The preferred Oligocene age result (Site 706 sediment) as well as the Eocene age result (Site 715 basalt) both indicate paleolatitudes of about 25° and are consistent, therefore, with the generation of these volcanic ridges by the Réunion hotspot. The pa-

Table 3. Summary of paleolatitude results from Leg 115.

Site	Mean (degrees)	Kappa	Alpha 95 (degrees)	Paleolatitude (°S)	Comment
706 (sediment)	44.4	30.5	4.7	26.1 ± 3.7	Internally consistent
706 (basement)	−24.2	10.2	10.5	12.7 ± 6.0	Internally consistent
707 (basement)	43.3	205.2	4.9	25.2 ± 3.8	Inadequate secular variation?
713 (basement)	24.4	29.2	4.6	12.8 ± 2.6	Excessive scatter
715 (basement)	−41.1	23.4	8.8	23.6 ± 6.5	All units
	−43.0	43.8	6.7	25.0 ± 5.1	Unit 5 excluded

Note: Maximum likelihood statistics are used to determine mean inclination and Fisher precision parameter kappa (see "Paleomagnetics" section, "Explanatory Notes" chapter, this volume).

leomagnetic results do not indicate, however, whether the shift of the hotspot latitude occurred uniformly or during some restricted interval.

SEDIMENTATION RATES

Site 715 recovered an approximately 105-m-thick Neogene sequence of calcareous ooze and a more than 106-m-thick sequence of Eocene shallow-water limestones overlying or intercalated into basalt. A hiatus spanning the interval from the middle Pleistocene to middle Miocene (approximately 14 m.y.) was observed in the Neogene sequence. There is possibly another hiatus between the Neogene sequence and the shallow-water limestone which may span the major part of the Oligocene and some portion of the Eocene.

Nannofossil and planktonic foraminiferal datum events observed in Hole 715A are listed in Table 4, and sedimentation rates based on these events are illustrated in Figure 9. The sedimentation rate for the late Pleistocene is the highest observed on Leg 115 (86 m/m.y.). Since the equivalent rate for Site 714, which is only a couple of miles away from Site 715, was measured as 39 m/m.y., the unusually high sedimentation rate may be a result of resedimentation. Sedimentary textures were badly disturbed in this rotary cored sequence, implying that the presence of slumps or turbidites could not be recognized.

Table 4. Depth ranges and ages of the biostratigraphic datum events observed at Site 715.

	Species event	Depth (mbsf)	Age (Ma)
FO	*E. huxleyi* (N)	16.0–17.8	0.27
LO	*P. lacunosa* (N)	39.0–40.5	0.46
LO	*S. heteromorphus* (N)	— –46.8	13.2
FO	*Orbulina* spp. (F)	56.5–66.1	15.2
LO	*H. ampliaperta*	74.9–75.7	16.0
FO	*G. sicanus* (F)	75.7–85.3	16.6
FO	*S. heteromorphus* (N)	88.7–89.6	18.6
FO	*S. belemnos* (N)	98.3–98.8	21.5
LO	*S. ciperoensis* (N)	104.6– —	<25.2

Note: FO = first occurrence, LO = last occurrence, N = calcareous nannoplanktons, and F = planktonic foraminifers.

GEOCHEMISTRY

Interstitial Water Studies

Interstitial water analyses were performed on seven samples from Hole 715A. The deepest sample taken was from 81.65 mbsf. Data are presented in Table 5 and Figure 10.

Calcium and Magnesium

The calcium and magnesium concentrations in Hole 715A are essentially constant throughout the entire depth interval over which samples were taken (Fig. 11). The absence of significant changes in Mg^{2+} and Ca^{2+} may suggest the occurrence of precipitation and dissolution reactions involving carbonate minerals.

Alkalinity, pH, and Sulfate

Alkalinity and sulfate show small changes typical of previous sites investigated during Leg 115 (Fig. 10). Perhaps the most interesting aspect of Hole 715A was the low pH of the pore waters, as low as 7.1 and lower than at any previous site investigated.

Carbonate and Organic Carbon Content

The carbonate concentration of sediments from Hole 715A varies from 58.9 to 91.4 wt% (see "Physical Properties" section, this chapter). The Pleistocene portion of the core is characterized by steadily rising carbonate content, similar to Hole 714A. The average carbonate content of the upper Miocene sediments is identical to that seen in Hole 714A for the same time interval. Substantial quantities of aragonite and quartz were detected throughout the Pleistocene interval. Below the hiatus marking the Pleistocene/Miocene boundary, the mineralogy is dominated by low-magnesium calcite.

Amounts of organic carbon were high in the Pleistocene portion of the core, similar to Site 714 (Table 6).

BASEMENT ROCKS

Introduction

After rotary coring through ~100 m of nannofossil ooze and 110 m of coralline limestone, basalt was intersected 40 cm into Core 115-715A-23R at a depth of 211.21 mbsf. The hole was stopped after Core 115-715A-31R at a depth of 287.8 mbsf, with 30.09 m of core recovered from the 76.6 m drilled (39.3%; see Fig. 12). The basalt flows encountered were for the most part aphyric and conspicuously oxidized and weathered in their upper parts. This alteration diminishes toward the more massive interiors of the flows, some parts of which appear only slightly altered. Immediately overlying, and intercalated with several flows, are basalt-limestone breccias or calcarenites with weathered reddish brown basaltic grains, fragments, or boulders. These sedimentary layers may well represent beach deposits or subaerial paleoregoliths.

Through visual examination the recovered core was subdivided into 21 units (including sedimentary intercalations—Units 1, 3, and 8) on the basis of lithostratigraphy, vesicularity, grain size, phenocryst type and abundance, and the presence of highly weathered/oxidized zones. The distribution of these units relative to the core actually recovered is illustrated in Figure 12. Note that we have arbitrarily assumed that the core segments recovered are continuous and located at the top of each core drilled. A detailed description of the macroscopic and microscopic characteristics of each unit is given below, features of which are summarized in Figure 13.

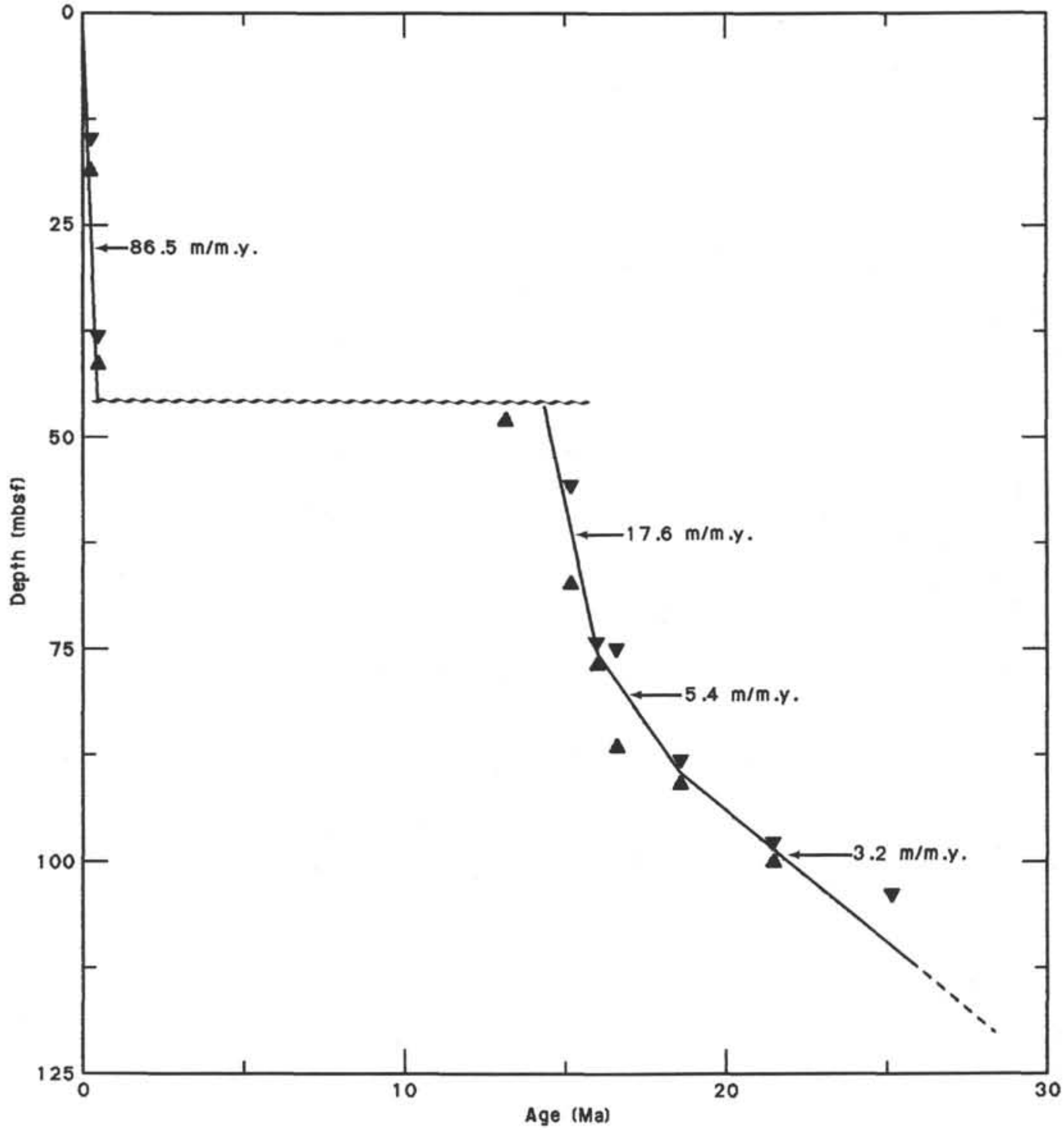

Figure 9. Age-depth plot for Hole 715A showing estimated sedimentation rates at Site 715.

Table 5. Interstitial water analyses, Hole 715A.

Sample interval (cm)	Depth (mbsf)	Ca (mmol/L)	Mg (mmol/L)	Cl (mmol/L)	Alk (mmol/L)	pH	Salinity (‰)	Si (μmol/L)	SO_4 (mmol/L)
Seawater	0	10.58	55.21	560.1	2.47	8.5	35.0	0	27.80
115-715A-									
1R-3, 145-150	4.45	10.43	51.67	552.5	3.38	7.8	34.4	671	27.25
2R-4, 145-150	14.05	10.52	52.57	556.2	3.97	7.7	34.5	662	26.92
3R-4, 145-150	23.75	10.52	52.97	546.0	4.20	7.1	34.2	727	26.37
4R-4, 145-150	33.45	10.62	53.44	540.4	4.38	7.5	35.0	702	26.70
5R-4, 145-150	43.05	10.49	51.94	562.7	4.40	7.3	34.8	783	26.70
6R-4, 145-150	52.75	10.65	53.16	546.0	4.33	7.6	34.5	714	26.50
9R-4, 145-150	81.65	10.60	53.30	564.6	3.45	7.8	35.0	479	27.48

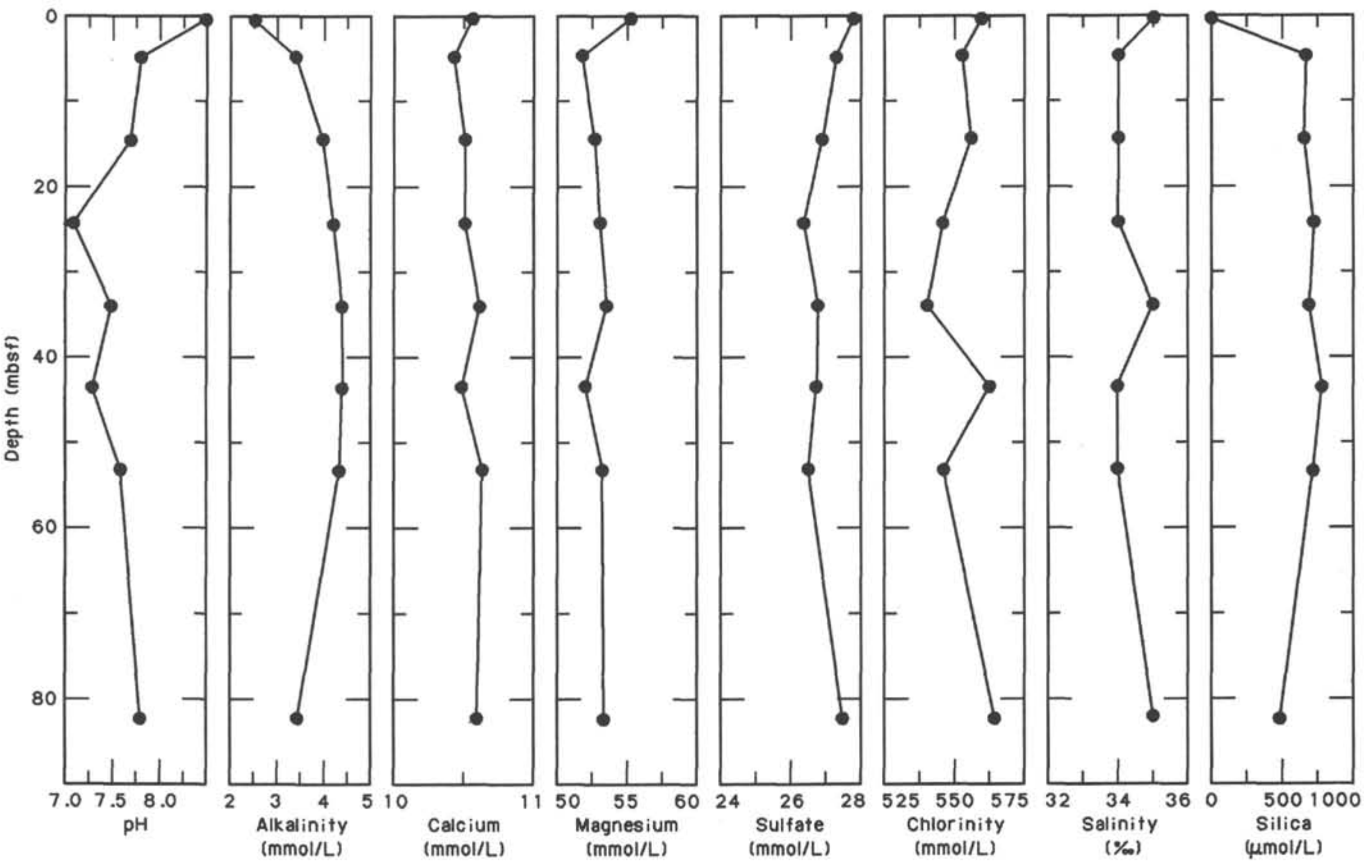

Figure 10. Summary of interstitial water analyses, Site 715, as a function of sub-bottom depth. Values for surface seawater are plotted at 0 mbsf.

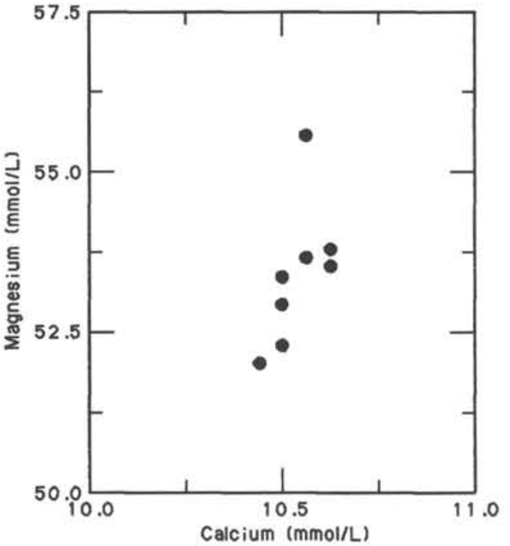

Figure 11. Relationship between calcium and magnesium concentrations, Site 715.

Table 6. Organic carbon analyses, Hole 715A.

Sample interval (cm)	Depth (mbsf)	Organic carbon (%)
115-715A-		
1R-2, 83–85	2.33	0.77
2R-5, 22–24	14.32	2.31
3R-5, 22–24	24.02	0.55
4R-5, 38–40	33.88	0
5R-5, 78–80	43.88	0
6R-5, 60–62	53.40	1.42
7R-5, 60–62	63.10	0.02
8R-5, 60–62	72.70	0.54
9R-5, 60–62	82.30	0
10R-5, 60–62	91.90	0.17
11R-5, 60–62	101.50	0.02

Macroscopic Characteristics

Unit 1 (0.38 m thick): Reefal limestones of Core 115-715-23R overlie Unit 1, which contains rounded to subangular basalt clasts set in a micritic carbonate matrix. The aphyric, fine-grained, moderately vesicular basalt clasts have vesicles filled with carbonate and minor sulfide minerals.

Unit 2 (0.09 m thick): Moderately altered, nearly aphyric basalt (plagioclase phenocrysts $<1\%$) composes this unit, which is moderately vesicular (10%). The typically spherical vesicles, up to 1 cm in diameter, are rimmed with clay, carbonate, and sulfide minerals.

Unit 3 (0.77 m thick): This unit is primarily a coarse calcarenite with basalt clasts (1 mm–5 cm in diameter), showing moderate to intense alteration and oxidation. Figure 14 shows the contact between the calcarenite and vesicular basalt. Some vesicles in the basalt are rimmed with calcite.

Units 4 and 5 (0.18 and 0.53 m thick, respectively): These two units consist of plagioclase-phyric (less than 5% phenocrysts), highly vesicular (20%), moderately altered basalts. The

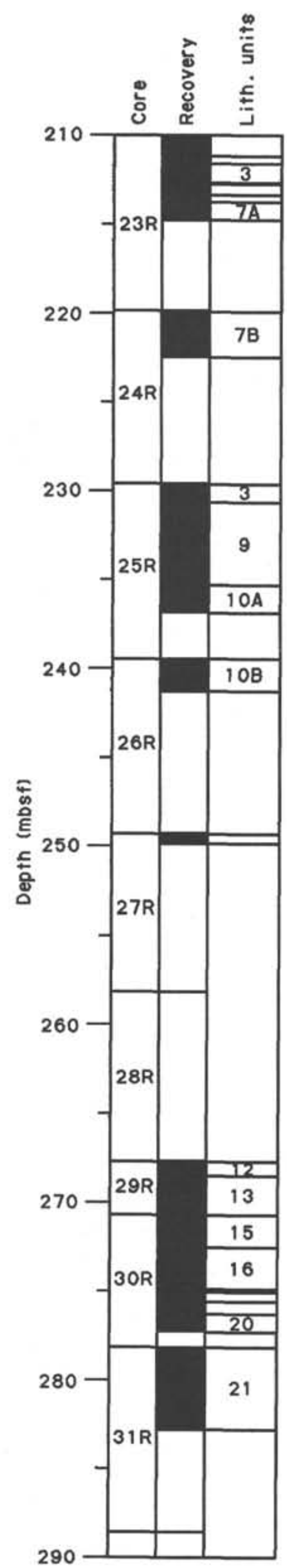

Figure 12. Site 715 basement rock unit numbers and core depths, with recovery indicated by black bars. Note that each numbered core represents about 9.5–10.0 m of drill penetration, but that actual core recovery is variable. Overall average recovery at the site was 39.9%.

tops of both units are marked by calcarenites containing rounded basalt clasts up to 1 cm across (Fig. 15). About 50% of the vesicles are filled with carbonate, 30% by dark green to yellow minerals, and the remainder are unfilled.

Unit 6 (0.37 m thick): A bed of basaltic calcarenite grading to conglomerate (clasts up to 6 cm wide) makes up the sixth unit. The vesicular basalt clasts are enclosed in a micritic matrix and appear moderately to highly altered (Fig. 16).

Unit 7 (4.00 m thick): We found this unit between the bottom 1.5 m of Core 115-715A-23R and the top 2.5 m of Core 115-715A-24R. As these segments could be separated by as much as 5.4 m (the recovery gap in Core 115-715A-23R), the unit has been separated into Subunits 7A and 7B. The unit consists of moderately altered, plagioclase-phyric (<5%), fine-grained basalt. Vesicles are rare in most of the unit (less than 2%) but are abundant in the top 30 cm (20%), where vesicles up to 6 mm in diameter are generally filled with yellow clay minerals and, less commonly, carbonates. The upper 3 m of the unit has a dark brown color, but a fresh black unoxidized portion occurs near the bottom of Unit 7B in Core 115-715A-24R. This change in color does not correspond with the break in recovery between Cores 115-715A-23R and 115-715A-24R. Units 7A and 7B are similar in terms of TiO_2 and zircon, and these elements distinguish Unit 7 from the lower units (Table 7).

Carbonate layer: A calcarenite layer 0.85 m thick occurs between basaltic Units 7 and 8.

Unit 8 (0.11 m thick): This unit is a carbonate-cemented basalt breccia with clasts 1–20 mm in diameter showing varying degrees of alteration and weathering.

Units 9 and 10 (4.54 and 5.41 m thick, respectively): Aphyric, moderately to highly altered, fine-grained basalts make up these two units, which are judged to represent two lava flow units. In both, vesicularity changes gradually; the central parts are characterized by very low (less than 1%) vesicularity, whereas the upper and lower parts are more highly vesicular (up to 50% and with vesicles up to 10 mm in diameter). Most of the vesicles are filled with carbonate and/or clay minerals. Highly vesicular parts of the units show a greater degree of alteration or oxidation (reddish brown in color), and the bottom of Unit 10 resembles the soil typically observed at the "clinker" base of subaerial lava flows. The boundary between these two units is not clearly defined. Unit 10 is contained in both Cores 115-715A-25R and 115-715A-26R. Although 2.4 m of core is missing between the bottom of Core 115-715A-25R and the top of Core 115-715A-26R, the similarity of lithology across this gap suggests that only one unit is represented.

Unit 11 (0.11 m thick): A single piece of basalt in the core catcher of Core 115-715A-27R represents the only retrieved portion of Unit 11. It is a dark grey, moderately to highly altered, slightly vesicular (up to 2 mm in diameter), fine-grained, aphyric basalt.

Unit 12 (0.76 m thick): Slightly altered, plagioclase-phyric basalt composes this unit. Vesicles (about 5%) are filled with clay and carbonate minerals.

Unit 13 (1.80 m thick): Basalt richer in plagioclase phenocrysts (total 5%–10%) than the basalt of Unit 12 comprises Unit 13. Vesicles occur mainly in the upper portion of the unit (around 20%), rapidly decreasing to less than 1% over a 10-cm interval 0.6 m below the top.

Unit 14 (0.07 m thick): This unit consists of a highly weathered, plagioclase-phyric (less than 5%) basalt with abundant vesicles (1.5 cm in average diameter and filled with clay and carbonate minerals).

Unit 15 (1.72 m thick): This unit is composed of a massive, olivine-bearing, plagioclase-phyric basalt with an oxidized zone at the top and bottom, 5 and 10 cm thick, respectively. Olivine

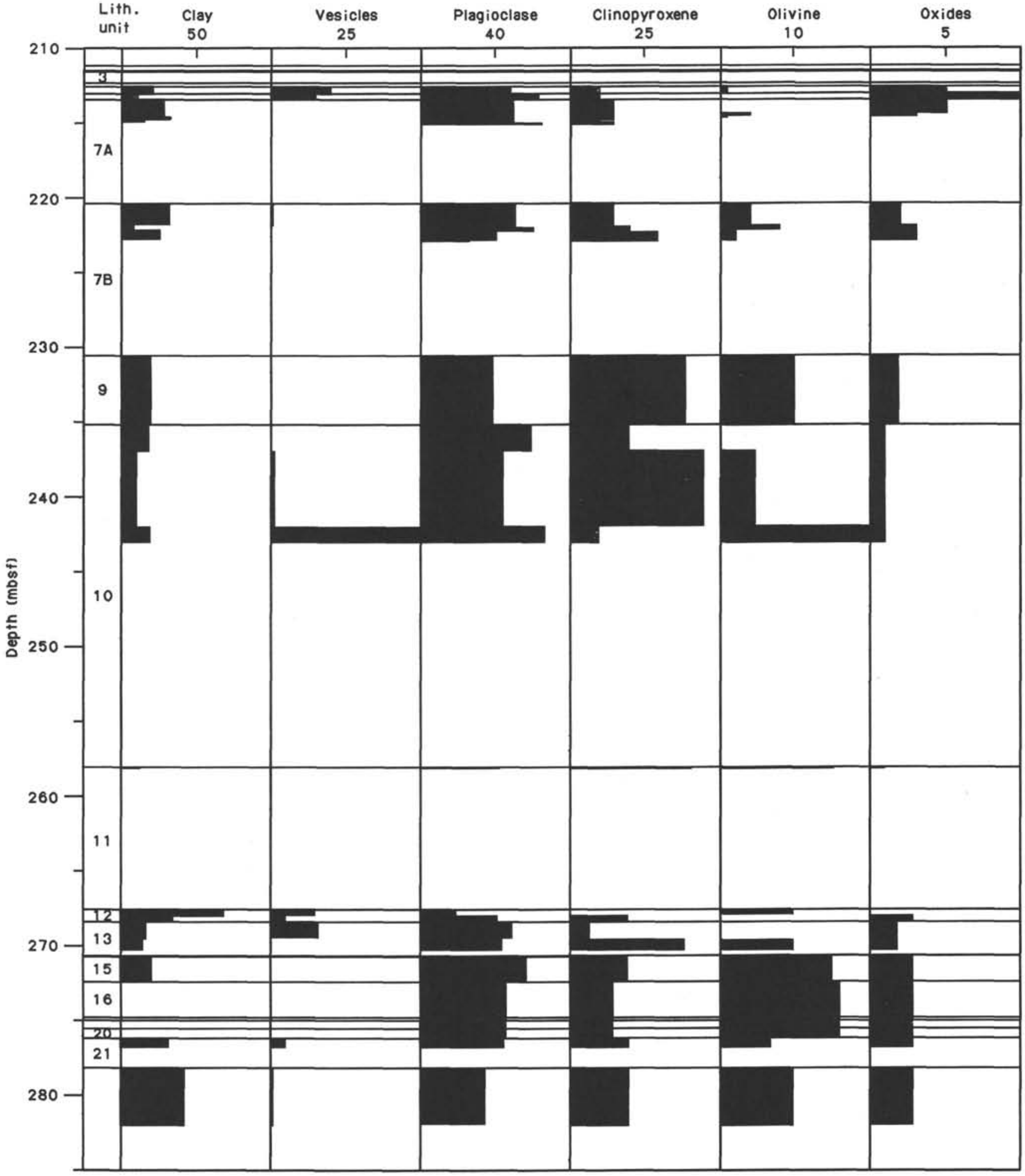

Figure 13. Graphic summary of the petrographic characteristics of basalts from Hole 715A. Alteration percentages appear in the second column as percent clay, and vesicle percentages are given in the third column. The columns marked "Plagioclase," "Clinopyroxene," and "Olivine" refer to the modal phenocryst percentages for each mineral. In most cases olivine has been altered to clay. The column marked "Oxides" refers to the total modal abundance of the iron-titanium oxides.

phenocrysts are completely altered to green (chlorite) or reddish brown (iddingsite) clay minerals.

Unit 16 (2.32 m thick): The massive, augite olivine plagioclase basalt of Unit 16 shows an oxidized top (5 cm thick) and vesicular bottom (15 cm thick). Rims of olivine are totally replaced by iddingsite.

Unit 17 (0.22 m thick): Unit 17 consists of an olivine plagioclase basalt which may comprise one lava flow. A concentration

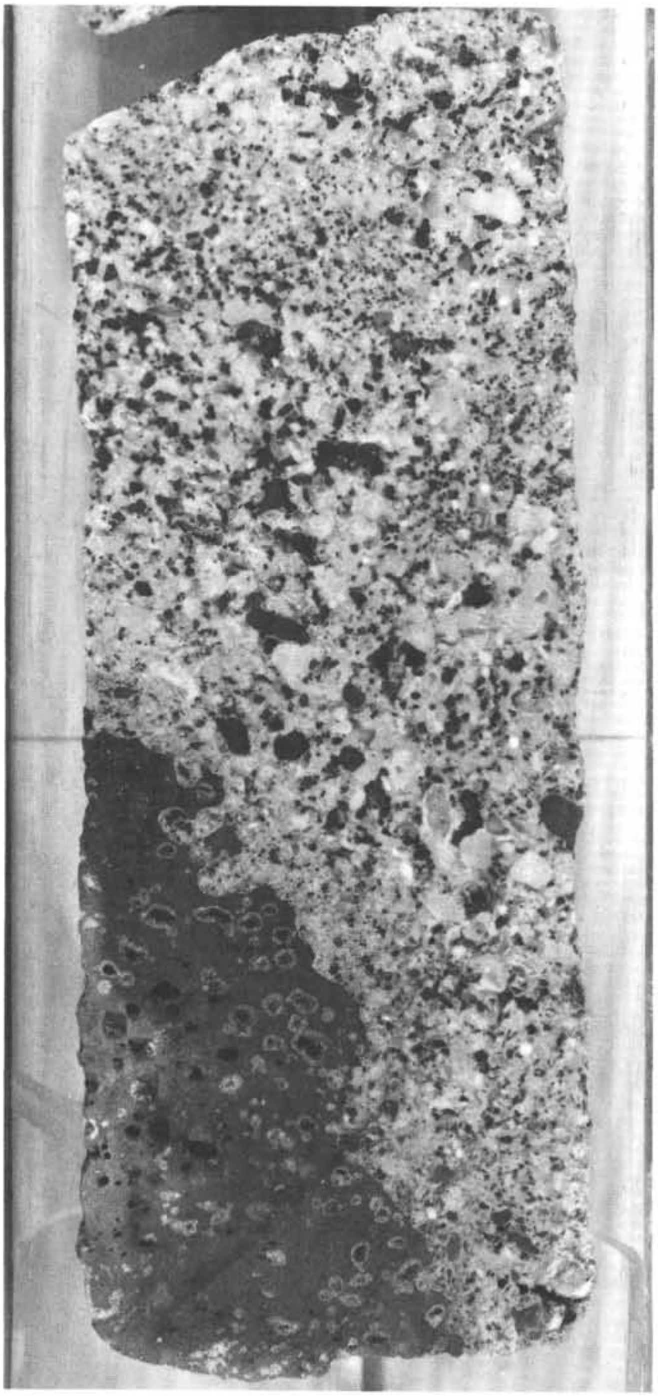

1 cm

Figure 14. Photograph of the contact between coarse carbonate-basalt sandstone and basalt in Unit 3 (115-715A-23R-1, 130–144 cm).

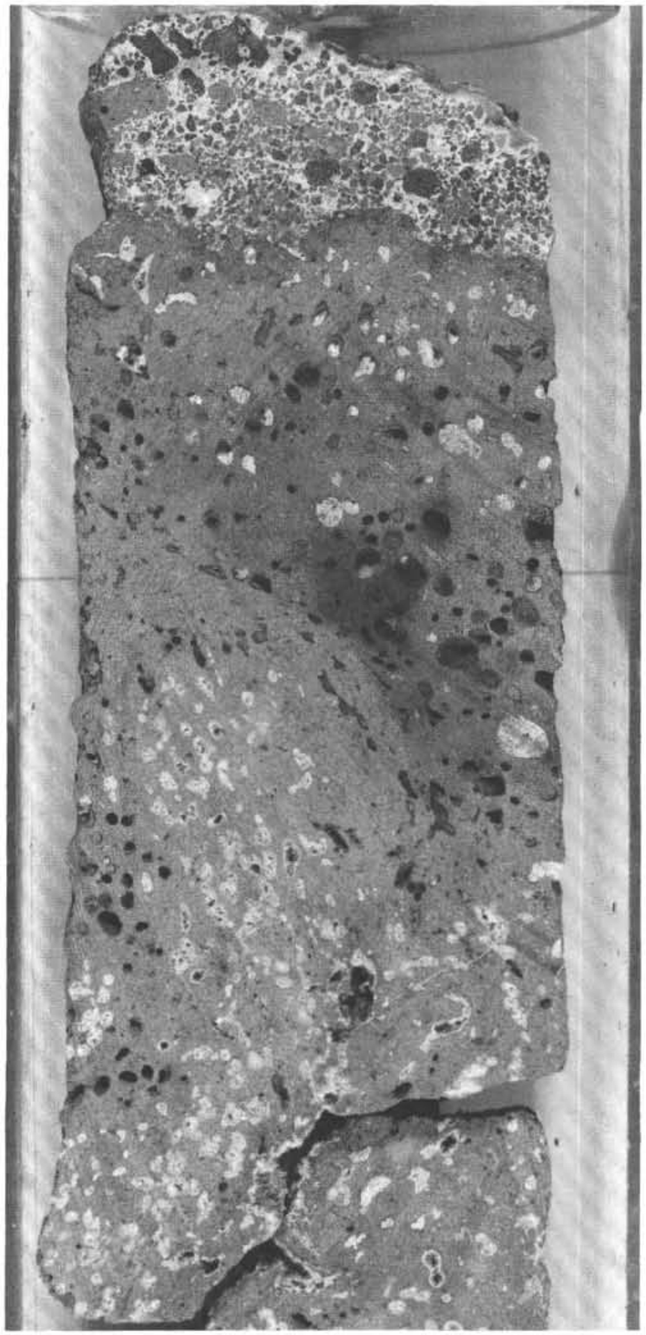

1 cm

Figure 15. Vesicular basalt with upper contact of carbonate sandstone in Unit 5 (115-715A-23R-2, 38–50 cm).

of vesicles is present at the top and bottom of the unit. Larger vesicles (more than 1 mm across) are filled with carbonate minerals.

Unit 18 (0.49 m thick): This unit is distinguished from Unit 17 by its higher vesicularity and the absence of carbonate filling.

Unit 19 (0.66 m thick): A highly vesicular (50% and filled with carbonate minerals), extensively oxidized, olivine plagioclase basalt makes up Unit 19.

Unit 20 (0.64 m thick): This unit is composed of a slightly to moderately altered olivine augite basalt with vesicles forming less than 5%.

Unit 21 (3.86 m thick): The last unit, Unit 21, consists of moderately altered, plagioclase-phyric basalt. Vesicles are typically subellipsoidal, up to 1 cm in diameter, and diminish in abundance downward to form a massive zone 30 cm thick in the middle of the unit. The color change from reddish brown at the unit's boundaries to dark grey in the middle reflects the transition from oxidized flow-top to fresh interior.

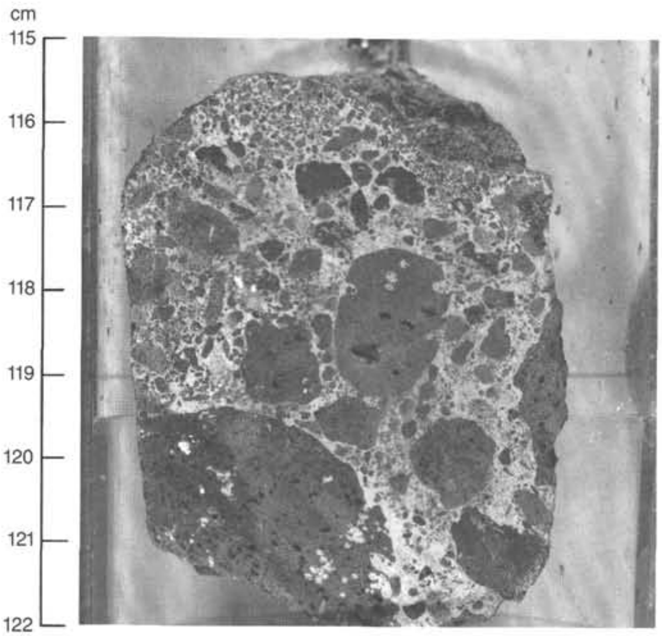

Figure 16. Top of Subunit 7A showing fine-grained vesicular basalt fragments in a carbonate matrix.

Petrography

Site 715 basalts (characteristics summarized in Fig. 13) comprise two distinct petrographic basalt groups which are separated by a limestone bed: an upper group (Units 2, 4, 5, and 7), and a lower group (Units 9 through 21). The upper group consists of plagioclase-bearing ($\sim 1\%$ phenocrysts ≤ 2 mm) basalts, which are aphanitic to fine-grained phaneritic (matrix pyroxene < 0.4 mm) and are massive to highly vesicular ($\leq 20\%$ by volume, ≤ 5 mm across). With the exception of the lower portion of Unit 7, all basalts appear somewhat oxidized with brownish yellow smectite, limonite, and hematite (15%-30%) replacing interstitial glass and filling vesicles. Iddingsite replaces minor olivine ($< 1\%$), and calcite locally fills vesicles. The colorless augite shows little alteration, but plagioclase can be moderately sericitized.

The lower basalt units are characterized by a higher color index; they include olivine-rich phyric to aphyric basalts where the percentage of olivine phenocrysts (0%-15%, ≤ 2 mm in length) tends to be higher toward the top and bottom of each unit. Colorless to pale brown matrix augite is typically ≤ 0.4 mm in size; but in ophitic samples from unit centers, grain sizes ≤ 1.2 mm occur. Plagioclase grains with compositions (determined optically) between An_{65} and An_{80} show minor normal zoning. The flows range from nonvesicular in the center to highly vesicular (50%) near their tops. Calcite and/or clay minerals fill the vesicles. Olivine is usually altered to iddingsite, chlorite, or serpentine, but relict grains were identified in Sample 115-715A-30R-3, 40-41 cm. In the oxidized upper portions of some units, plagioclase appears slightly sericitized, and interstitial glass and olivine are often altered to hematite and yellow brown smectite pigmented by limonite. Although the rocks appear quite fresh, chlorite and serpentine (together as low as 15%) occur as alteration "patches" surrounding altered olivine in the matrix of less oxidized samples.

Magnetic Susceptibility

Volume magnetic susceptibility was measured on 50 minicores that were cut for paleomagnetic study. The results are illustrated and compared with basalts drilled at previous Leg 115 sites in Figure 17. The Site 715 susceptibilities in general are very low (averaging $\sim 8 \times 10^{-5}$ cgs), particularly in Units 9, 10, and 21. Cursory examination of the poorly polished thin sections appeared to show a "normal" average abundance of opaques ($\sim 3\%$), with ilmenite present in at least some samples in addi-

Table 7. XRF major and trace element chemistry of Site 715 basalts.

Core, Section Interval (cm)	23R-3 91-95	23R-3[a] 91-95	24R-2 30-38	25R-3 25-34	25R-6 38-42	29R-1 33-38	29R-1 113-119	29R-2 42-48	30R-1 52-61	30R-3 41-51	30R-6 0-9	31R-2 89-94
wt%:												
SiO_2	46.40	45.61	48.62	48.08	47.93	48.34	49.40	48.55	48.43	47.29	48.19	48.00
TiO_2	2.34	2.31	2.18	0.97	0.98	1.32	2.48	1.31	1.35	1.24	1.16	1.32
Al_2O_3	15.21	14.96	14.18	15.09	14.98	15.49	13.76	15.54	15.30	15.53	15.67	15.51
Fe_2O_3	17.03	16.82	15.84	11.77	11.82	11.96	14.11	12.12	12.36	11.97	11.76	12.13
MnO	0.19	0.19	0.21	0.18	0.18	0.17	0.21	0.17	0.19	0.20	0.16	0.17
MgO	5.59	5.53	6.33	11.82	10.97	10.23	6.16	9.68	10.31	10.43	10.93	10.31
CaO	9.80	9.63	10.28	10.64	11.64	10.66	11.39	10.90	10.71	9.62	10.60	10.11
Na_2O	2.64	2.36	2.24	1.50	1.58	1.87	2.45	1.93	1.81	2.56	1.69	2.01
K_2O	0.75	0.75	0.28	0.18	0.26	0.21	0.49	0.21	0.31	1.58	0.26	0.52
P_2O_5	0.25	0.24	0.23	0.11	0.11	0.14	0.25	0.14	0.13	0.13	0.12	0.14
Total	100.20	98.40	100.39	100.37	100.45	100.39	100.70	100.55	100.90	100.55	100.54	100.22
ppm:												
Nb	16.1		15.5	7.6	8.1	10.1	18.6	9.5	9.4	9.2	8.4	11.1
Zr	138.8		136.2	55.8	54.1	78.3	142.0	77.2	74.1	69.2	65.0	79.3
Y	40.9		43.9	21.4	21.8	24.1	42.6	26.3	24.3	23.3	20.9	23.6
Sr	127.9		122.2	87.4	105.4	136.6	167.0	140.2	134.3	234.1	138.0	148.5
Rb	37.5		2.9	2.1	4.7	1.7	6.1	1.5	3.9	16.7	3.3	8.4
Zr	119.3		119.6	77.0	77.5	79.7	122.4	79.7	78.5	74.4	75.9	80.4
Cu	164.9		154.8	76.3	116.5	93.8	188.2	91.8	92.1	90.0	76.8	88.9
Ni	90.7		70.8	240.3	234.9	186.7	58.2	174.0	167.3	180.1	241.0	225.8
Cr	89.2		75.6	487.8	483.3	366.8	60.5	333.3	309.8	345.1	350.7	386.0
V	460.3		474.0	232.8	222.4	255.5	539.0	243.0	245.9	214.2	216.7	233.3
Ce	17.2		14.4	5.6	6.8	14.0	26.6	14.1	8.9	8.3	12.3	6.0
Ba	129.2		123.4	64.0	70.7	71.7	180.3	76.4	92.0	108.2	59.8	79.4

[a]These values represent duplicate measurements taken on this section interval for major elements only.

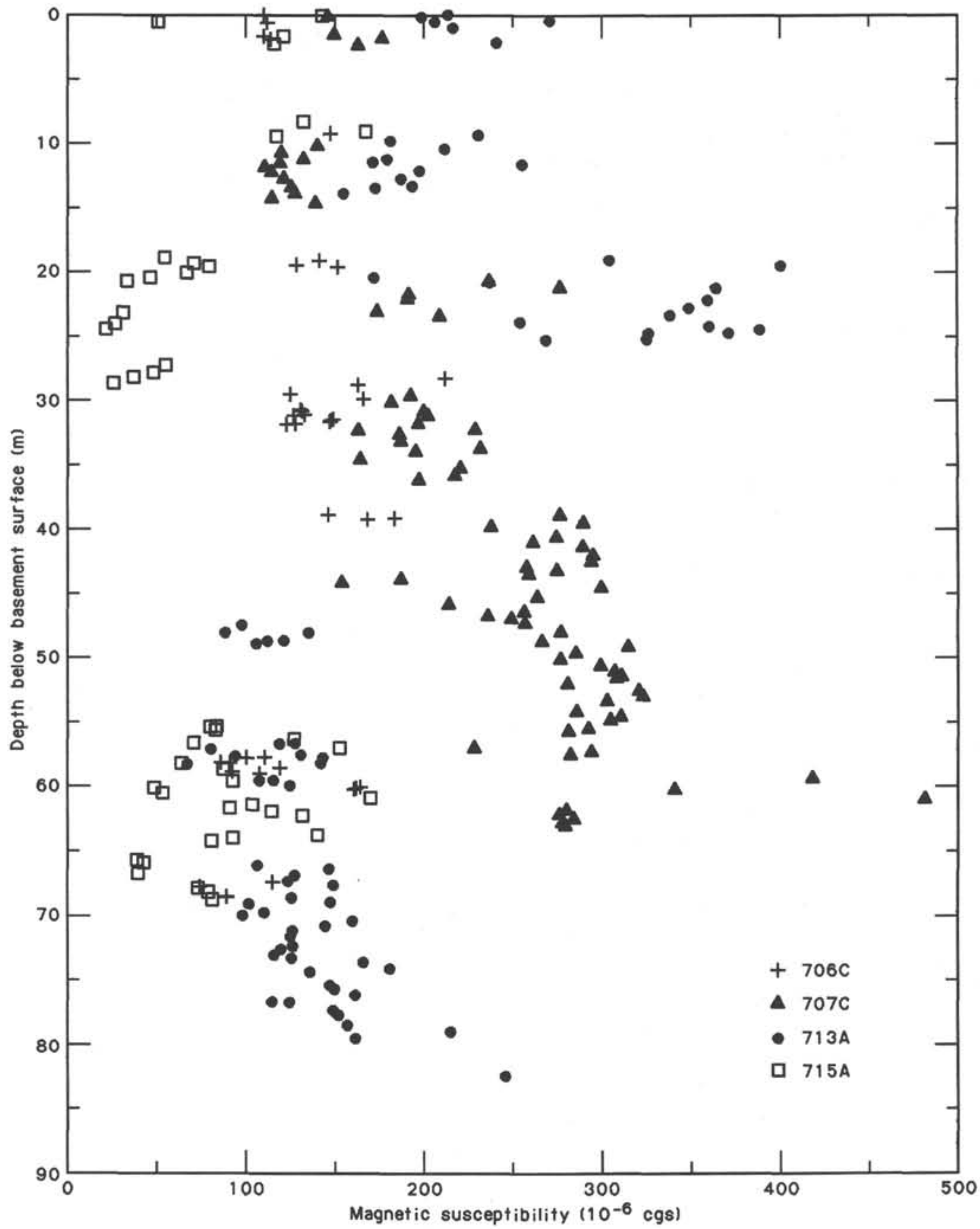

Figure 17. Plot of the magnetic susceptibility of Site 715 basalts in comparison with basalts from Sites 706, 707, and 713. Note the distinctly low susceptibility of Site 715 basalts. Magnetic susceptibility is presented in cgs units of emu/cm^3 /oersted.

tion to the titanomagnetite. The explanation for the anomalously low susceptibility (compare Site 715 with Sites 706, 707, and 713 in Fig. 17) remains to be established. A higher proportion of ilmenite or pervasive low-temperature oxidation are two possible explanations, but we could not determine the reason based on our shipboard examination.

Discussion

The unique feature of Site 715 basalts in comparison with all others encountered on Leg 115 is the conspicuous evidence of reddish brown lateritic(?) alteration. The upper parts of flow units are highly vesicular (as long as 1 cm) and invariably oxidized, with weathering decreasing inward. Even in the central parts of flow units, however, which look completely fresh, deuteric alteration patches spread out from original olivine grains. The immediately overlying and intercalated heterogeneous calcarenitic limestones may well have accumulated as the clinkery, oxidized, and weatherized subaerial lava tops became submerged and reefs began to grow.

Petrographically, these basalts are fine grained and more aphyric than the feldspar-phyric basalts recovered at previous sites. Particularly noteworthy is the relative abundance of olivine (or its alteration products) and the brownish color of the clinopyroxenes in the lower units. The former characteristic indicates that the basalts may be relatively primitive, and the latter suggests that they have alkaline tendencies.

The lower basalts appear more "primitive" petrochemically in that they have a relatively high magnesium-oxide content and magnesium numbers ($Mg/Mg + Fe^{2+}$ around 0.65) (Table 7). These magnesium numbers correspond with those expected of an unfractionated magma that formed in equilibrium with mantle olivine ($\sim Fo_{90}$) (Roedder and Emslie, 1970). In addition, their high nickel content (Table 7) is conspicuous and consistent with an unfractionated mantle-derived melt. The zircon/niobium ratios (~ 7.0) are low and more characteristic of transitional-alkaline, oceanic-island magmas than ocean-ridge basalts. Normatively, they appear transitional between tholeiitic basalts and alkali basalts, plotting close to the low-pressure thermal divide of the basalt tetrahedron.

The basalts fall into two groups based on magnesium oxide, ferric oxide, TiO_2, P_2O_5, zircon, niobium, yttrium, zinc, copper, nickel, chromium, and vanadium. This division is illustrated in Figure 18, which shows the distinction of Units 7 and 13 from the other units based on TiO_2 and MgO contents. The high-titanium basalts are also higher in total iron, phosphorus, niobium, zircon, yttrium, zinc, copper, and vanadium, but are lower in nickel and chromium (Table 7).

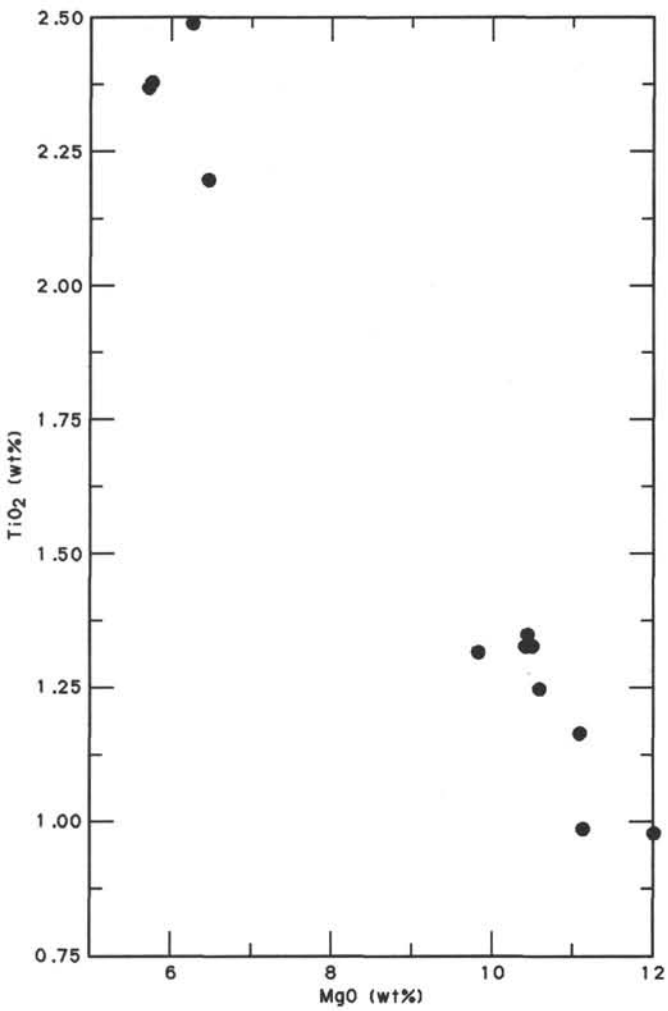

Figure 18. MgO-TiO_2 variation diagram for Site 715 basalts. Units 7 and 13 stand out because of their high TiO_2 and low MgO.

PHYSICAL PROPERTIES

Introduction

Sediments recovered at Site 715 consist of approximately 20 m of soft Pleistocene clay-bearing, foraminifer-bearing nannofossil ooze, which lies unconformably upon stiffer late Miocene nannofossil ooze and nannofossil chalk. We observed drilling disturbance in all Pleistocene and Miocene cores. At 105 mbsf there is a transition to well-lithified shallow-water limestones (see "Lithostratigraphy" section, this chapter). Recovery of the limestones below this level was poor to the top of basement (211.3 mbsf).

The following physical properties were measured on sediment samples: index properties, carbonate content, continuous GRAPE wet-bulk densities and compressional-wave velocities (*P*-wave logger), compressional velocity on discrete samples, shear strength, and thermal conductivity.

Index Properties

The results for the index properties at Site 715 are shown in Figure 19 and Table 8. The calcium carbonate contents of index property samples are shown in Figure 20 and Table 8.

Wet-bulk density gradually increases from 1.45 to 1.66 g/cm^3 from the seafloor to 100 mbsf. The wet-bulk density levels off below 40 mbsf (Fig. 19); there is also an increase in the scatter of measured densities. There are no lithologic boundaries at this depth, but we did observe a slight increase in the stiffness of the sediments. The occurrence of chalk "chunks" between 60 and 90 mbsf, as well as drilling-induced biscuiting of the chalks below 90 mbsf, has little apparent effect on the wet-bulk density. However, resolution is low and measurements were restricted to the more consolidated intervals.

Water content and porosity decrease from the seafloor to 42 mbsf—from 54% to 45% and 76% to 69%, respectively—and then remain constant (within 2%–4%) with depth. The increase of carbonate content with increasing depth (Fig. 20) has little effect upon grain density (Fig. 19). The saw-toothed variation in carbonate content in the top 50 m of sediments, shown in Figure 20, is a result of "aliasing" due to the large intervals between samples.

Compressional-Wave Velocity and Acoustic Impedance

The compressional-wave velocity (V_p) measurements taken in soft sediments at Site 715 are shown in Figures 21 and 22 and in Table 9. The measurements from the continuous *P*-wave logger (Fig. 22) show considerable variability, and they are offset by 50 m/s from the discrete data. The quality of the *P*-wave logger data from this site was greatly affected by the change of tracking systems (see "Physical Properties" section, "Site 714" chapter, this volume) and should be viewed with caution.

The nannofossil ooze in the upper 100 mbsf of Hole 715A was characterized by compressional-wave velocities (V_p) of 1483–1589 m/s, with a gradual increase of V_p downhole (Fig. 21 and Table 9). There was no major difference in the velocities measured at the transition from soft ooze to more plastic ooze, and to chalk at greater depths. The fairly constant compressional-wave velocities, together with a density profile that varies little with depth (see Fig. 21), generate an impedance profile which shows little contrast (Fig. 21). This is in good agreement with the 3.5-kHz record, which showed transparent layering in the near surface.

Shear Strength

The shear strength measurements taken at Site 715 are shown in Table 10 and Figure 23. The results show a fair amount of scatter, especially below 90 mbsf where biscuits of chalk lie within a softer oozelike paste. No data were collected in the soupy oozes in the top 50 m of core, nor in the more lithified sediments below 102 mbsf.

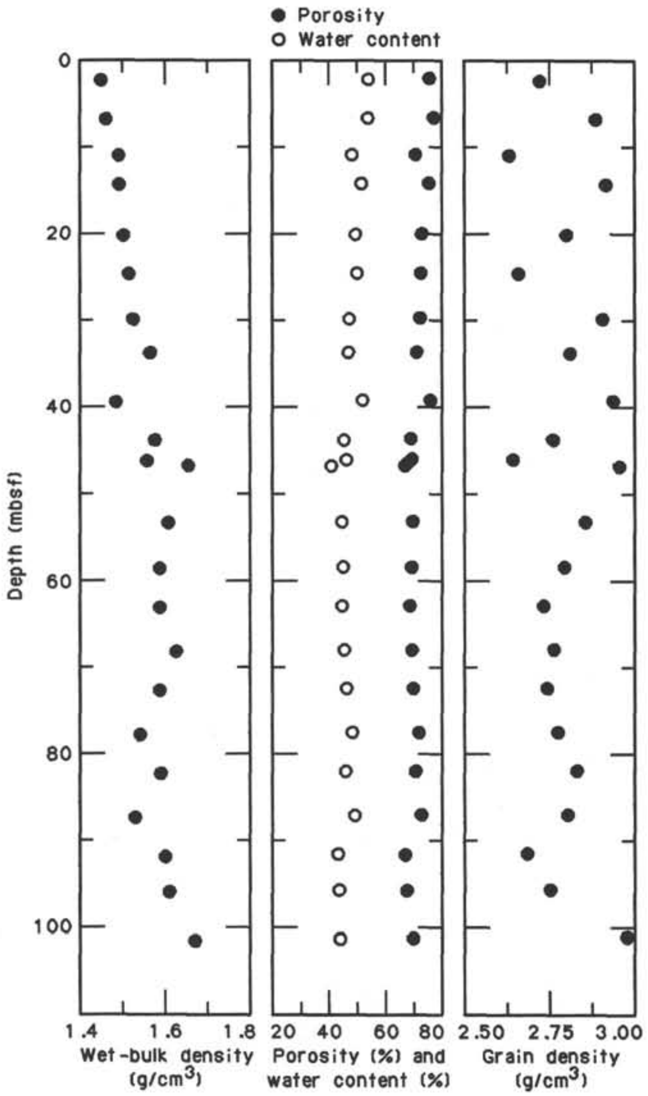

Figure 19. Index properties (wet-bulk density, water content, porosity, and grain density) at Site 715.

Thermal Conductivity

The results for thermal conductivity at Site 715 are shown in Figure 24 and Table 11. The thermal conductivity in the upper few meters of the sediment decreases rapidly from a high value of 1.4 $W \cdot m^{-1} \cdot K^{-1}$ to a value of 0.85 $W \cdot m^{-1} \cdot K^{-1}$; it then increases quickly to about 1.05 $W \cdot m^{-1} \cdot K^{-1}$. The rapid variation in the upper few meters was observed at other sites and is related to both near-surface compositional variation and the initial stages of consolidation. The trend for the next 100 mbsf is similar to that seen at nearby Site 714. A few isolated low values may result from disturbed cores with unusually high water contents.

The lithology changes from sediments to reef carbonates at 105 mbsf, where recovery dropped substantially. Few pieces of the recovered core were large enough to measure the thermal conductivity. The few values obtained were high and variable, due to the range in porosity and cementation observed in these carbonates.

Basement Rocks

The compressional-wave velocity (V_p), wet-bulk density, and acoustic impedance for basement rocks recovered from Site 715 are shown in Figure 25 and Table 12. Results for V_p are scattered in the limestones, ranging between 3350 and 5100 m/s. This variation in V_p was partly due to the physical differences between the limestone facies (see "Lithostratigraphy" section, this chapter), such as variations in porosity and the degree of recrystallization and cementation. The other contribution to the variability was due to such increased uncertainties in measurements (these effects were not quantified) as poor acoustic coupling from transducers, scattering of sound in the coarser samples, unevenness of the sample surfaces, and variations in the saturation of the samples. Some of these experimental uncertainties affected the V_p measurements on the basalts. However, there were also intrinsic differences between the 12 basaltic flow units from which the V_p measurements were obtained. These uncertainties combined with variations in the samples resulted in V_p ranging from 2500 to 6200 m/s. There is considerably less scatter in the V_p measurements on the basalts below 260 mbsf.

The bulk densities of the basalts between 212 and 222 mbsf are fairly scattered, but the next set of measurements between 222 and 242 mbsf are tightly grouped around 2.85 g/cm^3. Bulk density decreases slightly for the lower set of basalts to around 2.8 g/cm^3. The impedance profile is dominated by the scatter in the V_p data as the density is relatively constant. There are no observable contrasts above the scatter in data.

Thermal conductivity measurements in the basalts (Fig. 24) are related to the samples' alteration and vesicularity. The better preserved and less vesicular samples had fairly typical values of 1.66–1.70 $W \cdot m^{-1} \cdot K^{-1}$. The altered and vesicular samples had values as low as 1.4 $W \cdot m^{-1} \cdot K^{-1}$.

Summary

The soft to soupy clay-bearing Pleistocene ooze at Site 715 was characterized by a porosity of around 75% and a compressional-wave velocity (V_p) of 1500 m/s. Porosity, V_p, and impedance remained fairly constant through the more plastic Miocene oozes and chalks. Low shear strengths on the order of 15 kPa were measured in the oozes below 50 m, indicating the effects of disturbance.

The basement limestones showed considerable variation in porosity and recrystallization, although these observations were not quantified. Values for V_p ranged from 3300 to 5100 m/s, due to lithologic variations and increased experimental uncertainties. The V_p measurements ranged between 2500 and 6200 m/s for basalts recovered from 200 to 240 mbsf, and between 4400 and 5700 m/s for basalts cored from below 260 mbsf. The density of the basalts deviated little from 2.85 g/cm^3. The impedance profile within the basement was highly scattered due to the large variability in V_p. Thermal conductivities within the basalts show variations related to the sample alteration and vesicularity.

SEISMIC STRATIGRAPHY

Site 715 is located on the eastern shoulder of the Maldives Ridge, in 2262.3 m water depth (Fig. 26). This elevated plateau extends northward from the Chagos Bank to the Laccadive Islands and is part of the proposed volcanic trace of the Réunion hotspot left on the Indian plate. In this region, the ridge is capped by a 100-km-wide carbonate bank of 1–1.5 km thickness. We selected Site 715 to optimize our chance of penetrating the supposed basaltic basement rocks underlying the carbonates. From previous seismic surveys throughout the region (Fig. 27), it appeared that the basement reflector could be reached by drilling through pelagic and shallow-water carbonate sediments lying on the eastern slope of a narrow ridge connecting with the main platform.

In seismic sections perpendicular to the Maldives Ridge, basement appears as an irregular reflector which is seen only intermittently (Fig. 27). The first effect is due to the volcanic origin of the ridge, and the second is due to the dense, hard limestone

Table 8. Index-properties data and carbonate content measured at Site 715.

Section interval (cm)	Depth (mbsf)	Water content (%)	Porosity (%)	Wet-bulk density (g/cm^3)	Dry-bulk density (g/cm^3)	Grain density (g/cm^3)	Carbonate content (wt%)
115-715A-							
1R-2, 82	2.32	54.41	76.29	1.45	0.66	2.72	62.90
1R-5, 76	6.76	54.47	77.41	1.46	0.66	2.89	64.53
2R-2, 140	11.00	48.59	71.14	1.49	0.77	2.63	58.90
2R-5, 22	14.32	52.17	75.95	1.49	0.71	2.92	60.93
3R-2, 92	20.22	49.78	73.35	1.50	0.75	2.80	77.61
3R-5, 84	24.64	50.25	72.70	1.51	0.75	2.66	63.36
4R-2, 96	29.96	47.66	72.42	1.52	0.80	2.91	72.49
4R-5, 38	33.88	47.24	71.37	1.56	0.82	2.81	80.92
5R-2, 81	39.41	52.33	76.18	1.48	0.70	2.94	64.53
5R-5, 78	43.88	45.68	69.63	1.57	0.85	2.76	76.94
5R-7, 10	46.20	46.40	69.31	1.55	0.83	2.64	83.94
6R-1, 10	46.90	41.16	67.16	1.65	0.97	2.96	73.35
6R-5, 60	53.40	44.86	69.70	1.60	0.88	2.86	67.61
7R-2, 60	58.60	45.13	69.43	1.58	0.87	2.79	74.98
7R-5, 60	63.10	45.00	68.86	1.58	0.87	2.73	89.67
8R-2, 60	68.20	45.52	69.50	1.62	0.88	2.76	91.39
8R-5, 60	72.70	46.25	70.03	1.58	0.85	2.74	81.89
9R-2, 60	77.80	48.37	72.00	1.53	0.79	2.77	87.77
9R-5, 60	82.30	46.15	70.60	1.58	0.85	2.83	88.38
10R-2, 60	87.40	49.12	72.83	1.52	0.77	2.80	87.80
10R-5, 60	91.90	43.35	67.01	1.59	0.90	2.68	89.44
11R-2, 60	96.00	43.71	67.84	1.60	0.90	2.75	89.53
11R-5, 64	101.54	44.04	69.89	1.66	0.93	2.98	88.05

which has formed over the volcanic rocks and now produces extremely efficient seismic reflectors. Just to the east of Site 715 these strong reflectors are offset by about 0.40 s (two-way traveltime). This structure shows up on three east-west seismic profiles crossing this peripheral ridge and is probably fault-related.

The *JOIDES Resolution* single-channel seismic (SCS), watergun reflection profile over Site 715 (Fig. 28) clearly resolves the high impedance contrasts encountered during the drilling. The near-surface sediments appear to be disturbed, probably by downslope transport from the nearby ridge. These are fairly transparent Pleistocene and Miocene nannofossil oozes. At about 0.13 sbsf, a very strong reflector occurs that can be traced throughout the region. This is the top of an Eocene limestone first penetrated at 110 mbsf. *In-situ P*-wave velocities of about 1600 m/s would be appropriate for the overlying nannofossil oozes.

We can see a second strong reflector beneath the limestone to the west of Site 715. The two reflectors merge at the drilling site, however, making it difficult to pick their boundary. By tracing the deeper reflector from the west, we estimate that its top occurs at 0.18 sbsf, or 0.05 s below the top of the limestone. Drilling intersected basaltic basement at about 225 mbsf, so the limestone is 115 m thick at this site. This predicts an *in-situ P*-wave velocity for the limestone of about 4600 m/s, which is within the measured values (see "Physical Properties" section, this chapter).

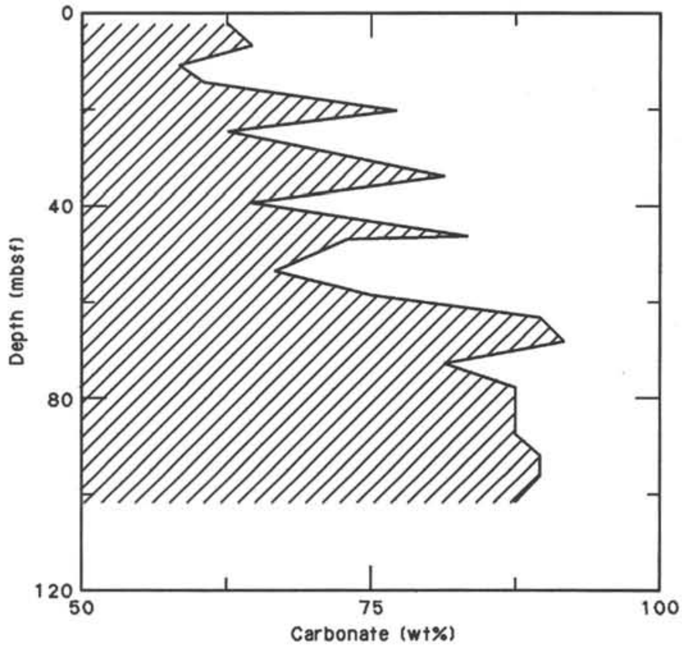

Figure 20. Carbonate content of samples for which the index properties were measured at Site 715.

DOWNHOLE MEASUREMENTS

Introduction

Site 715 was the second site where downhole logging was attempted on Leg 115. The logging program at this site was identical in plan to that of Site 707, with the three standard suites of Schlumberger logging tools. These are the seismic stratigraphy, geochemical, and lithoporosity combinations. All three logging runs were successful at this site.

Logging Results

Logging results are presented in the summary log plot (Fig. 29). All three of the tool strings worked extremely well. The important depths to consider for the logging runs are (1) the bottom of the drill pipe (70 mbsf for the first run and 129 mbsf for the second and third runs), (2) the sediment/reef carbonate boundary at 104 mbsf, and (3) the reef carbonate/basalt boundary at 212 mbsf. The bottom of the hole is at 286 mbsf.

The caliper data show that the hole was beginning to collapse from 90–100 mbsf. This squeezing in of the lowermost unconsolidated sediments of Unit I posed a danger to the subsequent logging runs and forced us to move the end of the pipe lower in the hole. Below that, in the uppermost reef carbonates, the hole rapidly increases in diameter to about 14 in. It then in-

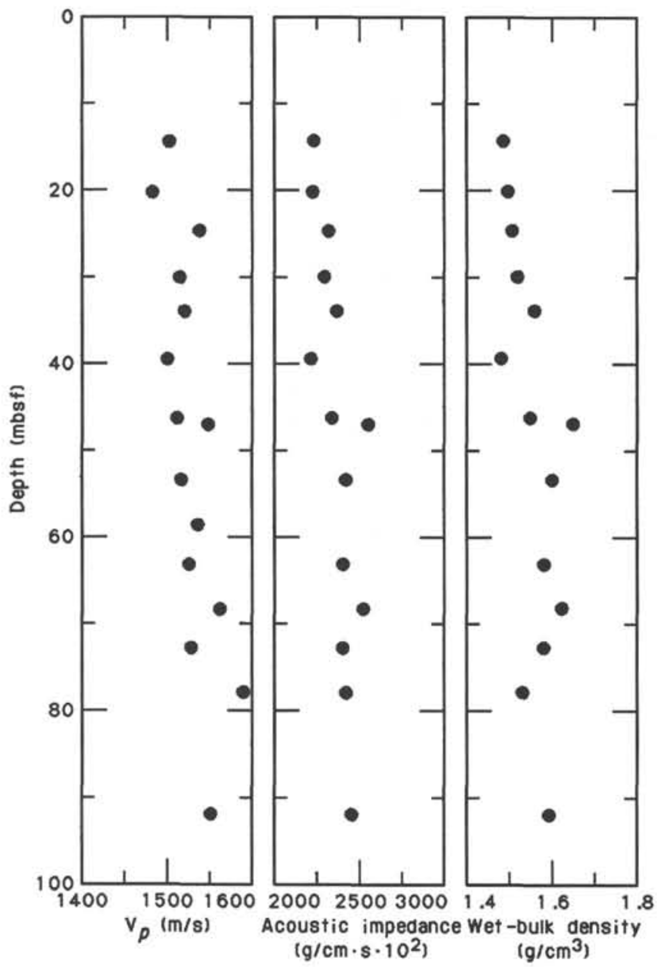

Figure 21. Compressional-wave velocity, acoustic impedance, and wet-bulk density of discrete samples at Site 715.

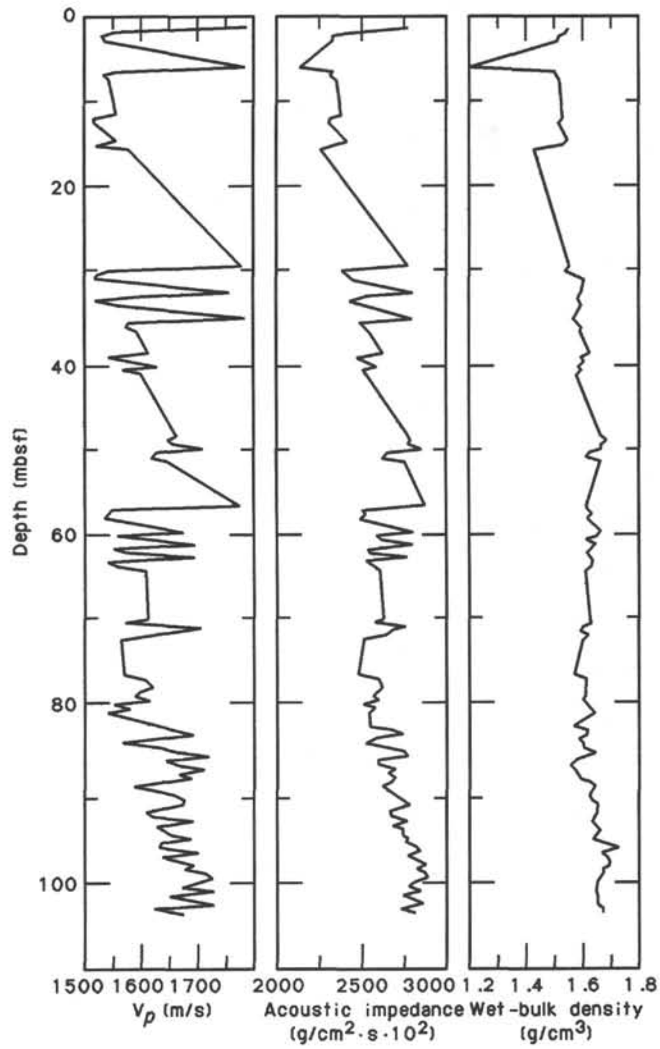

Figure 22. *P*-wave logger compressional-wave velocities, the calculated acoustic impedance profile, and GRAPE wet-bulk densities at Site 715.

creases irregularly with depth until it reaches the maximum the caliper can measure at 140 mbsf. The caliper does not return to scale until about 185 mbsf in the lower reef carbonates. The hole diameter decreases and then increases until basalts are reached at 212 mbsf. The diameter decreases again with depth but is somewhat irregular. The caliper shows a large excursion from 232 to 241 mbsf which may relate to partial bridging or to a piece of debris interfering with the proper operation of the caliper.

The gamma-ray data show an apparent high from 95 to 105 mbsf, but this is due to the small hole size. Below this, in the reef carbonates, the gamma values are about 10 API units with small-scale variability until the basalt is reached; the values then go up and show more variability. This reflects both alteration of the basalts and the presence of interbedded sediments and "soil" horizons.

The resistivity curves track reasonably well in the sediments and reef carbonates. The focused resistivity log, which penetrates the surrounding formation the least, does not track the other two in the basement units. This indicates that the drilling process has disturbed the formation more in this hole than was the case at Hole 707C. The large changes of resistivity in the basement sequence are consistent with the large changes in porosity, seismic velocity, density, and composition observed in this interval.

Table 9. Compressional-wave velocity and acoustic impedance data for soft-sediment section of Site 715.

Section interval (cm)	Depth (mbsf)	V_p (m/s)	Acoustic impedance ($g/cm^2 \cdot s \cdot 10^4$)
115-715A-			
2R-5, 22	14.32	1502	22.37
3R-2, 92	20.22	1483	22.24
3R-5, 84	24.64	1538	23.22
4R-2, 96	29.96	1515	23.02
4R-5, 38	33.88	1521	23.72
5R-2, 81	39.41	1501	22.21
5R-7, 10	46.20	1512	23.43
6R-1, 10	46.90	1550	25.57
6R-5, 60	53.40	1517	24.27
7R-2, 60	58.60	1537	—
7R-5, 60	63.10	1527	24.12
8R-2, 60	68.20	1563	25.32
8R-5, 60	72.70	1529	24.15
9R-2, 60	77.80	1589	24.31
10R-5, 60	91.90	1552	24.67

Table 10. Motorized shear strength data, Site 715.

Section interval (cm)	Depth (mbsf)	Peak (kPa)
115-715A-		
6R-5, 76	53.56	11.6
7R-2, 44	58.44	11.6
7R-5, 68	63.18	11.1
8R-2, 88	68.48	14.5
8R-5, 78	72.88	23.3
9R-2, 87	78.07	13.4
9R-5, 69	82.39	16.3
10R-2, 86	87.66	15.7
10R-5, 52	91.82	3.2
11R-2, 52	96.92	12.2
11R-5, 54	101.44	24.4

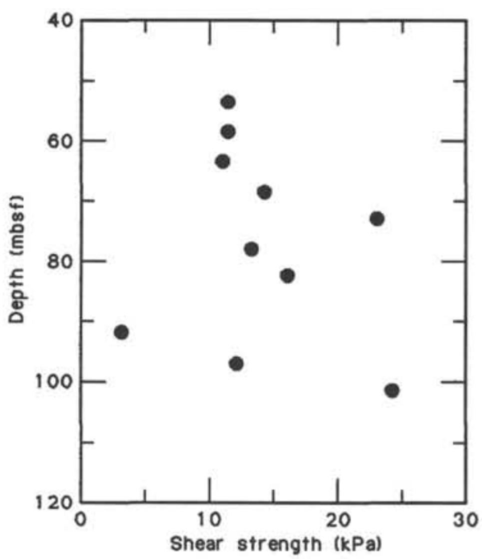

Figure 23. Measured shear strength on discrete samples from Hole 715A.

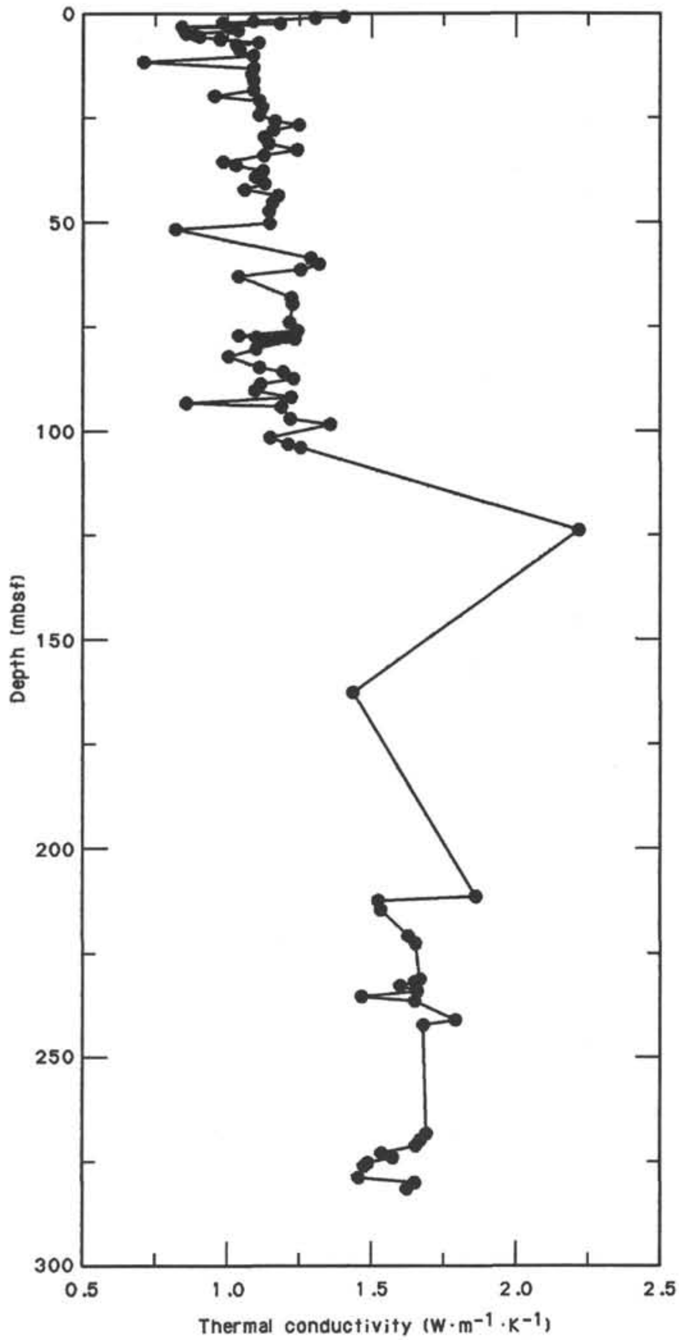

Figure 24. Thermal conductivity at Site 715.

Seismic-wave velocities are low (~1500 m/s) in the uppermost sediments. Velocities are quite variable in the reef carbonates, but they generally range from 3500 to 4000 m/s, which is similar to the few values measured on the recovered samples (see "Physical Properties" section, this chapter). We divided the velocity log within the reef carbonates into three zones with differing characteristics. This is similar to the lithologic division of the reef carbonates into three different environments.

The uppermost section, from 104 mbsf to 132 mbsf, is a sequence where the velocity rapidly alternates between layers below 3 km/s and above 4 km/s. These layers correspond well to layers in the caliper and resistivity logs. The high-velocity layers have higher resistivity and a smaller hole diameter. This is all consistent with alternating hard and soft layers in this upper reef section. Note that some, but not all, of these hard layers show increases in the natural gamma-ray counts. (All of the logs are corrected for variations in hole diameter.)

The next section of the reef, from 132 mbsf to 183 mbsf, shows much less variability in the velocity log, with a small increase in velocity with depth. The resistivity and gamma-ray logs also show reduced variability in this interval, with only one prominent high near 169 mbsf. The caliper log is at or near its maximum extension in this zone.

The lowermost zone of the reef, from 183 mbsf to 212 mbsf, again shows a highly variable velocity. The values change rapidly from somewhat above 3 km/s to over 5.5 km/s. Resistivity is also quite variable in this interval, with the high-velocity layers having high resistivity. There is also a distinct increase in resistivity in the lower 10 m of this zone by almost an order of magnitude. The caliper data show that the hole size is decreasing, but without sharp, distinct layers that were characteristic of the upper part of the reef unit.

The upper part of the basalt shows less variability than the lower part of the reef, with values near 5500 m/s. Variability increases deeper in the basalt; this is correlatable with the large amount of alteration and high variability in vesicularity of the

Table 11. Thermal conductivity data, Site 715.

Section interval (cm)	Depth (mbsf)	Thermal conductivity ($W \cdot m^{-1} \cdot K^{-1}$)
115-715A-		
1R-1, 80	0.80	1.404
1R-1, 120	1.20	1.305
1R-2, 40	1.90	1.090
1R-2, 80	2.30	0.978
1R-2, 120	2.70	1.182
1R-3, 40	3.40	0.841
1R-3, 80	3.80	1.014
1R-3, 120	4.20	1.034
1R-4, 40	4.90	0.856
1R-4, 80	5.30	0.885
1R-4, 120	5.70	0.902
1R-5, 40	6.40	0.974
1R-5, 120	7.20	1.104
1R-6, 25	7.75	1.028
2R-1, 80	8.90	1.040
2R-2, 80	10.40	1.088
2R-3, 80	11.90	0.711
2R-4, 80	13.40	1.087
2R-5, 80	14.90	1.082
2R-6, 81	16.41	1.087
3R-1, 82	18.62	1.089
3R-2, 83	20.13	0.954
3R-3, 80	21.60	1.109
3R-4, 50	22.80	1.121
3R-5, 80	24.60	1.111
3R-6, 80	26.10	1.169
3R-7, 20	27.00	1.251
4R-1, 80	28.30	1.160
4R-2, 80	29.80	1.127
4R-3, 80	31.30	1.147
4R-4, 80	32.80	1.245
4R-5, 80	34.30	1.127
4R-6, 80	35.80	0.985
4R-7, 15	36.65	1.030
5R-1, 80	37.90	1.124
5R-2, 80	39.40	1.099
5R-3, 80	40.90	1.132
5R-4, 80	42.40	1.062
5R-5, 80	43.90	1.179
5R-6, 80	45.40	1.161
6R-1, 80	47.60	1.149
6R-3, 80	50.60	1.146
6R-4, 50	51.80	0.819
7R-2, 80	58.80	1.293
7R-3, 80	60.30	1.323
7R-4, 80	61.80	1.259
7R-5, 80	63.30	1.040
8R-2, 80	68.40	1.226
8R-3, 80	69.90	1.231
8R-6, 80	74.40	1.220
9R-1, 80	76.50	1.249
9R-2, 40	77.60	1.040
9R-2, 50	77.70	1.200
9R-2, 60	77.80	1.169
9R-2, 80	78.00	1.208
9R-2, 90	78.10	1.103
9R-2, 100	78.20	1.179
9R-2, 130	78.50	1.129
9R-2, 140	78.60	1.237
9R-4, 80	81.00	1.101
9R-5, 80	82.50	1.008
9R-7, 25	84.95	1.114
10R-1, 70	86.00	1.197
10R-2, 80	87.60	1.233
10R-3, 80	89.10	1.117
10R-4, 80	90.60	1.096
10R-5, 80	92.10	1.226
10R-6, 80	93.60	0.862
10R-7, 25	94.55	1.192
11R-2, 80	97.20	1.226
11R-3, 80	98.70	1.362
11R-5, 80	101.70	1.155
11R-6, 80	103.20	1.215
11R-7, 20	104.10	1.259

Table 11 (continued).

Section interval (cm)	Depth (mbsf)	Thermal conductivity ($W \cdot m^{-1} \cdot K^{-1}$)
115-715A- (Cont.)		
14R-1, 33–35	124.23	2.220
18R-1, 26–32	162.86	1.440
23R-1, 117–127	211.97	1.870
23R-2, 52–60	212.78	1.530
23R-3, 118–129	214.94	1.540
24R-1, 61–73	221.11	1.640
24R-2, 81–89	222.71	1.660
25R-1, 110–118	231.10	1.680
25R-2, 65–72	231.97	1.660
25R-3, 56–71	232.95	1.610
25R-4, 21–30	234.04	1.670
25R-5, 12–19	235.40	1.470
25R-5, 115–129	236.43	1.660
26R-2, 42–56	241.04	1.800
26R-3, 1–11	242.07	1.690
29R-1, 61–69	268.31	1.700
29R-2, 66–75	269.76	1.680
30R-1, 62–76	271.32	1.660
30R-3, 52–58	273.06	1.540
30R-4, 1–12	273.93	1.580
30R-4, 137–146	275.29	1.490
30R-5, 54–60	275.93	1.480
31R-1, 72–81	278.92	1.460
31R-2, 57–66	280.27	1.660
31R-3, 35–42	281.55	1.630

rocks. For example, the velocity drops as low as 2000–3000 m/s from 260 to 263 mbsf.

The compensated gamma-ray log and the spectral gamma-ray log are used to correlate between different tool runs and to compute abundances of potassium, thorium, and uranium.

The photoelectric effect is a measure of the capture cross-section of the atomic nucleus and thus composition and density.

The neutron porosity log shows that porosity is generally in the 40%–50% range for the reef. The layer of higher resistivity at 169 mbsf corresponds to a decrease in porosity to 40%. The deeper zone in the reef with layers of higher velocity have corresponding decreases in the porosity, as low as 17% at 204 mbsf. The uppermost basalt has a very high porosity, up to almost 60%, corresponding with the large open vesicles on the recovered specimens. The porosity varies considerably in the basalts due to the variations in vesicularity, to alteration, and to compositional differences within the interbedded layers.

The bulk-density log is similar in character to the porosity log. The bulk density in the reef is generally 2.2–2.3 gm/cm^3. The bulk density in the basaltic basement is quite variable. It ranges from a high of 2.93 gm/cm^3 at 222 mbsf to a low of 1.6 gm/cm^3 at 252 mbsf in one of the interbedded zones between the basaltic units.

The thorium log (calculated from the compensated and spectral gamma-ray logs) shows quite low values in the carbonate reef, generally below 1 ppm. Thorium increases in the basalts to about 2 ppm but is quite variable. Several prominent peaks are present in thorium at 239 mbsf, 249 mbsf (6 ppm), 256 mbsf, and 264 mbsf. These generally do not correspond with the interbedded zones but rather appear to be within the basalt flows themselves.

The uranium log has low values, generally below 0.6 ppm, throughout the well. One section of the reef complex, from 182 to 197 mbsf, shows significantly higher uranium concentrations (as much as 1.5 ppm). There is also an increase in uranium concentration to 2 ppm near the bottom of the log, at 269 mbsf. One interesting observation is the differing responses of uranium and thorium at the locations of the thorium spikes. The spike at 239 mbsf has basically no change in the uranium. The

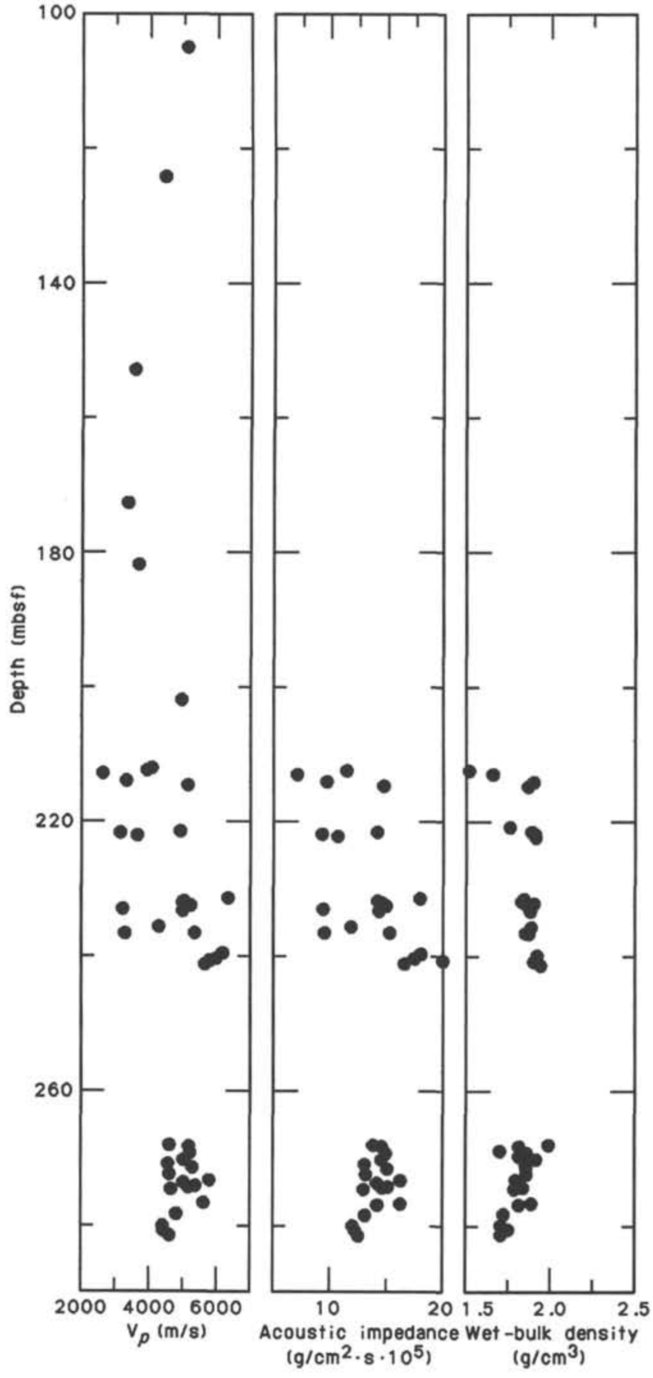

Figure 25. Compressional-wave velocities, acoustic impedance, and wet-bulk densities of discrete samples of limestones and basalts at Site 715.

spikes at 249, 256, and 264 mbsf show decreases in uranium when the thorium increases. The values of uranium concentration at the 249 and 256 mbsf levels drop to essentially zero.

Potassium values in the reef are quite low, about 0.1%, and show no particular systematic variations. The potassium content of the basalts is higher. The upper unit from 211 to 226 mbsf has a fairly uniform potassium content at about 0.3%. The values below that depth are more variable, reflecting the differing compositions of the basalts and the presence of interbedded sediments and weathering zones.

The remaining eight logs represent the processed output of the GST and ACT tools used for geochemical analysis. The GST tool measures the gamma-ray spectra of the formation after irradiating it with neutrons. The elemental data are then *summed* and *normalized*. The results presented for calcium, chlorine, silicon, iron, hydrogen, and sulfur are thus *relative* abundances. They have to be further processed to be turned into weight percent abundances of oxides. These data can be obtained through the drill pipe (except for iron, of course), but the processing must be done more carefully. Because of these complications, we will only briefly discuss these geochemical logs here.

We can briefly describe some broad features from the data. Calcium shows a large change at 104 mbsf at the boundary between the sediments and the carbonate reef. The calcium signal decreases at 211 mbsf where the reef/basalt boundary is located. Calcium increases in the calcarenite interbed at 230 mbsf. Corresponding behavior can be seen in the other components of the log. The calcarenite stands out quite distinctly from the basalt, with an increase in calcium and a decrease in silicon, iron, and aluminum. The interbedded "soil" horizons between some of the basalt flows stand out particularly well in the aluminum data.

Table 12. Compressional-wave velocity, wet-bulk density, and acoustic impedance for limestones and basalts at Site 715.

Lithology	Section interval (cm)	Depth (mbsf)	V_p (m/s)	Wet-bulk density (g/cm^3)	Acoustic impedance ($g/cm^2 \cdot s \cdot 10^4$)
Limestone	12R-1, 44	105.04	5093	—	—
Limestone	14R-1, 40	124.30	4450	—	—
Limestone	17R, CC, 11	153.01	3568	—	—
Limestone	19R, CC, 20	172.82	3374	—	—
Limestone	20R, CC, 15	181.95	3686	—	—
Limestone	22R-1, 90	202.00	4955	—	—
Basalt Unit 3	23R-1, 138	212.18	4089	—	—
Basalt Unit 4	23R-2, 26	212.52	3951	2.53	114.57
Basalt Unit 4	23R-2, 76	213.02	2654	2.66	70.59
Basalt Unit 7	23R-3, 44	214.20	3348	2.90	97.09
Basalt Unit 7	23R-3, 104	214.80	5145	2.87	147.66
Basalt Unit 7	24R-1, 30	220.80	—	2.76	—
Basalt Unit 7	24R-1, 109	221.59	4910	2.89	141.89
Basalt Unit 7	24R-2, 2	221.92	3184	2.91	92.65
Basalt Unit 7	24R-2, 37	222.27	3673	2.91	106.88
Basalt Unit 9	25R-2, 11	231.43	6342	2.84	180.11
Basalt Unit 9	25R-2, 53	231.85	5040	2.83	142.63
Basalt Unit 9	25R-2, 83	232.15	5018	2.90	145.52
Basalt Unit 9	25R-3, 19	232.58	5238	2.86	149.80
Basalt Unit 9	25R-3, 59	232.98	3248	2.88	93.54
Basalt Unit 9	25R-3, 83	233.22	5004	2.87	143.61
Basalt Unit 10	25R-5, 38	235.66	4301	2.88	118.16
Basalt Unit 10	25R-5, 126	236.54	3314	2.85	94.44
Basalt Unit 10	25R-6, 2	236.60	5341	2.87	153.28
Basalt Unit 10	26R-1, 26	239.76	6162	2.92	179.93
Basalt Unit 10	26R-1, 88	240.38	5991	2.92	174.93
Basalt Unit 10	26R-2, 12	240.74	5802	2.90	200.16
Basalt Unit 10	26R-2, 61	241.23	5646	2.94	165.99
Basalt Unit 12	29R-1, 28	267.98	4624	2.99	138.25
Basalt Unit 12	29R-1, 55	268.25	5188	2.81	145.78
Basalt Unit 13	29R-1, 124	268.94	—	2.70	—
Basalt Unit 13	29R-2, 10	269.20	5229	2.85	149.02
Basalt Unit 13	29R-2, 57	269.67	—	2.81	—
Basalt Unit 13	29R-2, 109	270.19	5024	2.91	146.19
Basalt Unit 14	30R-1, 18	270.88	4578	2.85	130.47
Basalt Unit 15	30R-1, 65	271.35	5295	2.85	150.90
Basalt Unit 15	30R-2, 87	272.34	4620	2.85	131.67
Basalt Unit 16	30R-3, 62	273.16	5799	2.79	161.79
Basalt Unit 16	30R-3, 107	273.61	5029	2.82	141.81
Basalt Unit 16	30R-4, 21	274.13	5376	2.81	151.06
Basalt Unit 16	30R-4, 45	274.37	5167	2.83	146.22
Basalt Unit 16	30R-4, 69	274.61	4667	2.78	129.74
Basalt Unit 20	30R-5, 130	276.69	5634	2.88	162.25
Basalt Unit 20	30R-6, 16	276.90	5045	2.81	141.76
Basalt Unit 21	31R-1, 15	278.35	4820	2.72	131.10
Basalt Unit 21	31R-2, 36	280.06	4430	2.70	119.61
Basalt Unit 21	31R-2, 81	280.51	4443	2.74	121.73
Basalt Unit 21	31R-3, 14	281.34	4613	2.70	124.55

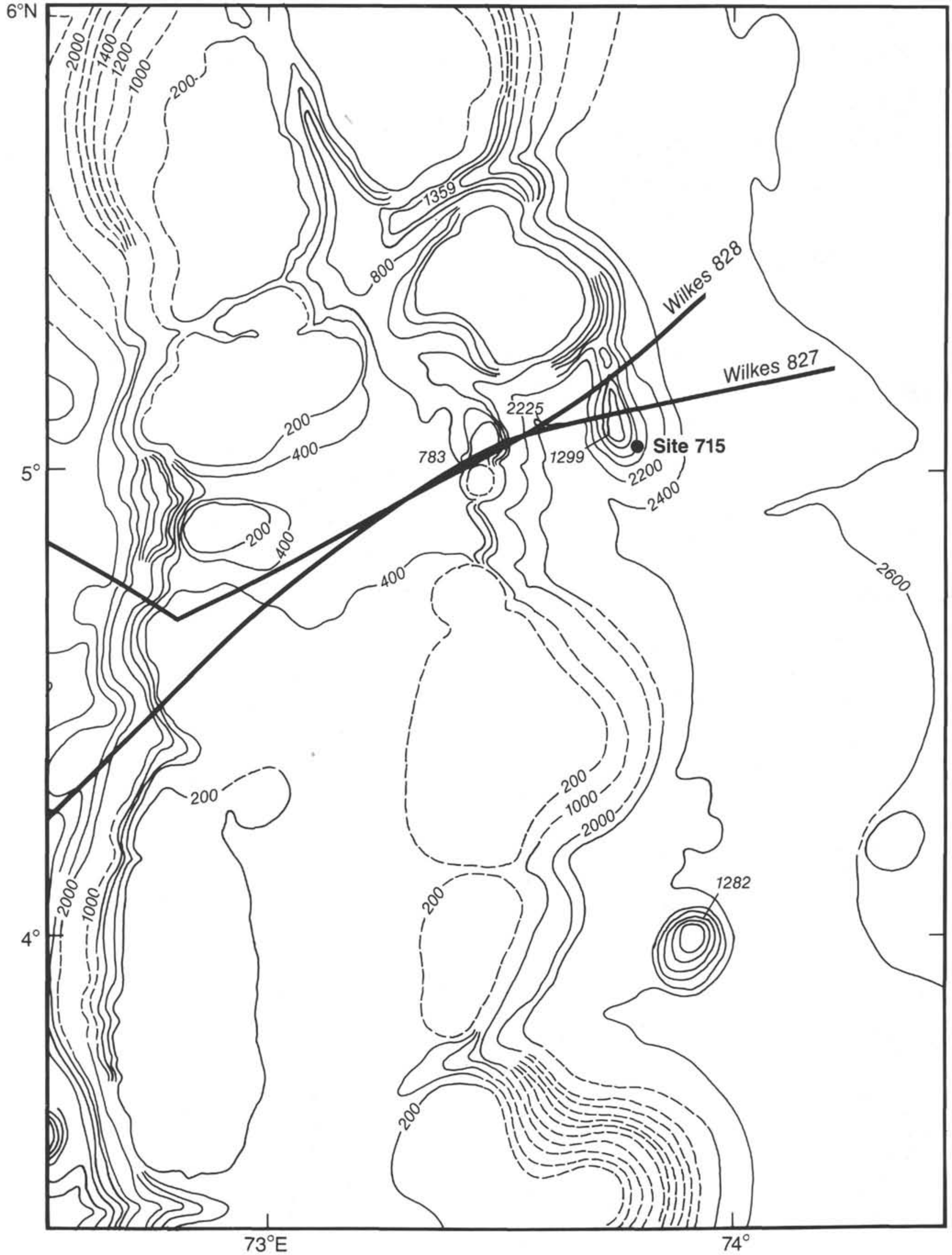

Figure 26. Bathymetry (in meters) in the region of Site 715, eastern margin of the Maldives Ridge (after unpublished data from NAVOCEANO, U.S. Navy surveys).

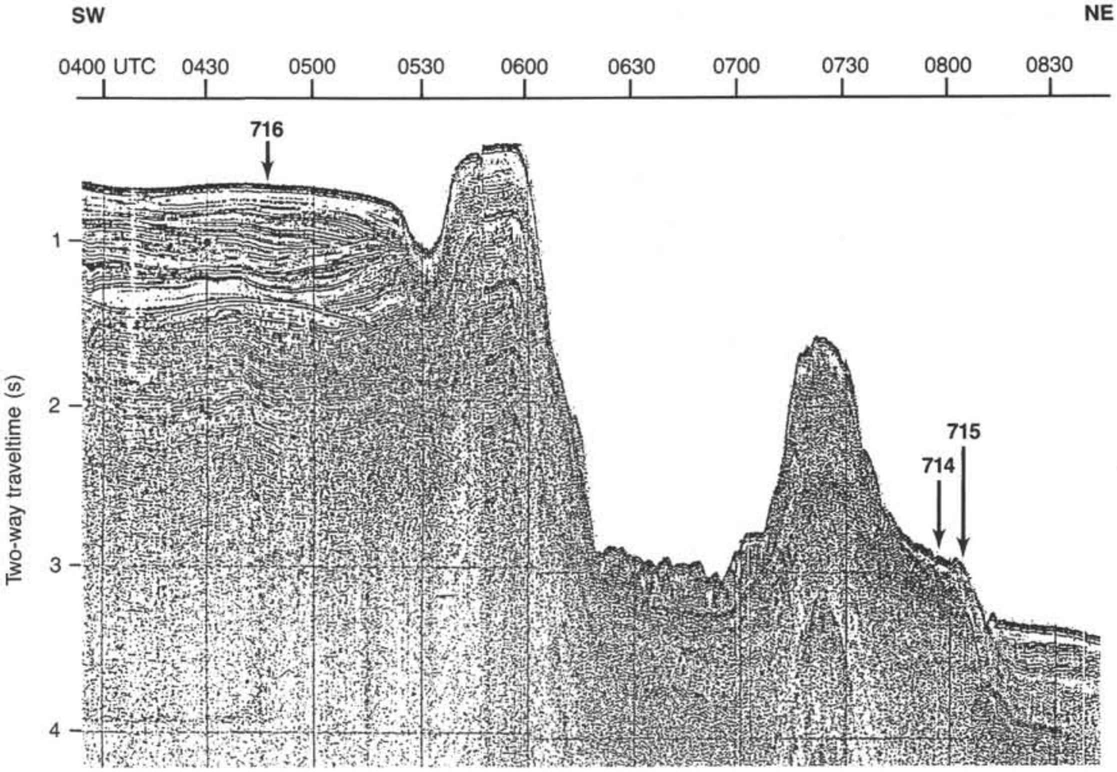

Figure 27. Wilkes 828 (17 September 1976) single-channel seismic (SCS), water-gun reflection line near Site 715. A narrow ridge peripheral to the main volcanic edifice affords the most accessible basement drilling target. Depth in meters.

The geochemical data presented in the summary log plots will be combined with the available analyses of the recovered core samples to calibrate the geochemical data to absolute abundance levels. These data will then be combined with mineralogic and petrologic data to produce lithologic interpretations.

Figure 30 presents the results of the first pass at processing the geochemical data. Some minor element concentrations are presented on the left part of Figure 31. We have not yet performed a careful cross-calibration of these data against the core analyses. Only the data outside the drill pipe are presented here. The shorter dotted and dashed lines on this figure represent the observed abundances in weight percent of TiO_2, MgO, $CaCO_3$, S, K_2O, SiO_2, Fe_2O_3, and Al_2O_3. The MgO values are most subject to error, and they are the most "processed" data; that is, the data determined as a result of differencing other observed signals.

The carbonate reef section is, of course, dominated by $CaCO_3$. The $CaCO_3$ amounts to 80%–90% by weight, though it drops below 80% in areas near the middle of the reef section. At the top of the reef, SiO_2 is low (about 5%), except for occasional layers up to 10% or 20%. Silica increases significantly in the middle of the reef but decreases again near the bottom. About 2% of the reef is Fe_2O_3, with concentrations very low near the top and increasing downward. There is a highly variable abundance pattern to MgO, with layers of about 8% in the upper part of the reef that decrease in frequency downward. From the middle of the reef to near the bottom, MgO abundance is very low, although it does increase just above the basalt. An irregular pattern, averaging about 0.5%, is evident for TiO_2, and K_2O is very low throughout the reef (at 0.1%–0.2%). Also present in low amounts is Al_2O_3, about 1%, but it shows little variability. Sulfur is highly variable in the reef, ranging from near 0% to 6% in some layers. The highest layers of concentration are near the middle of the reef. Gadolinium is present in small amounts (up to 2 ppm) in the middle of the reef; otherwise, it is below detection limits. Thorium is also present in small amounts (about 0.8 ppm) and has a variable distribution. Uranium averages about 0.5 ppm, but in the middle of the reef there is a concentration of uranium up to 1.5 ppm.

The abundances in the calcarenite interbed below the high iron-titanium basalt are similar to the abundances in the reef.

The abundance patterns in the basement sequence are, of course, much different. They are influenced by basalts of differing compositions, by alteration, and by interbedded layers of weathering products. The uppermost portion of the basement has a thick layer of basalt with a distinctive chemistry. It is characterized by high TiO_2 (about 2%), high Fe_2O_3 (about 14%–16%), and slightly lower SiO_2 (about 50%) than the deeper basalts. The gadolinium concentration of 6–8 ppm for the upper unit is also higher than the deeper units.

Abundances in the lower units are more variable. Averages for TiO_2 are about 1%, and for K_2O, at about 0.5% with occasional concentrations up to 1%. The level of MgO is generally about 8% and is somewhat variable. On the other hand, SiO_2 is higher in the deeper units (52%–56%) and is more variable, becoming as much as 60% in one unit near the bottom of the logged interval. Concentrations of $CaCO_3$ are variable at about 10%; and Fe_2O_3 is variable but is lower in the deeper units (about 10%–12%) than in the upper units (14%–16%). Sulfur concentrations are still variable, only ranging up to 1%. Concentrations of Al_2O_3 are higher and show evidence of being fairly coherent from unit to unit. The upper basalt has about 15% Al_2O_3, and this is similar to most of the others. One unit that has high SiO_2 (about 60%) has lower Al_2O_3, about 12%–13%. Gadolinium is variable in the lower units, averaging 4 ppm. Thorium is higher than in the reef. It is most prominent in several layers (discussed above) where it ranges up to 6 ppm. Uranium is comparable to its abundance in the reef, near 1

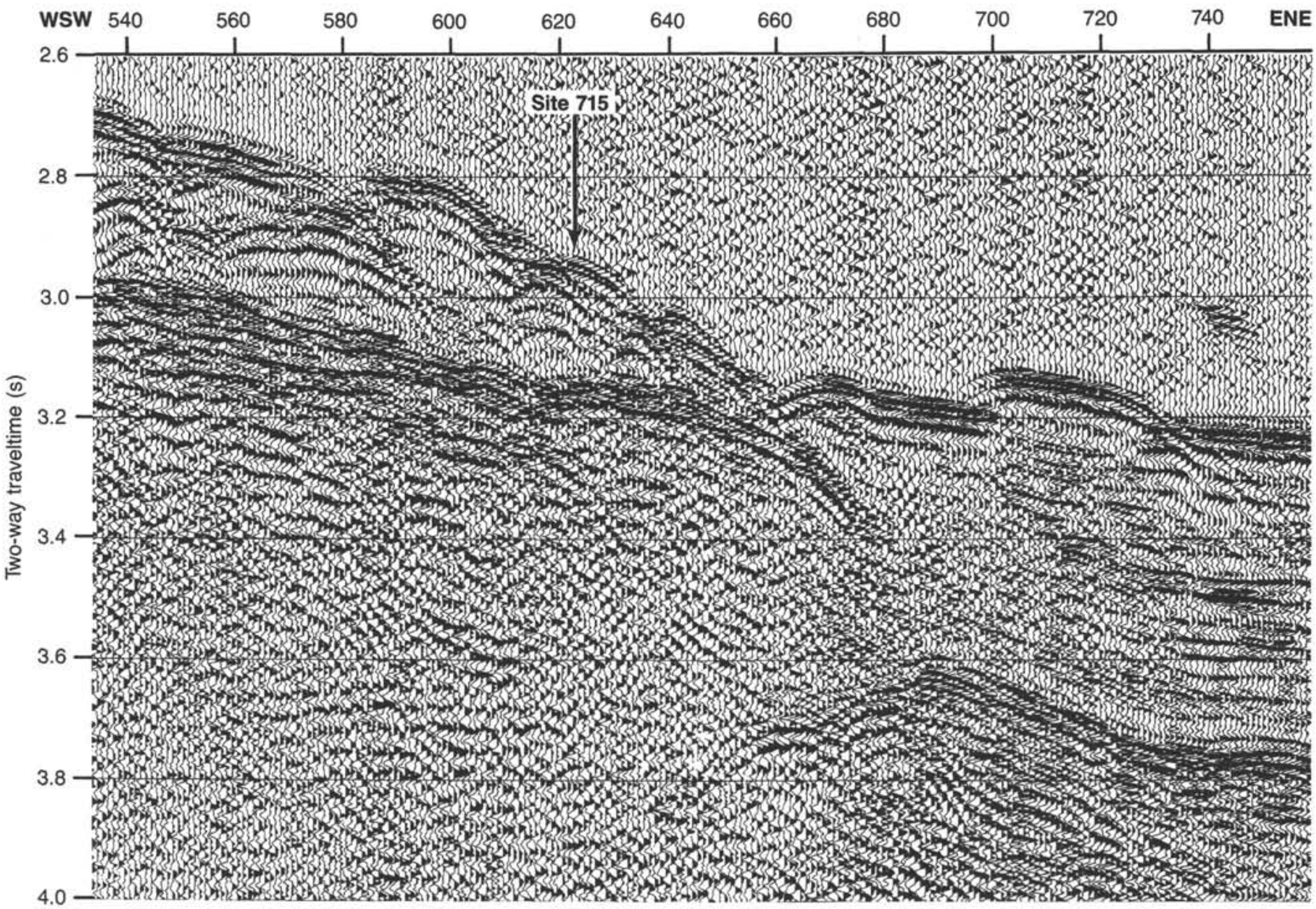

Figure 28. The *JOIDES Resolution* single-channel seismic (SCS), water-gun reflection profile over Site 715. Strong reflectors occur at 0.13 and 0.18 s (two-way traveltime) sub-seafloor and are correlated with the top of limestone and basaltic basement, respectively.

ppm, but shows an increase toward the bottom of the logged interval.

The interbedded weathering zones or "soil" horizons have distinctively higher Al_2O_3 (up to 36%) and lower Fe_2O_3 (down to 6%).

A preliminary attempt to incorporate the chemical results into a lithologic model is presented in the right-hand half of Figure 31. One model matrix was used for both the reef and the basement. The components for the model are quartz, calcite, anhydrite, dolomite, two different basalt compositions, and pyrite. The chemical compositions of these components are given in Table 13. The model that is calculated is then inverted and plotted as the solid and longitudinal lines on Figure 30. This permits us to examine where the model poorly fits the observations and thus requires revision.

Several trends become apparent upon examination of these results. For example, in the reef the abundance of pyrite decreases upward. "Anhydrite" is required in the upper sections to account for the remaining sulfur after the model has used up all the iron. (Note: It has been suggested that celestite, a strontium sulfate, would be more appropriate here.)

The calcite-bearing calcarenite below the "Basalt 1" unit stands out clearly. "Basalt 1" and "Basalt 2" differ primarily in TiO_2 and Fe_2O_3, with "Basalt 1" having higher concentrations. Examination of the core sample chemical analyses shows that we need to increase the SiO_2 concentration in the "Basalt 2" component. Comparison of the back-calculated chemistry on Figure 30 also will cause us to use a higher Al_2O_3 and lower SiO_2 clay component.

We have planned more analyses of the logging data and will report our results in the *Scientific Results* volume of the *Proceedings*. The absolute chemical abundances will be corrected, and the lithologic components will be revised. Normative mineralogies will also be calculated as a function of depth.

REFERENCES

Berggren, W. A., Kent, D. V., and Van Couvering, J. A., 1985. Neogene geochronology and chronostratigraphy. *In* Snelling, N. J. (Ed.), *The Chronology of the Geological Record*. London Geol. Soc. Mem., 10:211–260.

Courtillot, V., Besse, J., Vandamme, D., Montigny, R., Jaeger, J.-J., and Cappetta, H., 1986. Deccan flood basalts at the Cretaceous-Tertiary boundary? *Earth Planet. Sci. Lett.*, 80:361–374.

Crough, S. T., 1978. Thermal origin of mid-plate hotspot swells. *Geophys. J. R. Astron. Soc.*, 55:451–469.

Duncan, R. A., 1978. Geochronology of basalts from the Ninetyeast Ridge and continental dispersion in the eastern Indian Ocean. *J. Volcanol. Geotherm. Res.*, 4:283–305.

________, 1981. Hotspots in the southern oceans—an absolute frame of reference for motion of the Gondwana continents. *Tectonophysics*, 74:29–42.

Emerick, C. M., 1985. Age-progressive volcanism in the Comores Archipelago and northern Madagascar [Ph.D. dissert.]. Oregon State Univ., Corvallis.

Gordon, R. G., and Cape, C., 1981. Cenozoic latitudinal shift of the Hawaiian hotspot and its implication for true polar wander. *Earth Planet. Sci. Lett.*, 55:37–47.

Hottinger, L., 1960. Recherches sur les alvéolines du Paléocene et de l'Eocene. *Schweiz. Palaeontol. Abh.* (Mem. Soc. Pal. Suisse), 75/76:1–243.

McDougall, I., 1971. The geochronology and evolution of the young island of Réunion, Indian Ocean. *Geochim. Cosmochim. Acta*, 35: 261–270.

McKenzie, D. P., and Sclater, J. G., 1971. The evolution of the Indian Ocean since the Late Cretaceous. *Geophys. J. R. Astron. Soc.*, 25: 437–528.

Morgan, W. J., 1981. Hotspot tracks and the opening of the Atlantic and Indian Oceans. *In* Emiliani, C. (Ed.), *The Sea* (Vol. 7): New York (Wiley), 443–487.

Roedder, P. R., and Emslie, R. E., 1970. Olivine-melt equilibria. *Contrib. Mineral. Petrol.*, 29:275–289.

Sclater, J. G., Abbott, D., and Thiede, J., 1977. Paleobathymetry and sediments of the Indian Ocean. *In* Heirtzler, J., et al. (Eds.), *Indian Ocean Geology and Biostratigraphy*: Washington (American Geophysical Union), 25–59.

Ms 115A-113

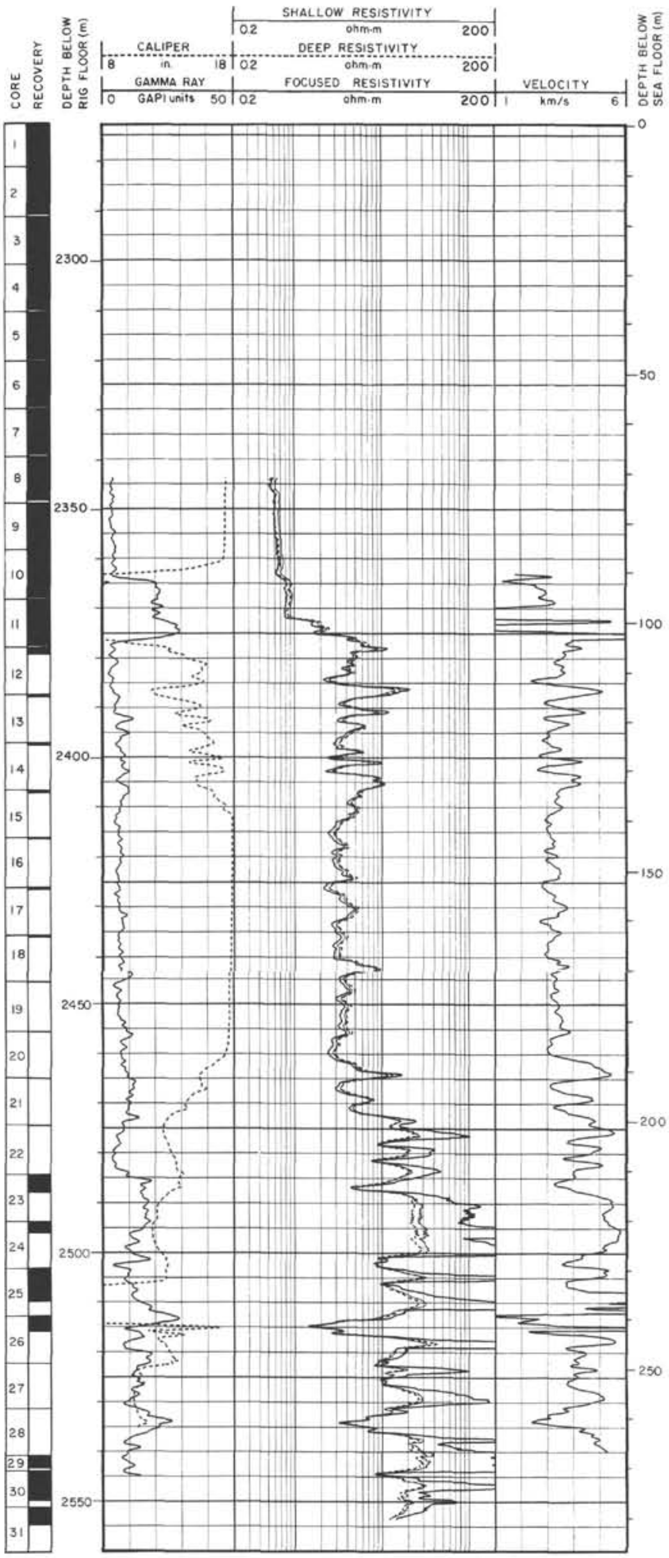

Figure 29. Summary log plot for Hole 715A. Units and scales as given on the figure.

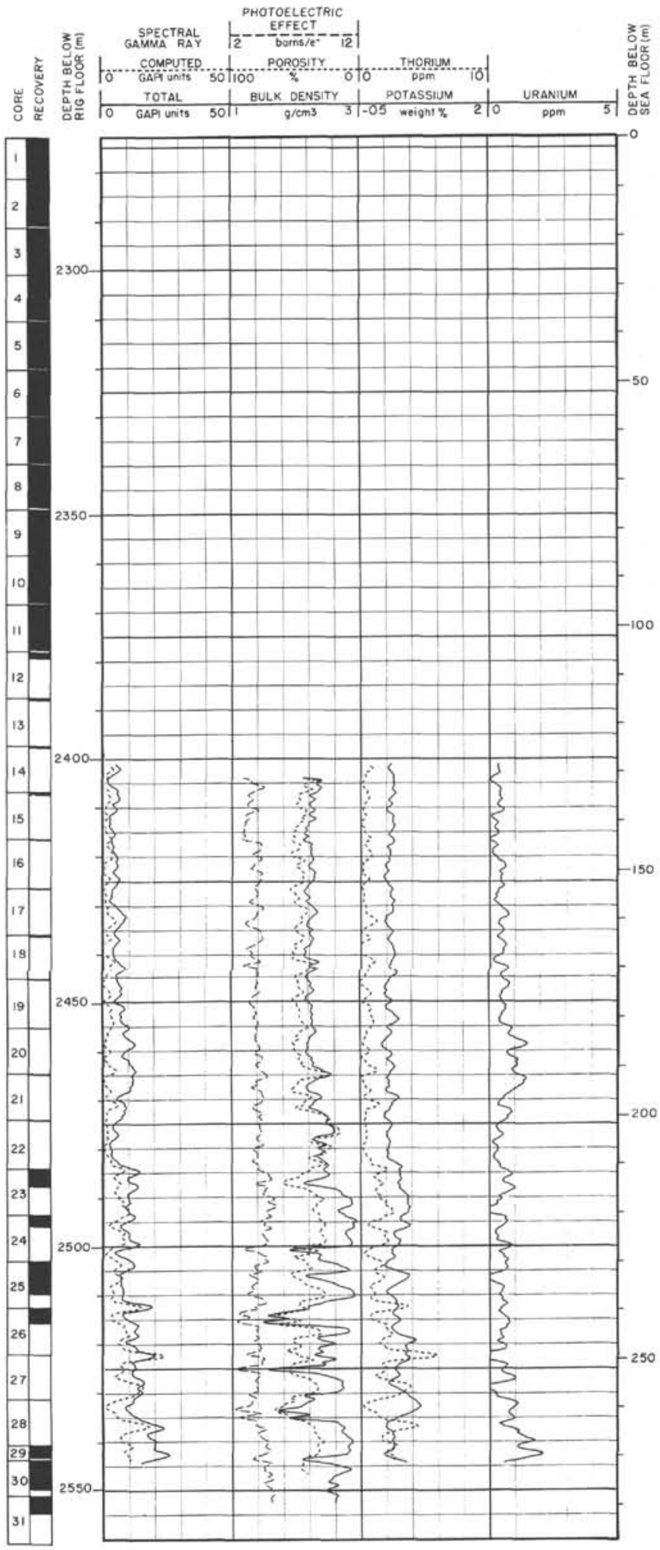

Figure 29 (continued).

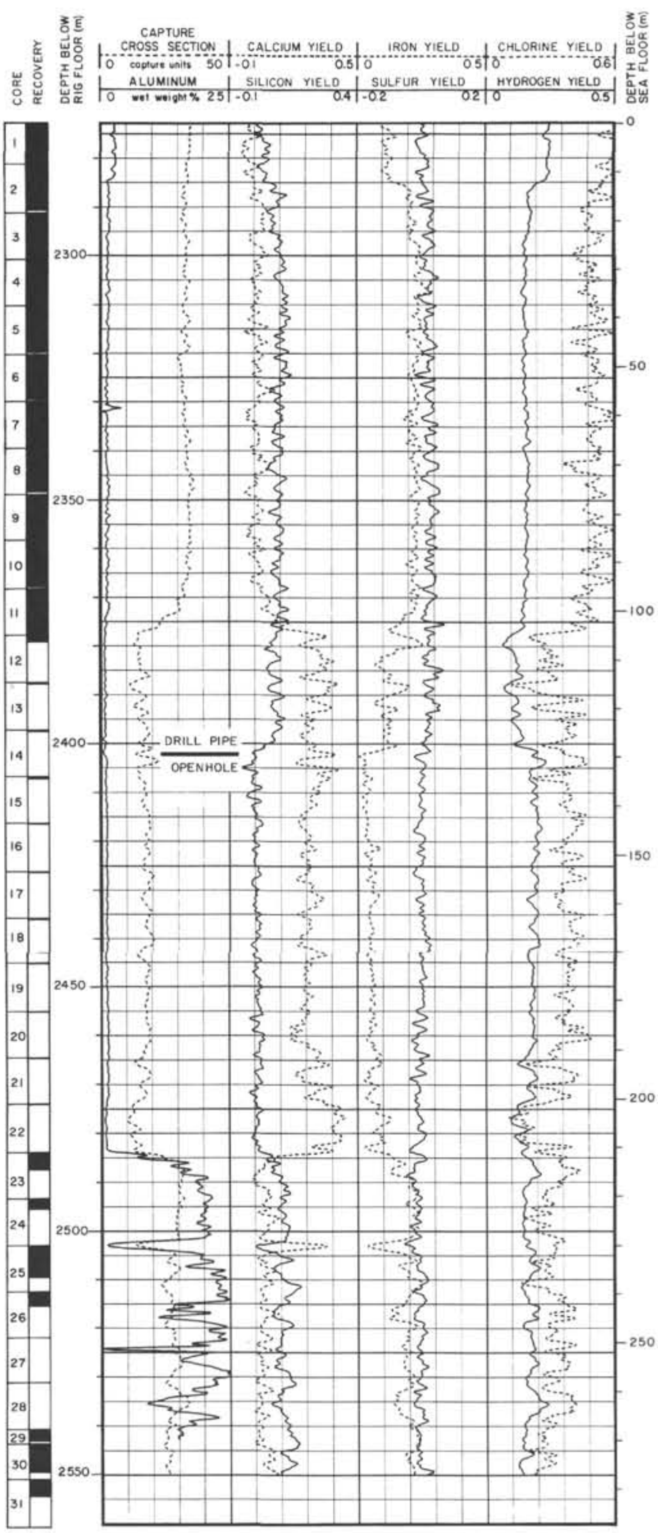

Figure 29 (continued).

Table 13. Component compositions used for preliminary lithologic model applied to logging data.

	TiO_2	K_2O	MgO	SiO_2	$CaCO_3$	Fe_2O_3	Sulfur	Al_2O_3
Quartz	—	—	—	100.0	—	—	—	—
Calcite	—	—	—	—	100.0	—	—	—
Dolomite	—	—	10.0	—	—	—	—	—
Anhydrite	—	—	—	—	30.0	—	23.0	—
Pyrite	—	—	—	—	—	63.0	37.0	—
Smectite	0.50	0.50	23.0	60.0	2.0	14.0	—	6.0
Basalt 1	2.0	0.40	8.0	50.0	12.0	14.0	—	15.0
Basalt 2	0.50	0.40	10.0	50.0	18.0	11.0	—	17.0

Note: All values are in dry weight percent.

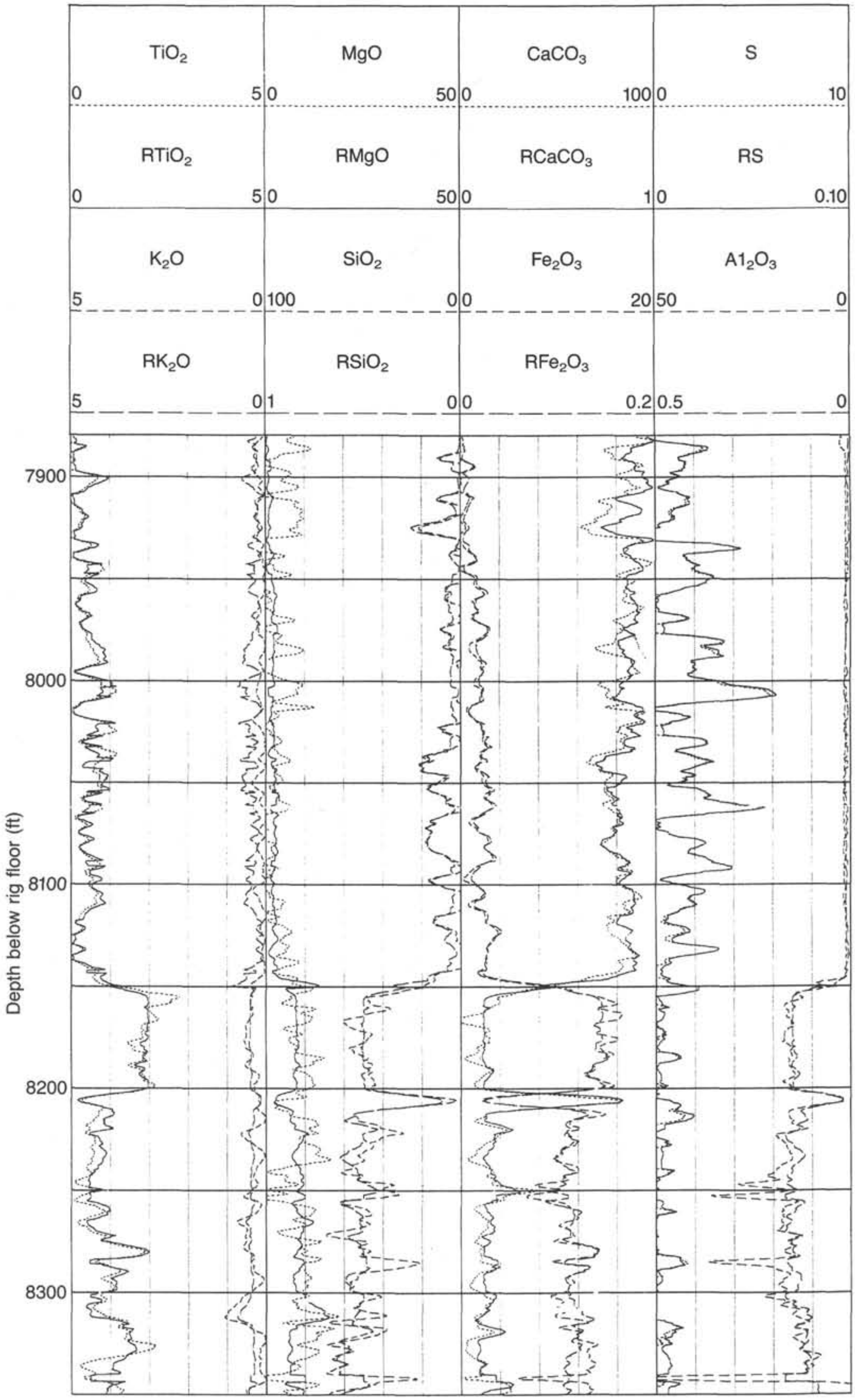

Figure 30. Oxides (in dry weight percent) for various elements. Short dashed lines represent observations. Solid and long dashed lines indicate recalculations (R) backward from fitted lithologies (see Fig. 31).

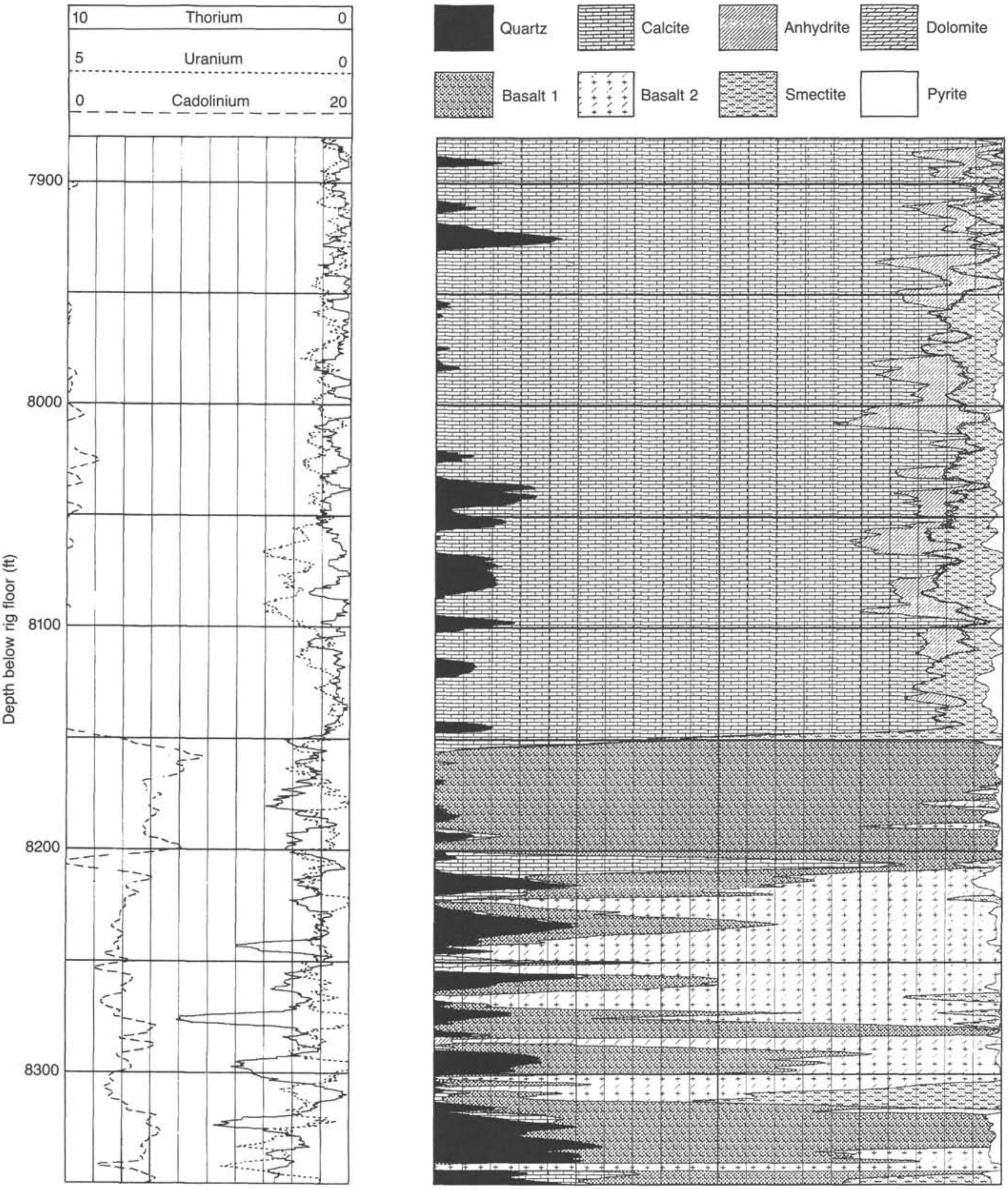

Figure 31. Trace element concentrations in ppm to the left. A preliminary lithologic log on the right. See Table 14 for composition of components in lithologic fit.

SITE 715 HOLE A CORE 1R CORED INTERVAL 2262.3-2270.4 mbsl; 0.0-8.1 mbsf

TIME-ROCK UNIT	BIOSTRAT. ZONE/ FOSSIL CHARACTER: FORAMINIFERS	NANNOFOSSILS	RADIOLARIANS	DIATOMS	PALEOMAGNETICS	PHYS. PROPERTIES	CHEMISTRY	SECTION	METERS	GRAPHIC LITHOLOGY	DRILLING DISTURB.	SED. STRUCTURES	SAMPLES
UPPER PLEISTOCENE	N 23-N 22	CN 15 (NN 21)	PLEISTOCENE	Barren				1	0.5, 1.0				
								2					
								3					*
								4					
								5					
								6					
	AG	AG	AG					CC					

LITHOLOGIC DESCRIPTION

CLAY-BEARING FORAMINIFER-BEARING NANNOFOSSIL OOZE

Major lithology: Clay-bearing, foraminifer-bearing nannofossil ooze, greenish gray (5GY 5/1), dark greenish gray (5GY 4/1), and brown (10YR 5/3), no distinct color changes. Soft, quite homogeneous, disturbed by drilling.

SMEAR SLIDE SUMMARY (%):

	3, 80
	D
TEXTURE:	
Sand	15
Silt	30
Clay	55
COMPOSITION:	
Clay	20
Foraminifers	20
Nannofossils	51
Radiolarians	5
Sponge spicules	2
Fish remains	2

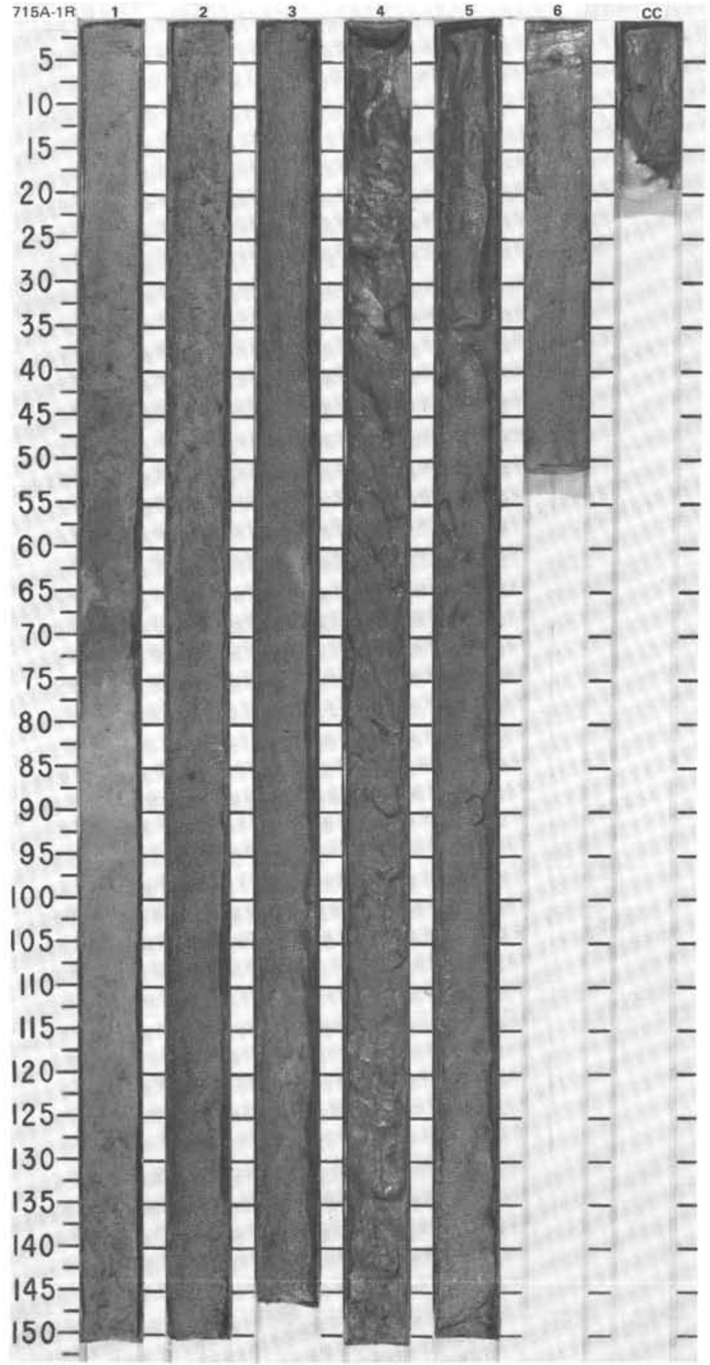

SITE 715 HOLE A CORE 2R CORED INTERVAL 2270.4-2280.1 mbsl; 8.1-17.8 mbsf

TIME-ROCK UNIT	FORAMINIFERS	NANNOFOSSILS	RADIOLARIANS	DIATOMS	PALEOMAGNETICS	PHYS. PROPERTIES	CHEMISTRY	SECTION	METERS	GRAPHIC LITHOLOGY	DRILLING DISTURB.	SED. STRUCTURES	SAMPLES
UPPER PLEISTOCENE	N 23-N 22	CN 15 (NN 21)		Barren				1, 2, 3, 4, 5, 6, 7, CC	0.5, 1.0				* *
	AG	AG CN 14b											

LITHOLOGIC DESCRIPTION

CLAY-BEARING NANNOFOSSIL OOZE

Major lithology: Clay-bearing nannofossil ooze, greenish gray (5GY 5/1, 6/1), gray (5Y 5/1, 6/1), dark greenish gray (5GY 4/1), and light gray (5Y 7/1), subtle gradational color changes.

SMEAR SLIDE SUMMARY (%):

	1, 68 D	5, 67 D
TEXTURE:		
Sand	5	3
Silt	30	40
Clay	65	57
COMPOSITION:		
Clay	20	18
Volcanic glass	1	—
Accessory minerals	—	1
Foraminifers	5	5
Nannofossils	72	74
Radiolarians	1	1
Sponge spicules	1	1

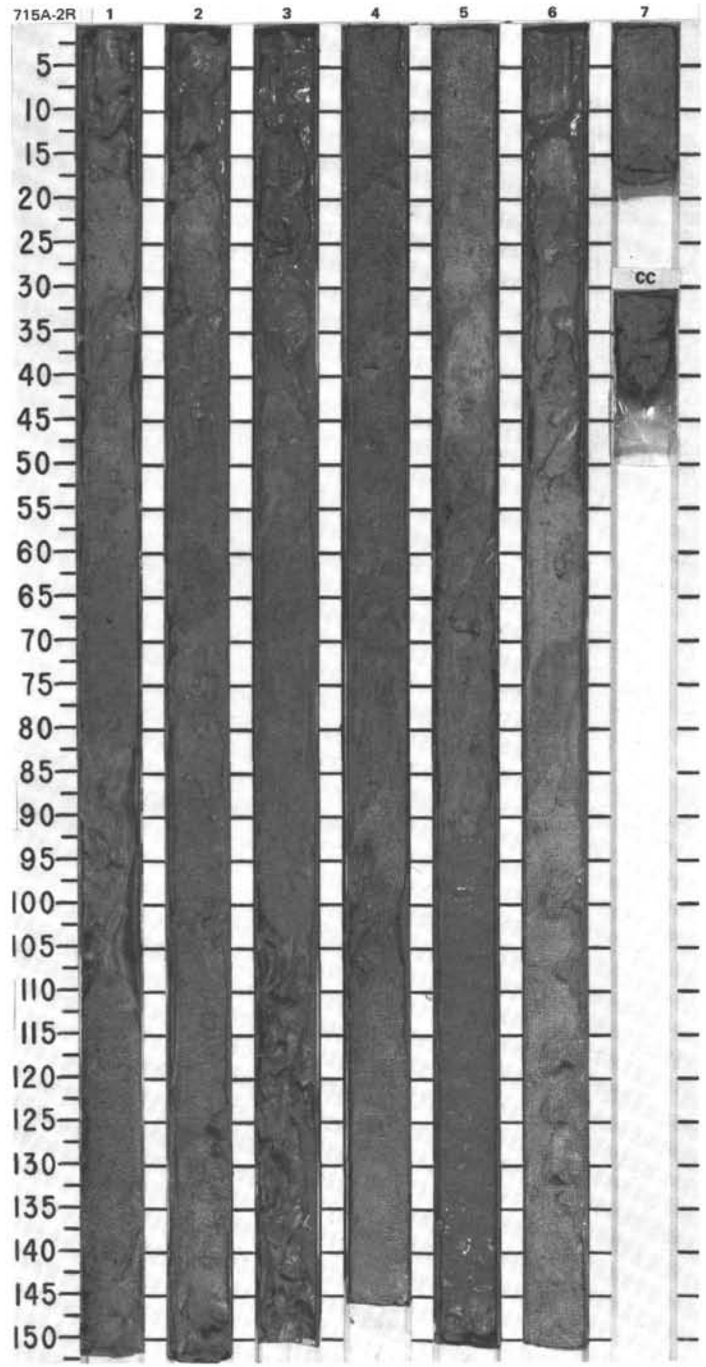

SITE 715 HOLE A CORE 3R CORED INTERVAL 2280.1-2289.8 mbsl; 17.8-27.5 mbsf

TIME-ROCK UNIT	BIOSTRAT. ZONE/ FOSSIL CHARACTER: FORAMINIFERS	NANNOFOSSILS	RADIOLARIANS	DIATOMS	PALEOMAGNETICS	PHYS. PROPERTIES	CHEMISTRY	SECTION	METERS	GRAPHIC LITHOLOGY	DRILLING DISTURB.	SED. STRUCTURES	SAMPLES
PLEISTOCENE	N 23 - N 22	AG CN 14b (NN 20)		Barren				1 2 3 4 5 6 7 CC	0.5 1.0				* OG IW *
	AM	AG											

LITHOLOGIC DESCRIPTION

CLAY-BEARING NANNOFOSSIL OOZE

Major lithology: Clay-bearing nannofossil ooze, greenish gray (5GY 6/1), light yellowish gray (5Y 7/2), gray (5Y 6/1, 5/1), light greenish gray (5GY 7/1), and yellowish gray (5Y 6/2).

SMEAR SLIDE SUMMARY (%):

	3, 80 D	5, 80 D
TEXTURE:		
Sand	2	5
Silt	40	30
Clay	58	65
COMPOSITION:		
Clay	15	15
Volcanic glass	1	Tr
Foraminifers	2	7
Nannofossils	80	75
Radiolarians	1	2
Sponge spicules	1	1

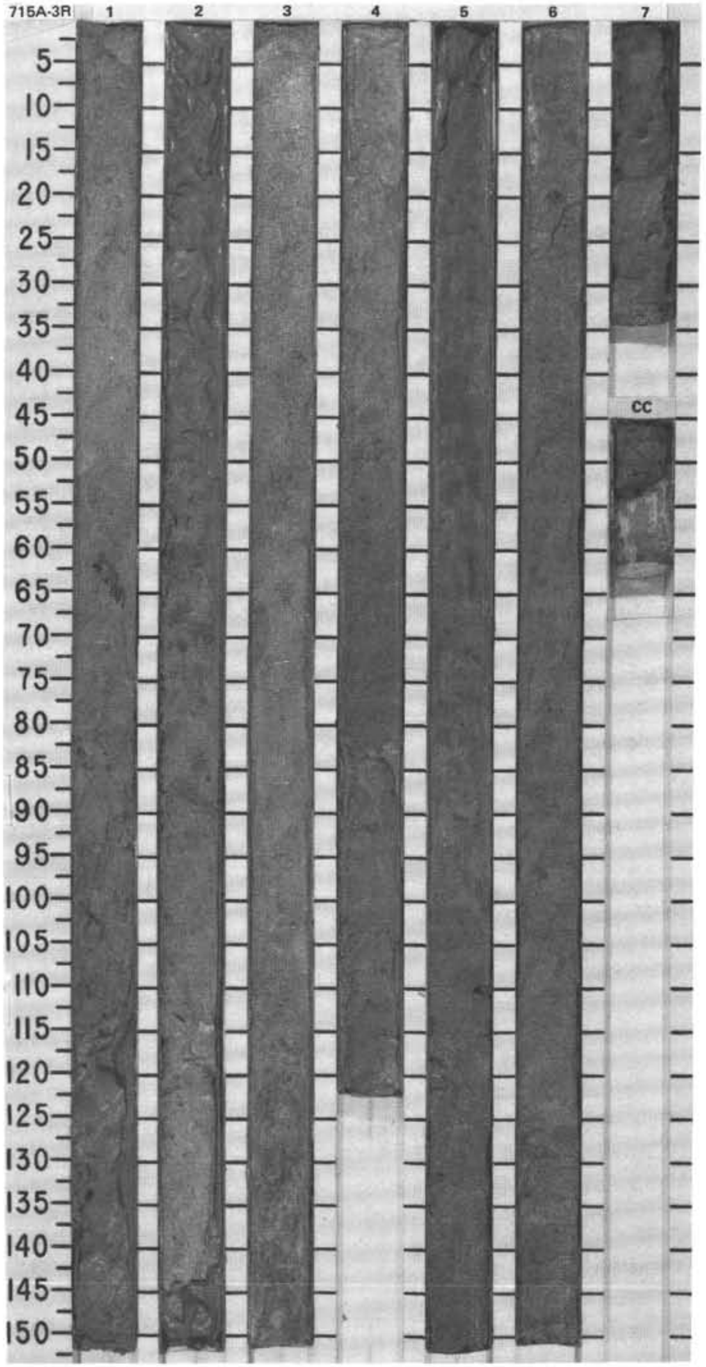

SITE 715 HOLE A CORE 4R CORED INTERVAL 2289.8-2299.4 mbsl; 27.5-37.1 mbsf

TIME-ROCK UNIT	BIOSTRAT. ZONE/FOSSIL CHARACTER: FORAMINIFERS	NANNOFOSSILS	RADIOLARIANS	DIATOMS	PALEOMAGNETICS	PHYS. PROPERTIES	CHEMISTRY	SECTION	METERS	GRAPHIC LITHOLOGY	DRILLING DISTURB.	SED. STRUCTURES	SAMPLES
PLEISTOCENE	N 23-N 22	CN 14b (NN 20)		*P. doliolus*				1	0.5 / 1.0				*
								2					
								3					*
								4					IW
								5					
								6					
	AG	AG		RP				7					
								CC					

LITHOLOGIC DESCRIPTION

CLAY-BEARING NANNOFOSSIL OOZE

Major lithology: Clay-bearing nannofossil ooze, greenish gray (5GY 6/1, 5/1).

SMEAR SLIDE SUMMARY (%):

	1, 80 D	3, 80 D
TEXTURE:		
Sand	5	5
Silt	30	30
Clay	65	65
COMPOSITION:		
Clay	12	12
Volcanic glass	—	Tr
Accessory minerals	Tr	—
Foraminifers	8	5
Nannofossils	79	83
Radiolarians	1	Tr
Sponge spicules	Tr	Tr
Fish remains	Tr	—

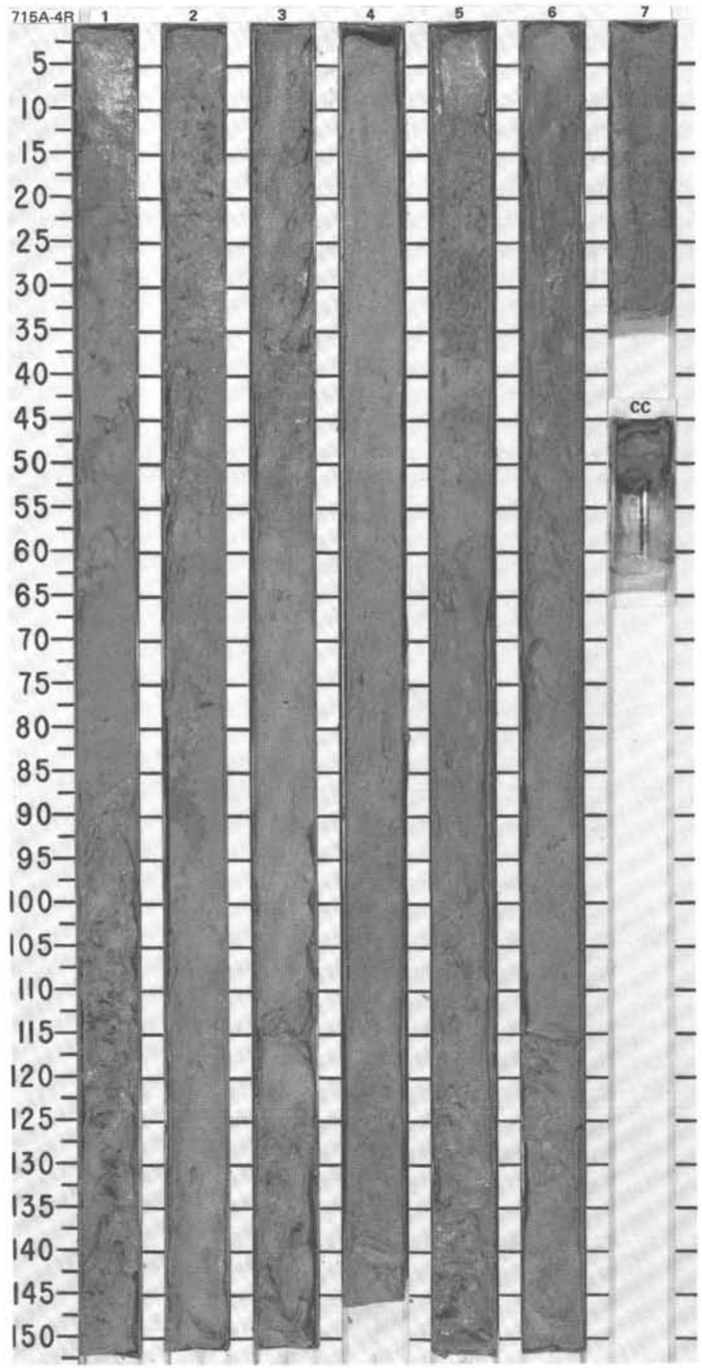

SITE 715 HOLE A CORE 5R CORED INTERVAL 2299.4-2309.1 mbsl; 37.1-46.8 mbsf

TIME-ROCK UNIT	BIOSTRAT. ZONE/ FOSSIL CHARACTER: FORAMINIFERS	NANNOFOSSILS	RADIOLARIANS	DIATOMS	PALEOMAGNETICS	PHYS. PROPERTIES	CHEMISTRY	SECTION	METERS	GRAPHIC LITHOLOGY	DRILLING DISTURB.	SED. STRUCTURES	SAMPLES
PLEISTOCENE	N 23-N 22	CN 14b (NN 20)	*A. ypsilon*	Barren				1	0.5, 1.0				
								2					*
		AG						3					
		CN 14a (NN 19)						4					* IW
								5					
								6					
								7					
	AM	AG	CM					CC					

CLAY-BEARING NANNOFOSSIL OOZE

Major lithology: Clay-bearing nannofossil ooze, greenish gray (5GY 5/1, 6/1; 5G 6/1), mottled.

SMEAR SLIDE SUMMARY (%):

	2, 79 D	4, 82 D
TEXTURE:		
Sand	5	5
Silt	40	30
Clay	55	65
COMPOSITION:		
Clay	12	20
Volcanic glass	Tr	Tr
Foraminifers	8	8
Nannofossils	71	71
Diatoms	Tr	Tr
Radiolarians	4	Tr
Sponge spicules	5	1
Fish remains	Tr	Tr

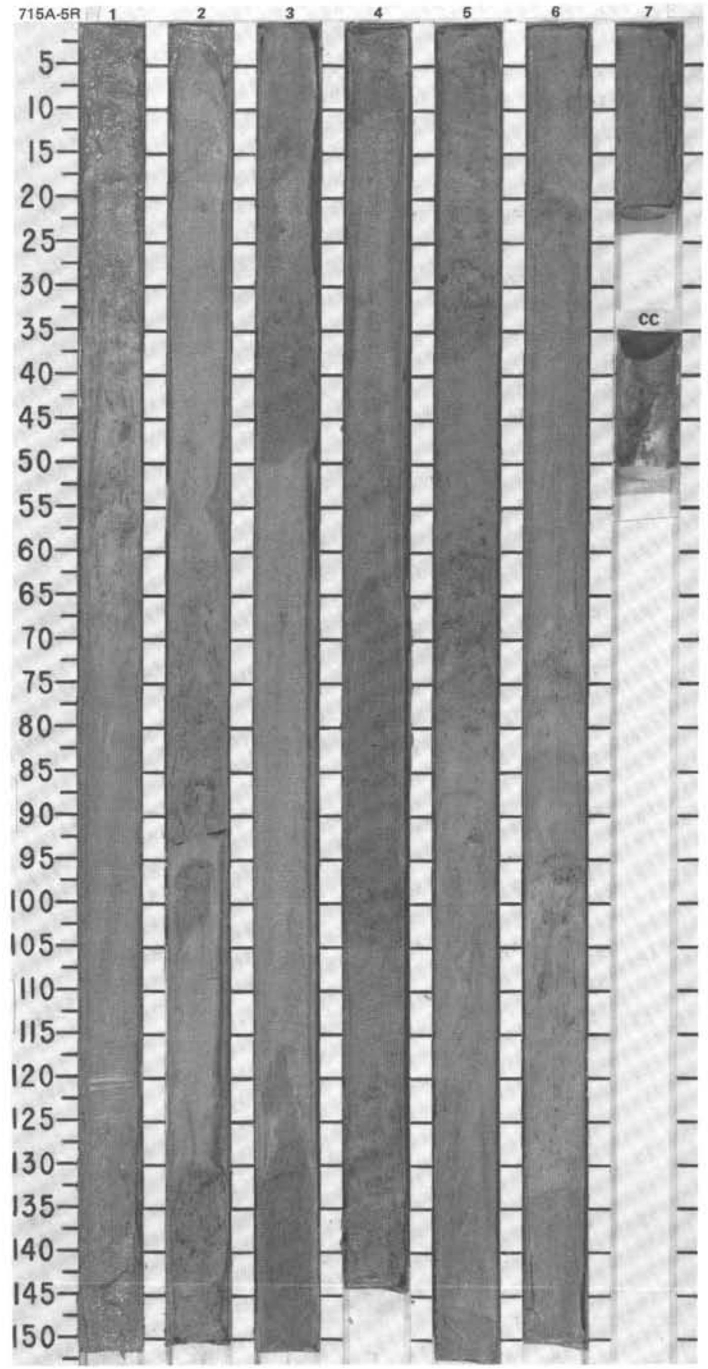

SITE 715 HOLE A CORE 6R CORED INTERVAL 2309.1-2318.8 mbsl; 46.8-56.5 mbsf

TIME-ROCK UNIT	BIOSTRAT. ZONE/FOSSIL CHARACTER: FORAMINIFERS	NANNOFOSSILS	RADIOLARIANS	DIATOMS	PALEOMAGNETICS	PHYS. PROPERTIES	CHEMISTRY	SECTION	METERS	GRAPHIC LITHOLOGY	DRILLING DISTURB.	SED. STRUCTURES	SAMPLES
MIDDLE MIOCENE	N 9	AM CN 4 (NN 5)	*C. costata*	Barren				1	0.5 1.0				*
								2					
								3					
								4					OG IW
								5					*
								6					
								7					
	AM	AM	FM					CC					

LITHOLOGIC DESCRIPTION

FORAMINIFER-BEARING NANNOFOSSIL OOZE

Major lithology: Foraminifer-bearing, very light greenish gray (5G 8/1), very homogeneous, minor pyrite staining.

SMEAR SLIDE SUMMARY (%):

	1, 80 D	5, 80 D
TEXTURE:		
Sand	10	15
Silt	40	40
Clay	50	45
COMPOSITION:		
Clay	5	5
Volcanic glass	Tr	—
Foraminifers	15	20
Nannofossils	79	73
Radiolarians	Tr	Tr
Sponge spicules	1	2

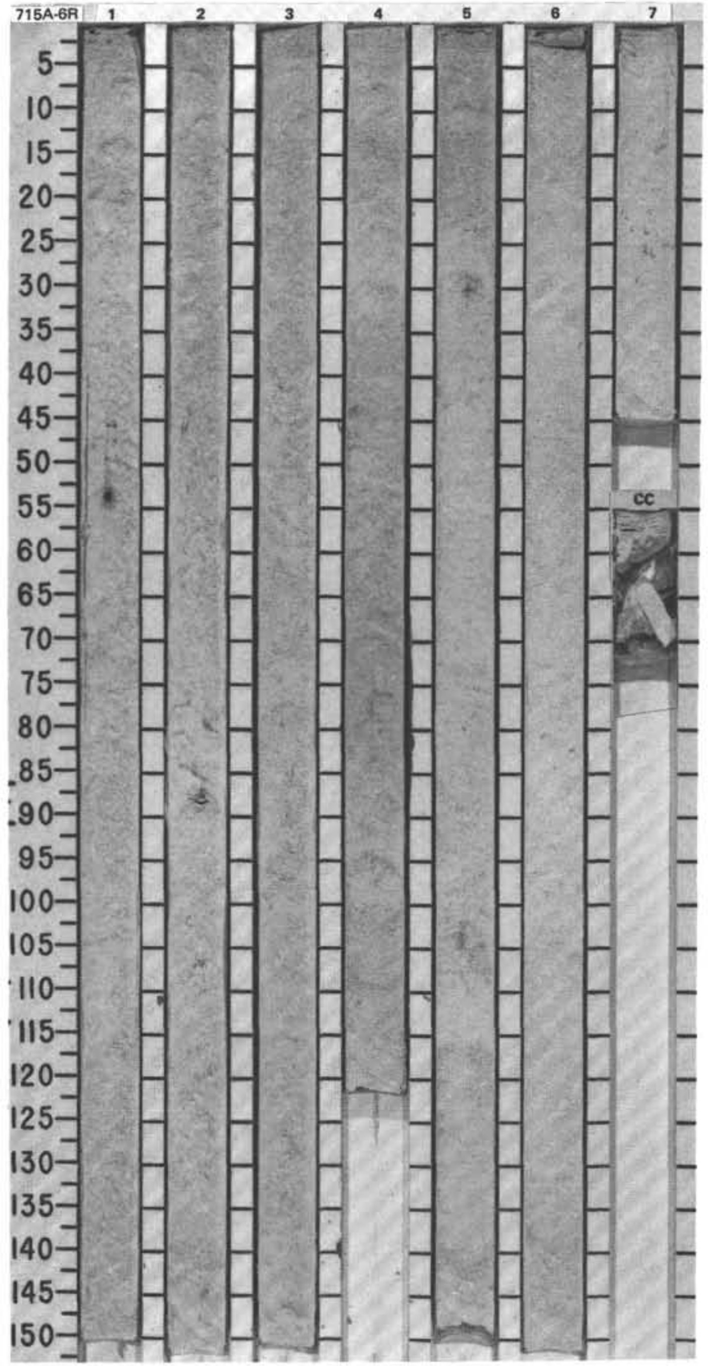

SITE 715 HOLE A CORE 7R CORED INTERVAL 2318.8-2328.4 mbsl; 56.5-66.1 mbsf

TIME-ROCK UNIT	FORAMINIFERS	NANNOFOSSILS	RADIOLARIANS	DIATOMS	PALEOMAGNETICS	PHYS. PROPERTIES	CHEMISTRY	SECTION	METERS	GRAPHIC LITHOLOGY	DRILLING DISTURB.	SED. STRUCTURES	SAMPLES
MIDDLE MIOCENE	N 8	CN 4 (NN 5)	Barren	Barren				1	0.5, 1.0				
		AM						2					*
								3					
								4					
								5					*
								6					
	AM	AM						7					
								CC					

BIOSTRAT. ZONE/ FOSSIL CHARACTER

LITHOLOGIC DESCRIPTION

FORAMINIFER-BEARING NANNOFOSSIL OOZE

Major lithology: Foraminifer-bearing nannofossil ooze, white (10Y 8/1), very homogeneous, featureless.

SMEAR SLIDE SUMMARY (%):

	2, 80 D	5, 80 D
TEXTURE:		
Sand	10	10
Silt	40	40
Clay	50	50
COMPOSITION:		
Clay	5	5
Volcanic glass	Tr	Tr
Foraminifers	12	15
Nannofossils	83	80
Radiolarians	Tr	—
Sponge spicules	Tr	—

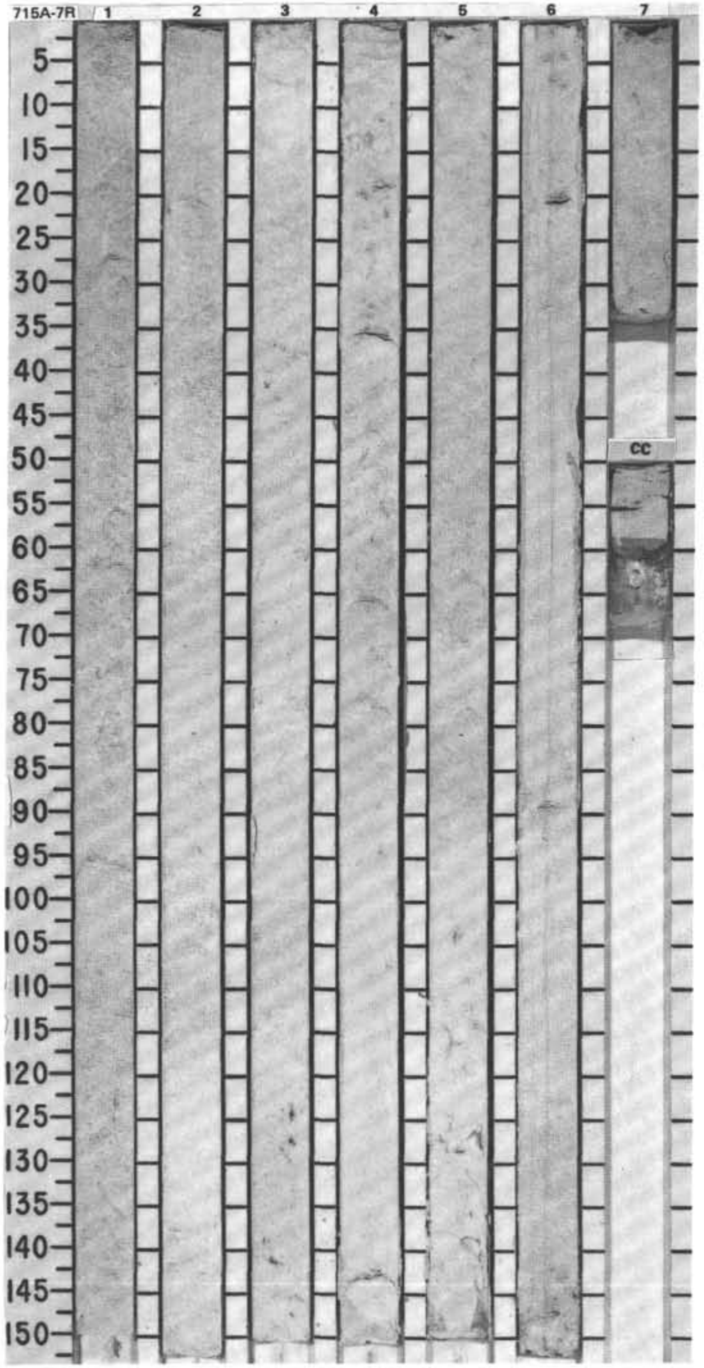

SITE 715 HOLE A CORE 8R CORED INTERVAL 2328.4-2338.0 mbsl; 66.1-75.7 mbsf

TIME-ROCK UNIT	BIOSTRAT. ZONE/FOSSIL CHARACTER: FORAMINIFERS	NANNOFOSSILS	RADIOLARIANS	DIATOMS	PALEOMAGNETICS	PHYS. PROPERTIES	CHEMISTRY	SECTION	METERS	GRAPHIC LITHOLOGY	DRILLING DISTURB.	SED. STRUCTURES	SAMPLES
MIDDLE MIOCENE	N 8	AM; CN 4 (NN 5)	Barren	Barren				1	0.5; 1.0				
								2					
								3				*	
								4					
								5					
								6					
	AM	AM						CC					

LITHOLOGIC DESCRIPTION

FORAMINIFER-BEARING NANNOFOSSIL OOZE and FORAMINIFER-BEARING NANNOFOSSIL CHALK

Major lithology: Foraminifer-bearing nannofossil ooze and foraminifer-bearing nannofossil chalk, white (5G 8/1), very homogeneous and featureless, some pyrite staining, about 20% lumps of harder chalk starting at top of Section 2.

SMEAR SLIDE SUMMARY (%):

	3, 80 D
TEXTURE:	
Sand	15
Silt	10
Clay	75
COMPOSITION:	
Clay	5
Volcanic glass	Tr
Foraminifers	24
Nannofossils	71
Radiolarians	Tr
Sponge spicules	Tr

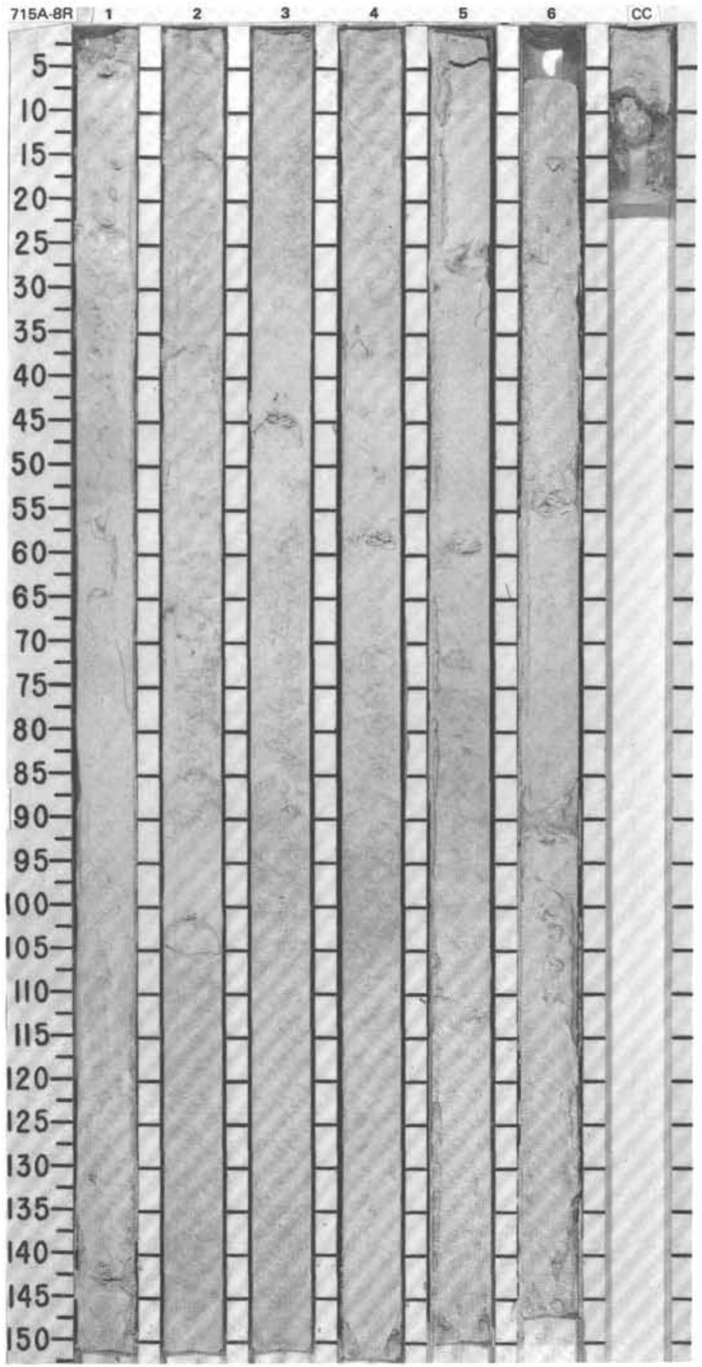

SITE 715 HOLE A CORE 9R CORED INTERVAL 2338.0-2347.6 mbsl; 75.7-85.3 mbsf

TIME-ROCK UNIT	BIOSTRAT. ZONE/FOSSIL CHARACTER: FORAMINIFERS	NANNOFOSSILS	RADIOLARIANS	DIATOMS	PALEOMAGNETICS	PHYS. PROPERTIES	CHEMISTRY	SECTION	METERS	GRAPHIC LITHOLOGY	DRILLING DISTURB.	SED. STRUCTURES	SAMPLES
LOWER MIOCENE	N 7? - N 5	AM CN 3	Barren	Barren				1	0.5 1.0				
								2					*
								3					
								4					IW OG
								5				OO	
								6					
								7					
	AM	AM						CC					

LITHOLOGIC DESCRIPTION

FORAMINIFER-BEARING NANNOFOSSIL OOZE and FORAMINIFER-BEARING NANNOFOSSIL CHALK

Major lithology: Foraminifer-bearing nannofossil ooze and foraminifer-bearing nannofossil chalk, white (5G 8/1), about 30% chalk, very homogeneous, some flow-in between chalk lumps, minor pyrite, hydrogen sulfide smell upon opening.

SMEAR SLIDE SUMMARY (%):

	2, 50 D
TEXTURE:	
Sand	20
Silt	10
Clay	70
COMPOSITION:	
Clay	8
Volcanic glass	Tr
Micrite	5
Accessory minerals	Tr
Foraminifers	20
Nannofossils	67
Radiolarians	Tr

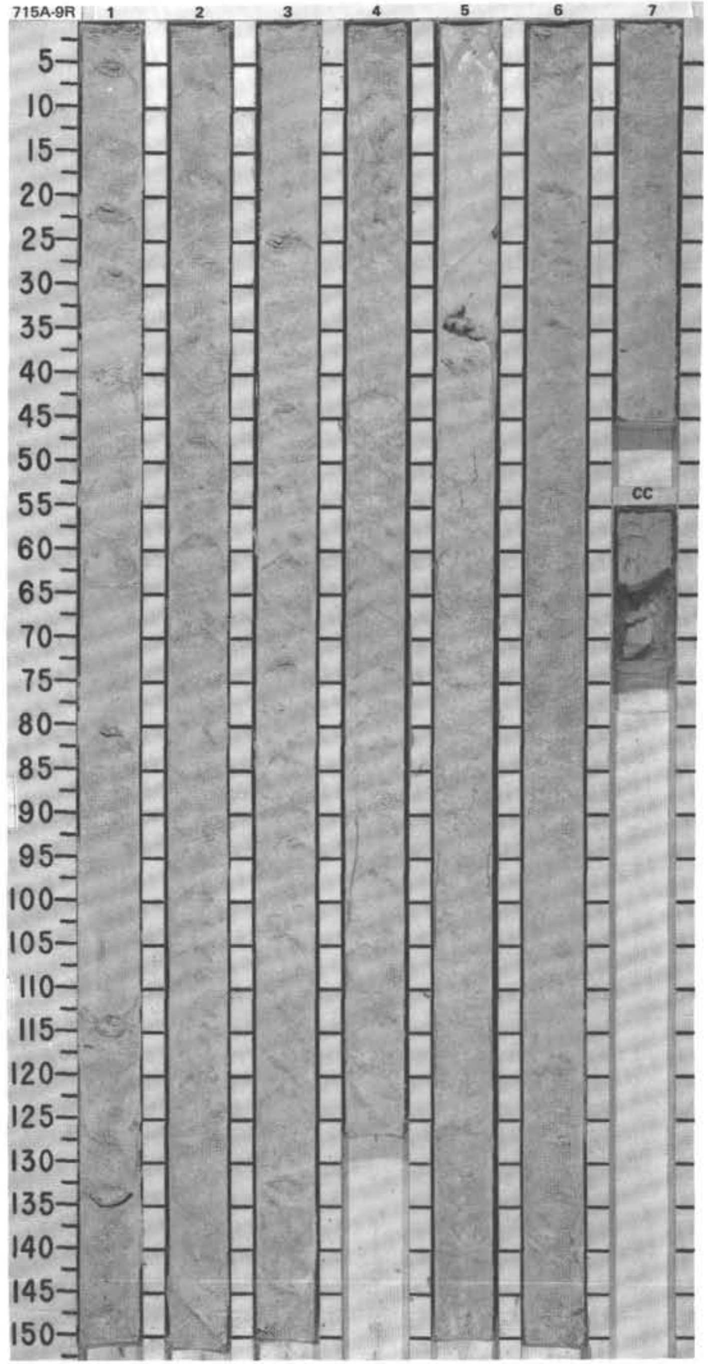

SITE 715 HOLE A CORE 10R CORED INTERVAL 2347.6-2357.2 mbsl; 85.3-94.9 mbsf

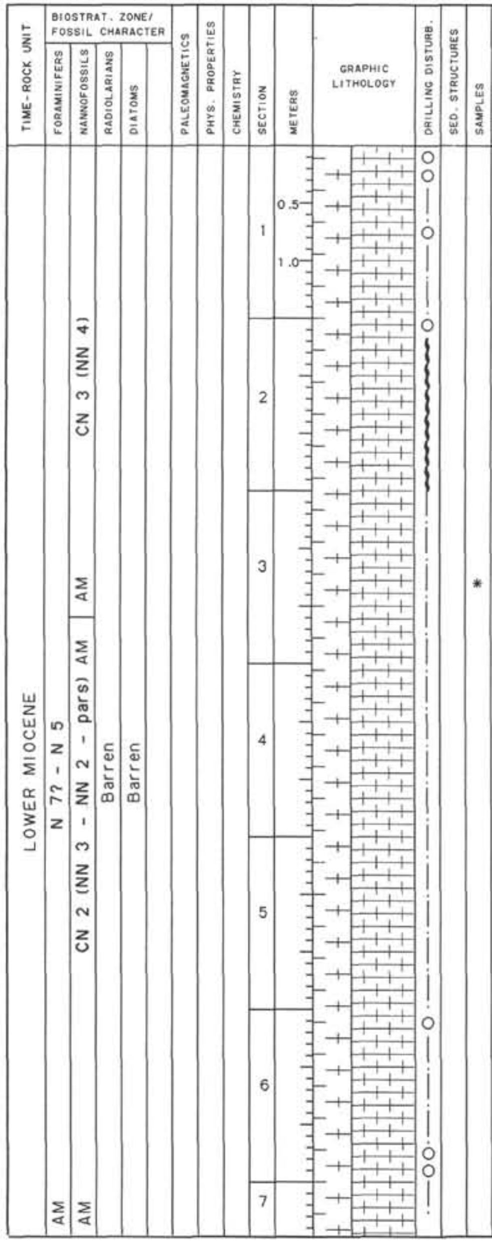

LITHOLOGIC DESCRIPTION

FORAMINIFER-NANNOFOSSIL CHALK AND FORAMINIFER-BEARING NANNOFOSSIL OOZE

Major lithology: Foraminifer-nannofossil chalk and foraminifer-bearing nannofossil ooze with disturbed ooze in between, white (5G 8/1), very homogeneous, minor pyrite staining, about 60% chalk.

SMEAR SLIDE SUMMARY (%):

	3, 80
	D
TEXTURE:	
Sand	25
Silt	15
Clay	60
COMPOSITION:	
Quartz	Tr
Feldspar	Tr
Clay	5
Accessory minerals	Tr
Foraminifers	35
Nannofossils	60
Radiolarians	Tr

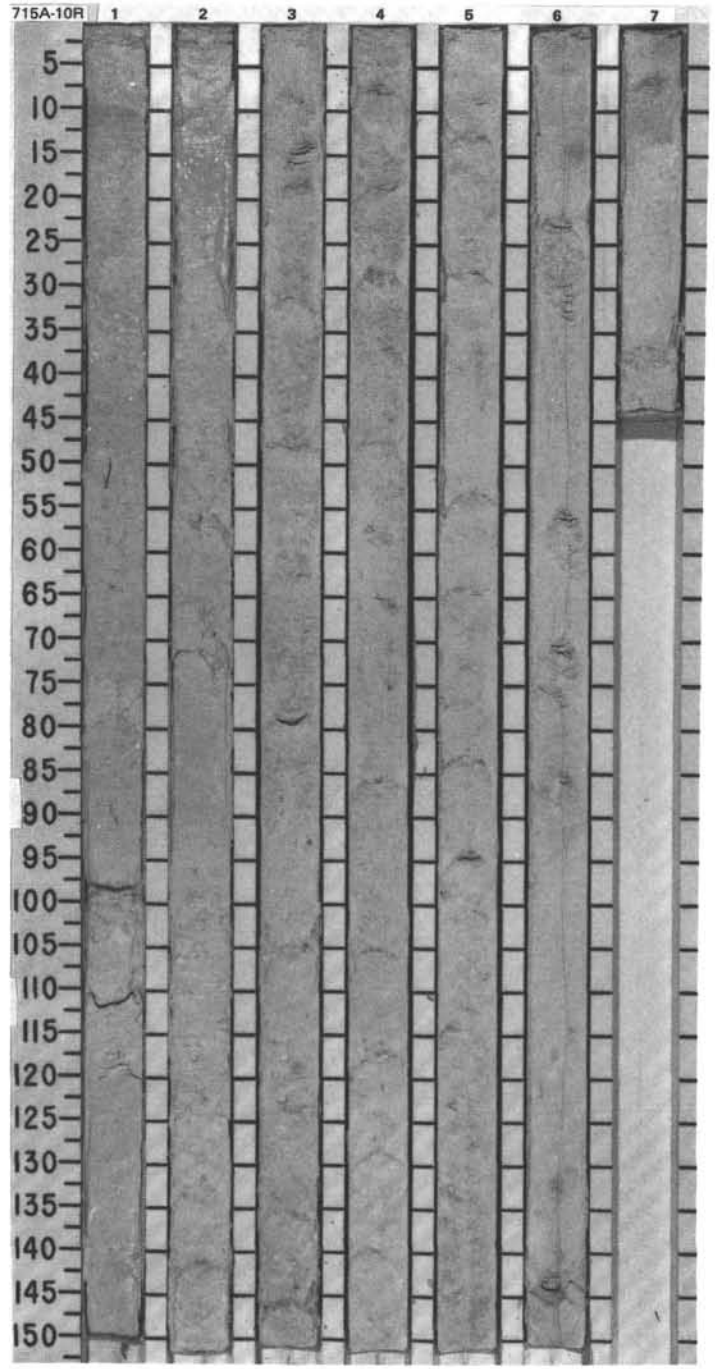

SITE 715 HOLE A CORE 11R CORED INTERVAL 2357.2-2366.9 mbsl; 94.9-104.6 mbsf

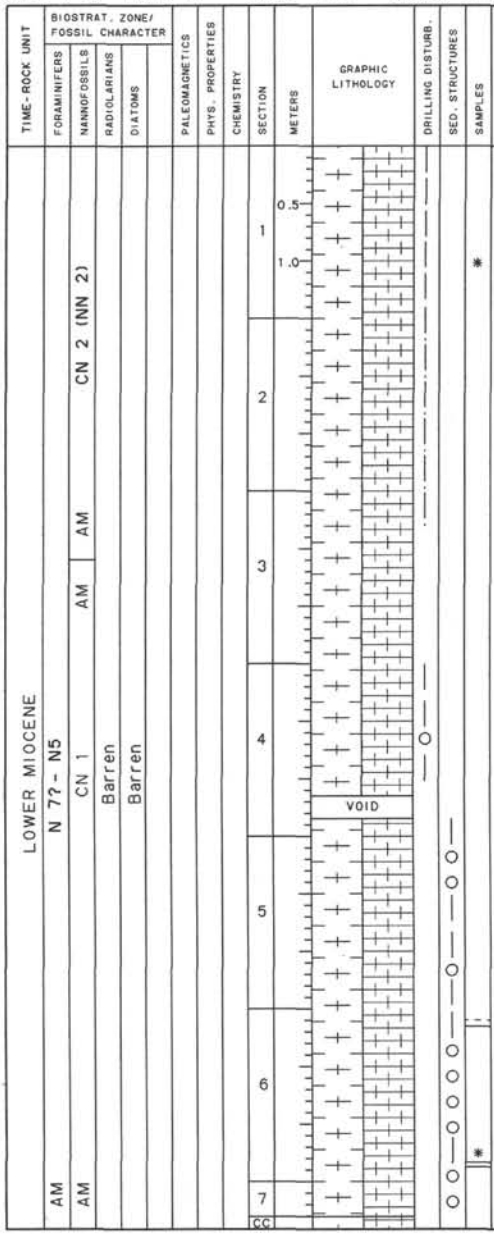

LITHOLOGIC DESCRIPTION

FORAMINIFER-NANNOFOSSIL CHALK AND FORAMINIFER-BEARING NANNOFOSSIL OOZE

Major lithology: Foraminifer-nannofossil chalk and foraminifer-bearing nannofossil ooze, about 50% chalk, white (5G 8/1), homogeneous throughout, minor pyrite staining, gray (N6) pyrite-stained horizons at Section 6, 7-17 and 136-138 cm.

Note: Void at Section 4, 118-134 cm, was created by soupy core extruding upon opening the liner.

SMEAR SLIDE SUMMARY (%):

	1, 80	6, 138
	D	D
TEXTURE:		
Sand	25	25
Silt	10	15
Clay	65	60
COMPOSITION:		
Clay	5	8
Volcanic glass	Tr	Tr
Accessory minerals	Tr	Tr
Foraminifers	30	28
Nannofossils	65	64
Radiolarians	Tr	Tr
Sponge spicules	—	Tr

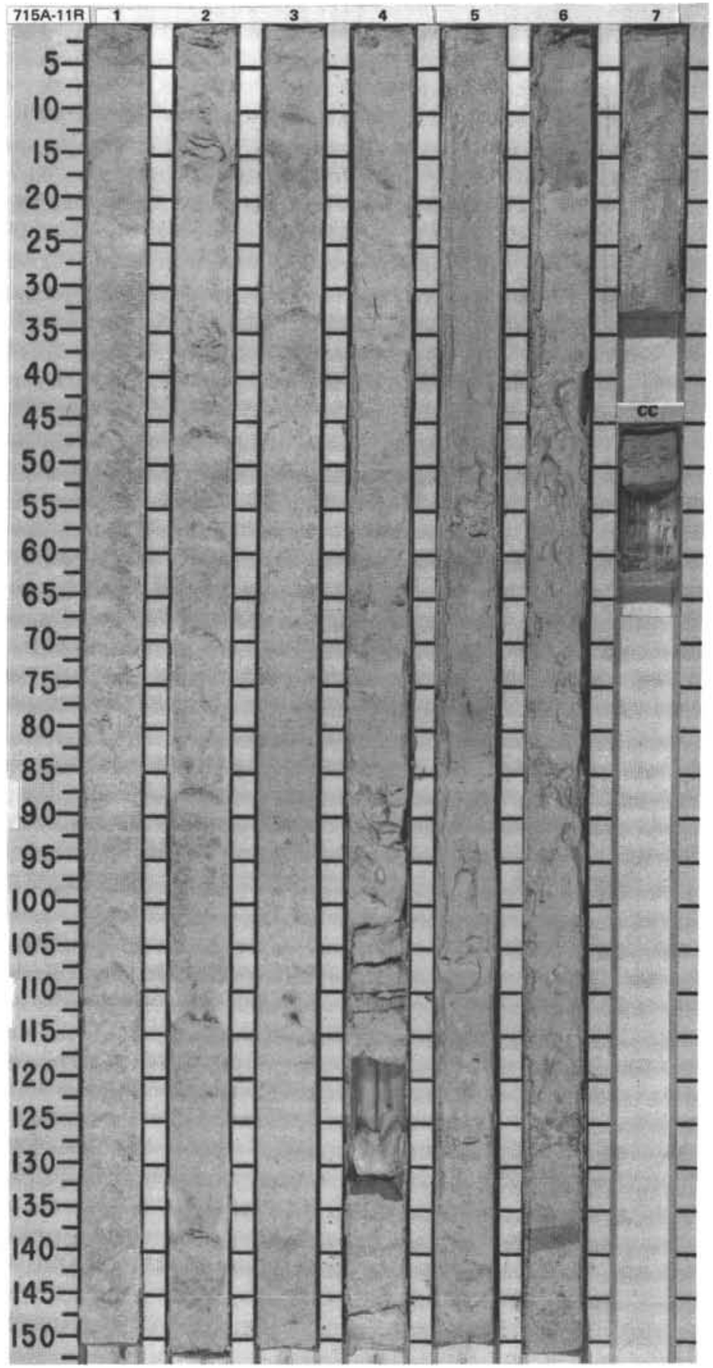

SITE 715 HOLE A CORE 12R CORED INTERVAL 2366.9-2376.6 mbsl; 104.6-114.3 mbsf

TIME-ROCK UNIT	FORAMINIFERS	NANNOFOSSILS	RADIOLARIANS	DIATOMS	PALEOMAGNETICS	PHYS. PROPERTIES	CHEMISTRY	SECTION	METERS	GRAPHIC LITHOLOGY	DRILLING DISTURB.	SED. STRUCTURES	SAMPLES	LITHOLOGIC DESCRIPTION
LOWER MIOCENE	P7	RP	Barren	Barren				1 CC	0.5 1.0					WACKESTONE Major lithology: Wackestone, white (10YR 8/2) and very pale brown (10YR 8/3), about 15% skeletal grains and remainder micrite. Recognizable grains include mostly large shallow-water benthic foraminifers and bivalve fragments, aligned parallel to bedding, some brachiopods and pelecypods. Grain moldic porosity. Several pieces have glauconite-stained hardgrounds.

SITE 715 HOLE A CORE 13R CORED INTERVAL 2376.6-2386.2 mbsl; 114.3-123.9 mbsf

TIME-ROCK UNIT	FORAMINIFERS	NANNOFOSSILS	RADIOLARIANS	DIATOMS	PALEOMAGNETICS	PHYS. PROPERTIES	CHEMISTRY	SECTION	METERS	GRAPHIC LITHOLOGY	DRILLING DISTURB.	SED. STRUCTURES	SAMPLES	LITHOLOGIC DESCRIPTION
EOCENE	P7	CP 14 - CP 15 (NP 16 - NP 20) RM		Barren				1						PACKSTONE Major lithology: Packstone, white (10YR 8/2) or very pale brown (10YR 7/3). Less mud, more grains than previous core. Still mostly benthic foraminifers and one coral mold. One fragment of black manganese oxide-stained, highly porous, packstone.

SITE 715 HOLE A CORE 14R CORED INTERVAL 2386.2-2395.8 mbsl; 123.9-133.5 mbsf

TIME-ROCK UNIT	FORAMINIFERS	NANNOFOSSILS	RADIOLARIANS	DIATOMS	PALEOMAGNETICS	PHYS. PROPERTIES	CHEMISTRY	SECTION	METERS	GRAPHIC LITHOLOGY	DRILLING DISTURB.	SED. STRUCTURES	SAMPLES	LITHOLOGIC DESCRIPTION
LOWER EOCENE	P7	Barren						1						PACKSTONE Major lithology: Packstone fragments, white (10YR 8/2). Major constituents include benthic foraminifers, oysters, solitary corals, and bryozoans. Moldic porosity. Coarser grains and shallower water than previous two cores. One dark green chert nodule.

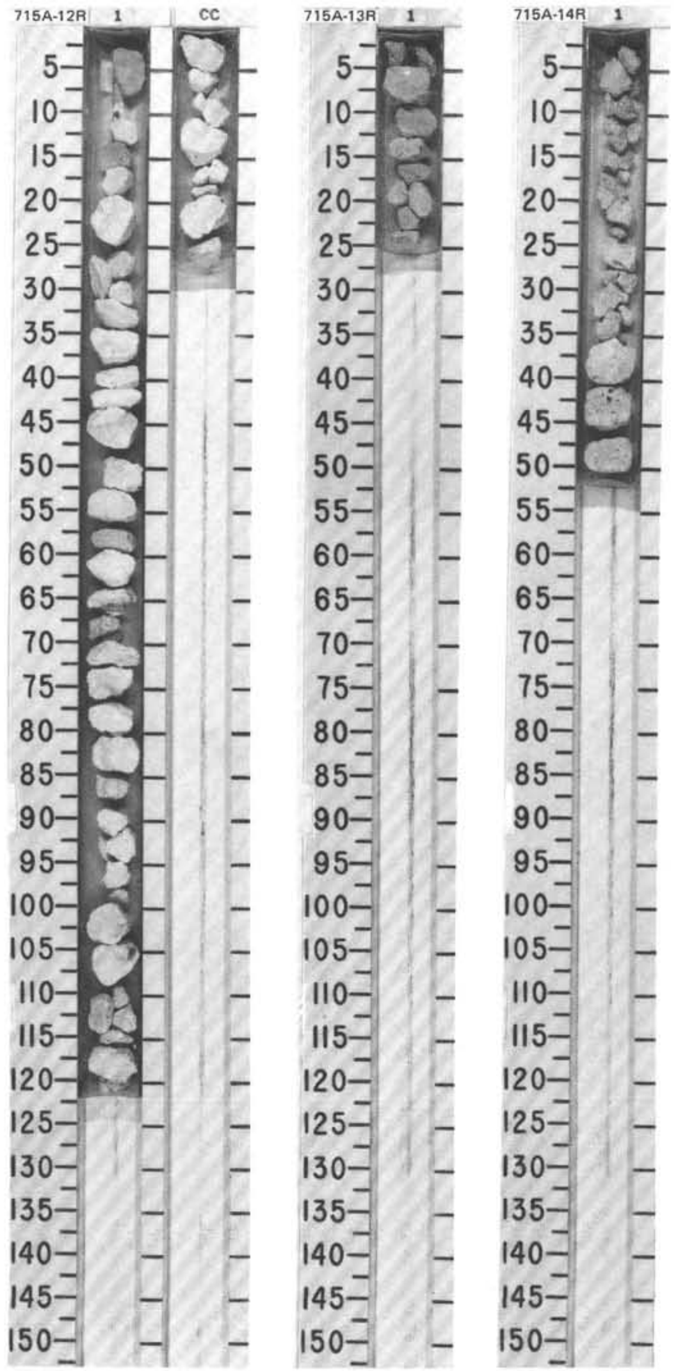

SITE 715 HOLE A CORE 15R CORED INTERVAL 2395.8-2405.5 mbsl; 133.5-143.2 mbsf

TIME-ROCK UNIT	FORAMINIFERS	NANNOFOSSILS	RADIOLARIANS	DIATOMS	PALEOMAGNETICS	PHYS. PROPERTIES	CHEMISTRY	SECTION	METERS	GRAPHIC LITHOLOGY	DRILLING DISTURB.	SED. STRUCTURES	SAMPLES	LITHOLOGIC DESCRIPTION
LOWER EOCENE	P7	Barren						1	0.5 1.0					PACKSTONE Major lithology: Packstone, very pale brown (10YR 7/3). Contains large benthic foraminifers, large bivalves, bryozoans, gastropods, and boring clams.

SITE 715 HOLE A CORE 16R CORED INTERVAL 2405.5-2415.2 mbsl; 143.2-152.9 mbsf

TIME-ROCK UNIT	FORAMINIFERS	NANNOFOSSILS	RADIOLARIANS	DIATOMS	PALEOMAGNETICS	PHYS. PROPERTIES	CHEMISTRY	SECTION	METERS	GRAPHIC LITHOLOGY	DRILLING DISTURB.	SED. STRUCTURES	SAMPLES	LITHOLOGIC DESCRIPTION
		Barren						1						PACKSTONE and GRAINSTONE Major lithology: Pebble-size fragments of shelly, coquina-like packstone and grainstone, very pale brown (10YR 7/3), high porosity, recrystallized matrix. Contains large benthic foraminifers, coral molds, bryozoans, mollusks, and mollusk fragments.

SITE 715 HOLE A CORE 17R CORED INTERVAL 2415.2-2424.9 mbsl; 152.9-162.6 mbsf

TIME-ROCK UNIT	FORAMINIFERS	NANNOFOSSILS	RADIOLARIANS	DIATOMS	PALEOMAGNETICS	PHYS. PROPERTIES	CHEMISTRY	SECTION	METERS	GRAPHIC LITHOLOGY	DRILLING DISTURB.	SED. STRUCTURES	SAMPLES	LITHOLOGIC DESCRIPTION
		Barren						1						PACKSTONE and GRAINSTONE Major lithology: Packstone and grainstone, pebble-size fragments, and shelly coquina. High moldic porosity, recrystallized. Very pale brown (10YR 7/3). Contains large benthic foraminifers, solitary and colonial coral fragments, and bryozoans.

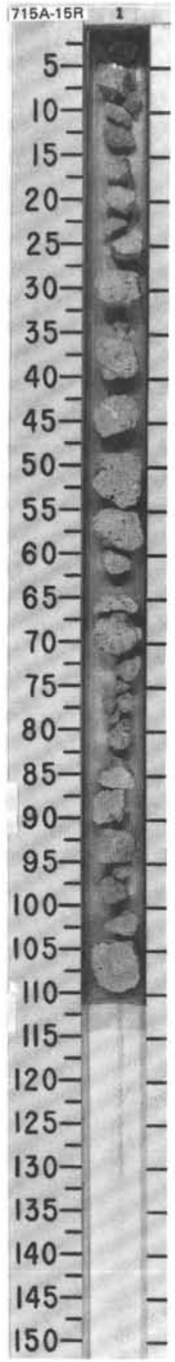

SITE 715 HOLE A CORE 18R CORED INTERVAL 2424.9-2434.5 mbsl; 162.6-172.2 mbsf

TIME-ROCK UNIT	FORAMINIFERS	NANNOFOSSILS	RADIOLARIANS	DIATOMS	PALEOMAGNETICS	PHYS. PROPERTIES	CHEMISTRY	SECTION	METERS	GRAPHIC LITHOLOGY	DRILLING DISTURB.	SED. STRUCTURES	SAMPLES	LITHOLOGIC DESCRIPTION
LOWER EOCENE	P7	Barren						1 CC	0.5					PACKSTONE and GRAINSTONE Major lithology: Shelly packstone and grainstone, very pale brown (10YR 7/3), coarse-grained, high porosity shell hash. Contains large benthic foraminifers, coral fragments, and bryozoans. Interpretation: high energy, shallow-water environment.

SITE 715 HOLE A CORE 19R CORED INTERVAL 2434.5-2444.1 mbsl; 172.2-181.8 mbsf

TIME-ROCK UNIT	FORAMINIFERS	NANNOFOSSILS	RADIOLARIANS	DIATOMS	PALEOMAGNETICS	PHYS. PROPERTIES	CHEMISTRY	SECTION	METERS	GRAPHIC LITHOLOGY	DRILLING DISTURB.	SED. STRUCTURES	SAMPLES	LITHOLOGIC DESCRIPTION
LOWER EOCENE	P7	Barren						1 CC	0.5					SHELLY GRAINSTONE and PACKSTONE Major lithology: Shelly grainstone and packstone, pebble-size fragments. Contains abundant benthic foraminifers, coral molds, and a few small coiled gastropods. Finer-grained and less porous than previous cores, recrystallized.

SITE 715 HOLE A CORE 20R CORED INTERVAL 2441.1-2453.7 mbsl; 181.8-191.4 mbsf

TIME-ROCK UNIT	FORAMINIFERS	NANNOFOSSILS	RADIOLARIANS	DIATOMS	PALEOMAGNETICS	PHYS. PROPERTIES	CHEMISTRY	SECTION	METERS	GRAPHIC LITHOLOGY	DRILLING DISTURB.	SED. STRUCTURES	SAMPLES	LITHOLOGIC DESCRIPTION
LOWER EOCENE	P7	Barren						CC						GRAINSTONE AND PACKSTONE Major lithology: Grainstone and packstone, very light brown (10YR 7/3), moldic porosity. Contains mollusk and coral debris, and benthic foraminifers.

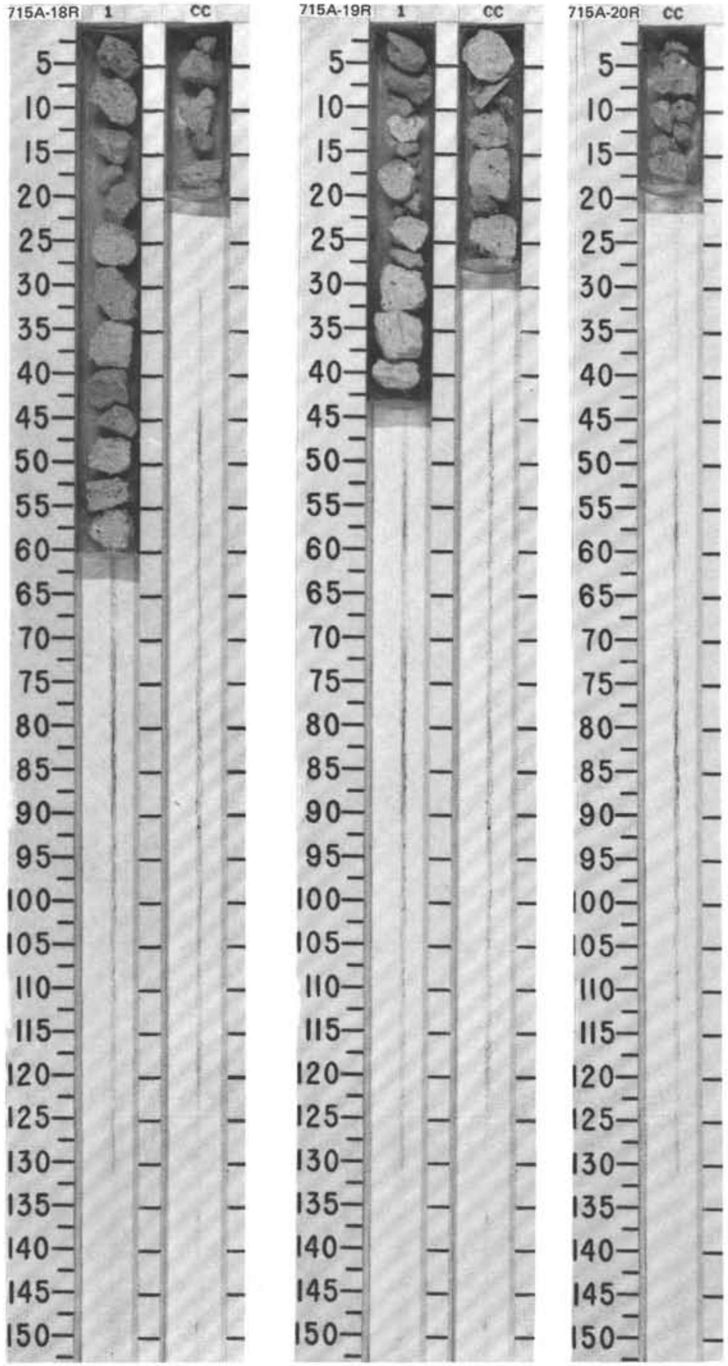

SITE 715 HOLE A CORE 21R CORED INTERVAL 2453.7-2463.4 mbsl; 191.4-201.1 mbsf

TIME-ROCK UNIT	BIOSTRAT. ZONE/ FOSSIL CHARACTER: FORAMINIFERS	NANNOFOSSILS	RADIOLARIANS	DIATOMS	PALEOMAGNETICS	PHYS. PROPERTIES	CHEMISTRY	SECTION	METERS	GRAPHIC LITHOLOGY	DRILLING DISTURB.	SED. STRUCTURES	SAMPLES	LITHOLOGIC DESCRIPTION
LOWER EOCENE	P7	Barren						1	0.5					GRAINSTONE AND PACKSTONE Major lithology: Grainstone and packstone, pale brown (10YR 7/3) and gray (N6) or light gray (N7). Filled with many fine inclusions of black pyrite or possibly manganese oxide. Otherwise similar to the overlying limestone.

SITE 715 HOLE A CORE 22R CORED INTERVAL 2463.4-2473.1 mbsl; 201.1-210.8 mbsf

TIME-ROCK UNIT	BIOSTRAT. ZONE/ FOSSIL CHARACTER: FORAMINIFERS	NANNOFOSSILS	RADIOLARIANS	DIATOMS	PALEOMAGNETICS	PHYS. PROPERTIES	CHEMISTRY	SECTION	METERS	GRAPHIC LITHOLOGY	DRILLING DISTURB.	SED. STRUCTURES	SAMPLES	LITHOLOGIC DESCRIPTION
EOCENE		Barren						1	0.5					GRAINSTONE Major lithology: Grainstone, porous, bioclastic, some fine black inclusions of pyrite or manganese oxide in upper Section 1, 0-67 cm; in Section 1, 67-93 cm, white (10YR 8/2), less porous packstone.

SITE 715 HOLE A CORE 23R CORED INTERVAL 2473.1-2482.8 mbsl; 210.8-210.5 mbsf

TIME-ROCK UNIT	BIOSTRAT. ZONE/ FOSSIL CHARACTER: FORAMINIFERS	NANNOFOSSILS	RADIOLARIANS	DIATOMS	PALEOMAGNETICS	PHYS. PROPERTIES	CHEMISTRY	SECTION	METERS	GRAPHIC LITHOLOGY	DRILLING DISTURB.	SED. STRUCTURES	SAMPLES	LITHOLOGIC DESCRIPTION
EOCENE		Barren						1						PACKSTONE Major lithology: Dense packstone, white (10YR 8/2) and light gray (10YR 7/2). Similar to limestone in overlying core.

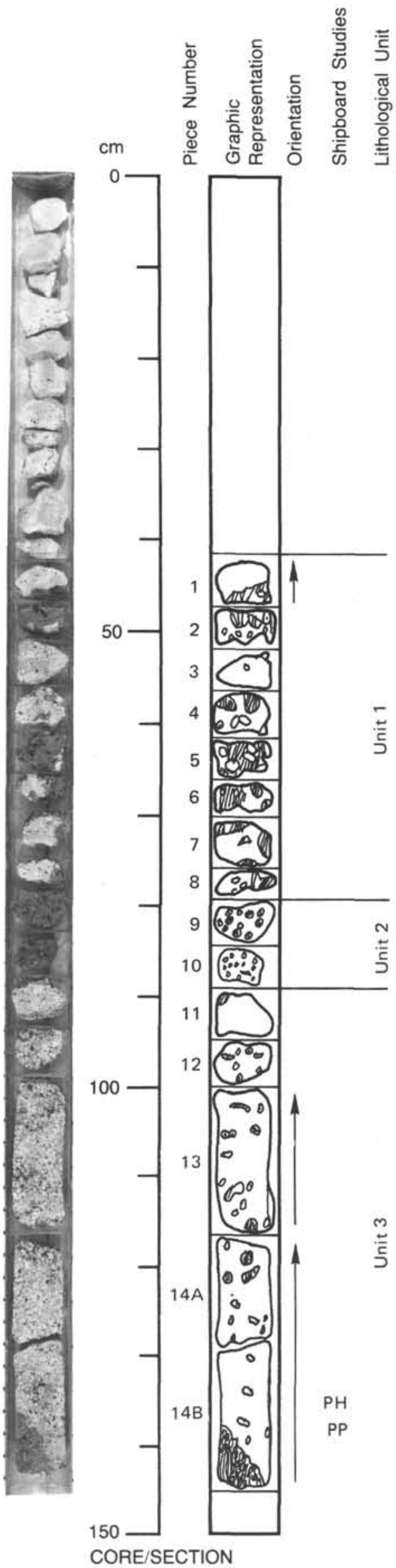

115-715A-23R-1

0-42 cm: CARBONATE (Described elsewhere)

UNIT 1: BRECCIA: ALTERED BASALT CLASTS IN CARBONATE

Pieces 1-8

CONTACTS: Pieces are oriented by microstromatolite.
COLOR: Dark basalt clasts in carbonate matrix.
VESICLES: Contain filaments of brown mineral, calcite, and sulfide.
ALTERATION: Altered basalt clasts.
VEINS/FRACTURES: None.

UNIT 2: FINE-GRAINED VESICULAR BASALT/HAWAIITE

Pieces 9-10

PHENOCRYSTS: Feldspar, 1-2 mm in size, 1%.
COLOR: Dark grayish brown to very dark grayish brown (10YR 3/2, 4/2).
VESICLES: Round to connected long shapes, 1-10 cm in size, 10%, rimmed with clay, calcite, and sulfide.
ALTERATION: Moderately altered. Groundmass appears to be altered clay.

UNIT 3: CARBONATE-BASALT BRECCIA: ALTERED BASALT FRAGMENTS IN CARBONATE

Pieces 11-14B

SIZE: Basalt fragments from <1 mm-5 cm in size.
ALTERATION: Basalt moderately to completely altered.

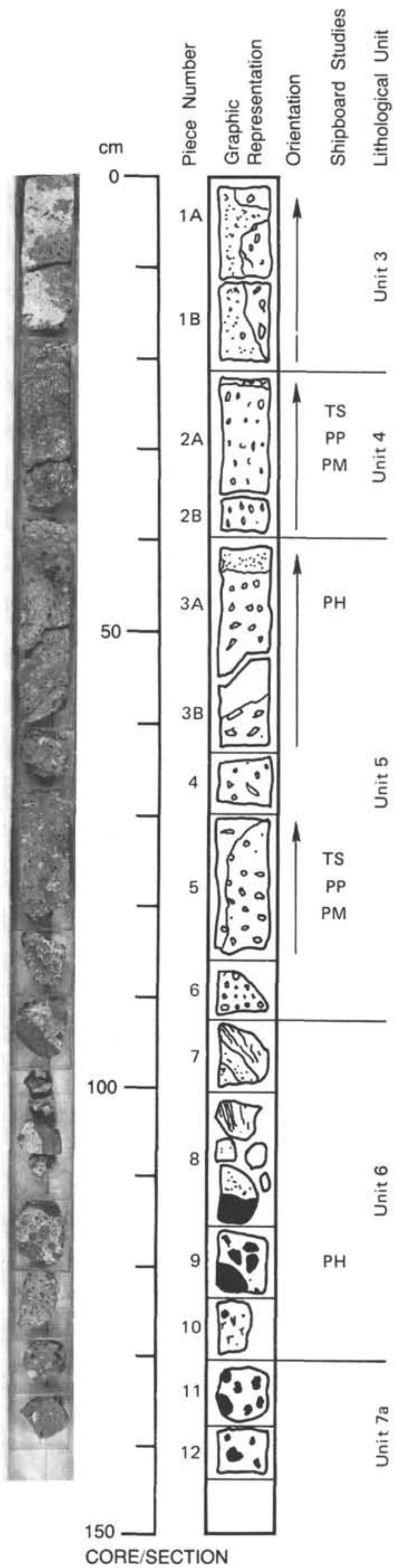

115-715A-23R-2

UNIT 3 (CONTINUED): CARBONATE-BASALT BRECCIA

Pieces 1A–1B

Continuous with 115-715A-23R-1, Unit 3

SIZE: One large basalt clast.
VESICLES: Beautiful, 1 mm large "dog tooth" calcite crystals line vesicle cavities.

UNIT 4: VERY FINE-GRAINED VESICULAR BASALT

Pieces 2A–2B

PHENOCRYSTS: Plagioclase - 0.5 mm long, <5%.
Ferromagnesian mineral (pyroxene) - 0.5 mm in size, <5%. Entirely altered to limonite.
GROUNDMASS: Very fine grained, altered and/or weathered in part.
COLOR: Dark reddish brown (5YR 3/2).
VESICLES: Oval, 1–2 mm wide, 20% of total.
30% of vesicles unfilled.
50% of vesicles filled with calcite, 0.5 mm crystals of "dog tooth" calcite in some vesicles.
20% of vesicles filled with dark green grading to yellow brown ("limonite" color) clay minerals.
ALTERATION: Basalt is altered in part.
CONTACTS: Upper contact is with carbonate sandstone, bearing abundant basalt fragments.

UNIT 5: VERY FINE-GRAINED VESICULAR BASALT

Pieces 3A–6

Similar to 115-715A-23R-2, Unit 4

CONTACTS: Upper contact is with carbonate sandstone, bearing abundant basalt fragments.
VESICLES: Percentage of vesicles drops to 15% in Piece 5. Vesicles as long as 4 mm in Piece 5.
VEINS/FRACTURES: Calcite-filled fractures in Pieces 3B and 5.

UNIT 6: BASALT COBBLE SANDSTONE-CONGLOMERATE

Pieces 7–10

GROUNDMASS: Micrite matrix to pebbles. Cobbles are surrounded by white carbonate sand (see sedimentary sheets for description).
SIZE: Well-rounded cobbles typically 2 cm long, some as long as 6 cm.
COLOR: Dark brown (10YR 4/3) and reddish brown (5Y 4/4) to olive gray (5Y 4/2).
VESICLES: Cobbles vesicular.

UNIT 7A: VERY FINE-GRAINED PYROXENE-PLAGIOCLASE BASALT

Pieces 11 and 12

See 115-715A-23R-3, Unit 7, for description.

VESICLES: Highly vesicular.

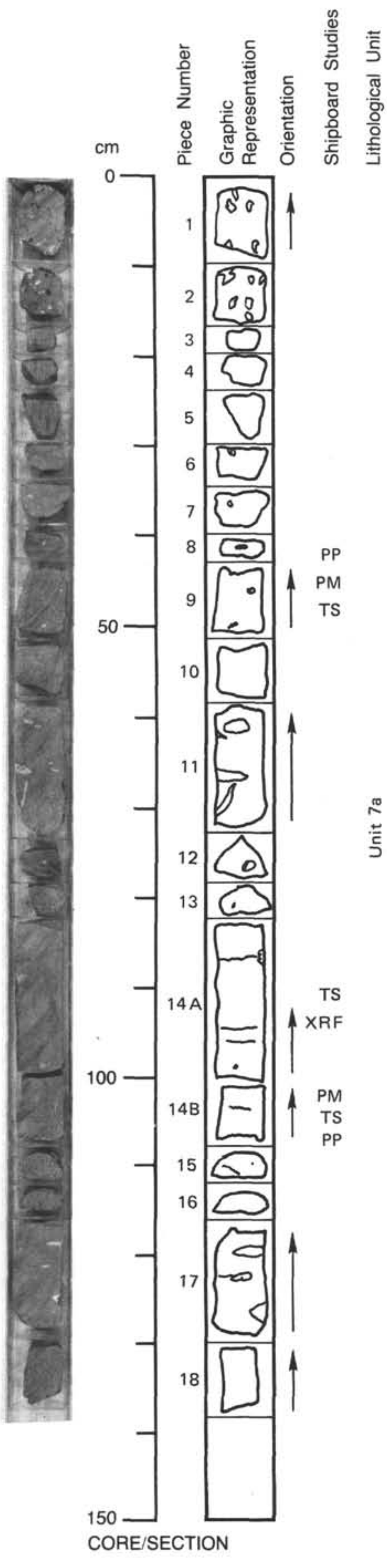

115-715A-23R-3

UNIT 7A (CONTINUED): VERY FINE-GRAINED PYROXENE-PLAGIOCLASE BASALT

Pieces 1–18

Continuous with 115-715A-23R-2, Unit 7A

PHENOCRYSTS: Plagioclase, ≤3 mm in size, <5%.
GROUNDMASS: Very fine grained, ≤0.08 mm. Pyroxene + plagioclase. Altered/weathered abundant limonite(?).
COLOR: Dark brown (10YR 3/3).
VESICLES:
115-715A-23R-2, Pieces 11 and 12, and 115-715A-23R-3, Pieces 1 and 2: Highly vesicular. Vesicles as wide as 6 mm, oval and round to irregular in shape, 20%. Some vesicles filled with calcite, others lined with brownish yellow (10YR 6/8) mineral (limonite?), forming microbotryoidal texture.
115-715A-23R-3, Pieces 3–18, and 115-715A-24R-1: Rare (<2%) vesicles, filled with calcite. Some "vugs" 1 cm long.
ALTERATION: Dark brown color (10YR 3/3) may be due to weathering or alteration; amount and effect are unknown.
VEINS/FRACTURES: Minor fractures filled with yellow brown mineral (limonite), e.g., Piece 14A. One fracture in Piece 14A has minor calcite.

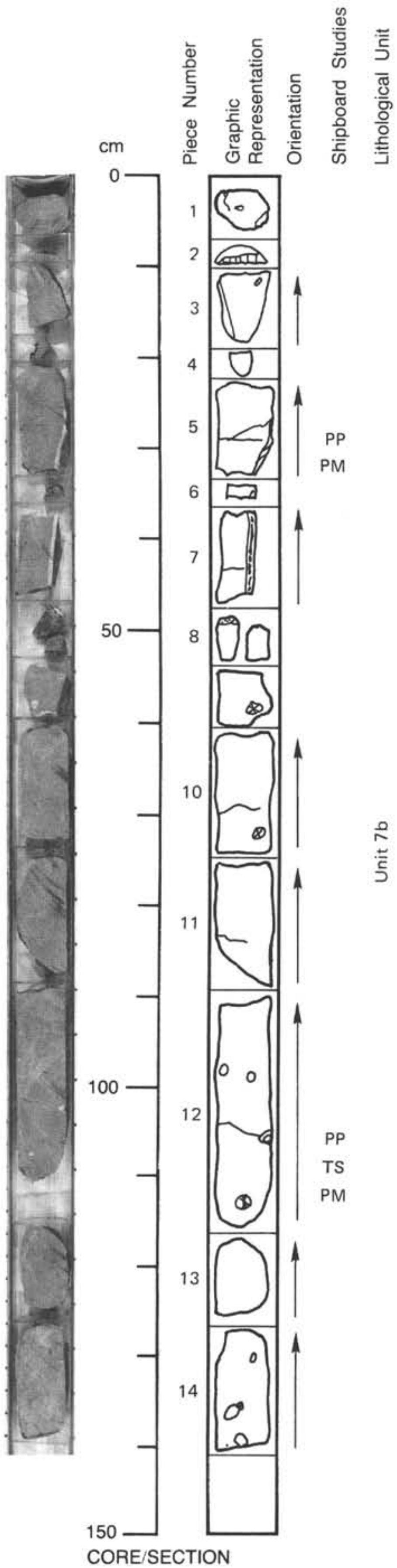

115-715A-24R-1

UNIT 7B: VERY FINE-GRAINED PYROXENE-PLAGIOCLASE BASALT

Pieces 1–14

Possibly continuous with 115-715A-23R-3, Unit 7A

COLOR: Grades from dark brown (10YR 3/3) at top of 115-715A-24R-1 to very dark gray (10YR 3/1) at bottom of 115-715A-24R-2.
VESICLES: Rare (<2%) vesicles, filled with calcite. Piece 9: Vesicle.
VEINS/FRACTURES: Piece 2: 5 mm thick vein.
Piece 5: Cracks, vein.
Piece 7: Vertical vein, 5 mm wide, filled with calcite.
Piece 9: Vein.
VOIDS: On back of Piece 10, 2 cm wide void filled with clay + calcite.

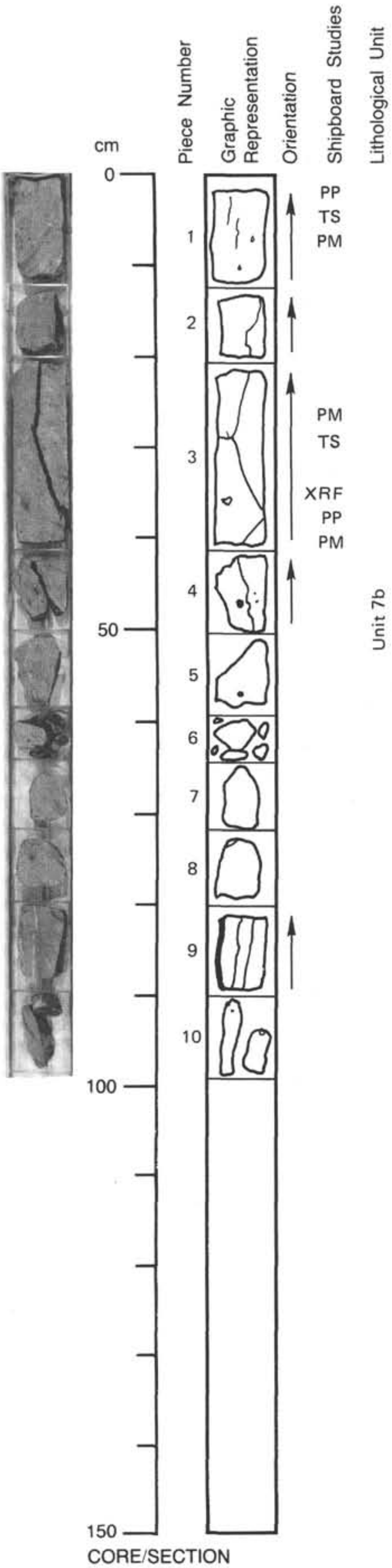

115-715A-24R-2

UNIT 7 B (CONTINUED): VERY FINE-GRAINED PYROXENE-PLAGIOCLASE BASALT

Pieces 1-10

Continuous with 115-715A-24R-1, Unit 7B

COLOR: Grades from dark brown (10YR 3/3) at top of 115-715A-24R-1 to very dark gray (10YR 3/1) at bottom of 115-715A-24R-2. Color change is most rapid at the top of 115-715A-24R-2, Piece 1, where rock changes dramatically from dark brown oxidized rock in 115-715A-24R-1, Piece 14, to black rock in 115-715A-24R-2, Piece 2.

VESICLES: Represent $\leq 1\%$ of rock, filled with green celadonite.

VEINS/FRACTURES: Pieces 1-3: Dark green clay mineral on surface of fractures.
Piece 9: Calcite-filled fracture. Next to fracture, a crack and a 1 cm wide parallel band of oxidation.

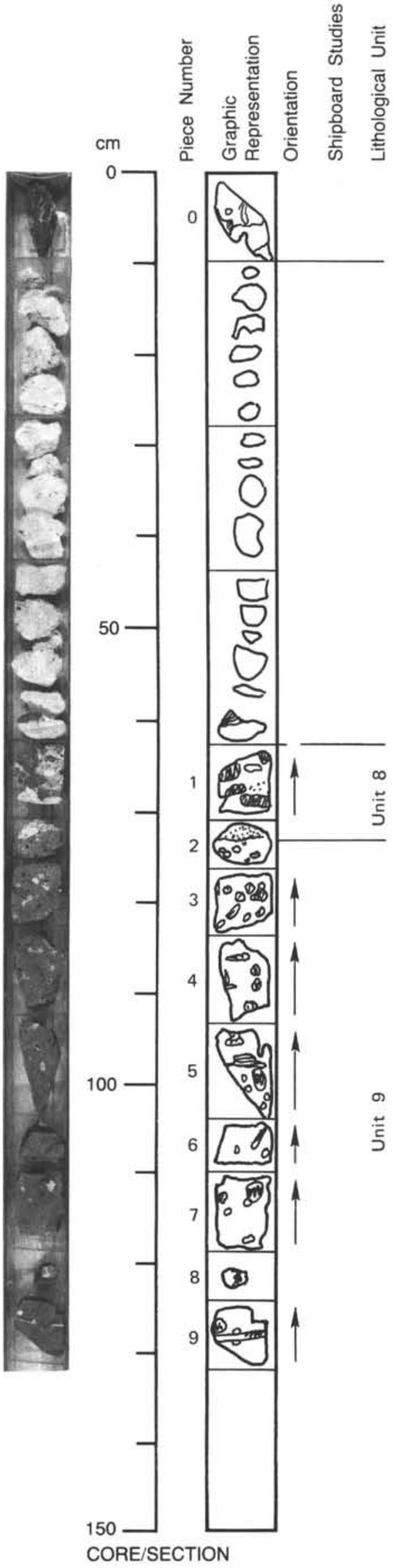

115-715A-25R-1

0–9 cm: VESICULAR BASALT FRAGMENT

VEINS/FRACTURES: Veins filled with calcite + zeolite.

9–63 cm: CARBONATE

CONTACTS: Lowest piece of sediment (60 cm) contains carbonate + basalt + clay.

UNIT 8: BASALT BRECCIA

Piece 1

GROUNDMASS: Carbonate matrix cementing basalt clasts.
ALTERATION: Clasts 1–20 mm in size include basalt in various stages of alteration. Clasts of coral also present.

UNIT 9: APHYRIC BASALT

Pieces 2–9

CONTACTS: Piece 2, top: Basalt breccia contact.
PHENOCRYSTS: None.
GROUNDMASS: Fine grained.
COLOR: Very dark gray (10YR 3/1) at 115-715A-25R-1, top of Unit 9, grading to very dark gray (5Y 3/1) at 115-715A-25R-3, 20 cm, dark grayish brown (10YR 4/2) at 115-715A-25R-3, 100 cm, reddish and yellowish brown (10YR 5/4) in lower part of 115-715A-25R-3, and reddish brown and red (10R 4/6) in 115-715A-25R-4, at base of Unit 9.
VESICLES: Filled with clay, calcite, and zeolite. Vesicles 1 cm in size at top (115-715A-25R-1, 76–111 cm), grading to vesicle-free zone (115-715A-25R-1, 125 cm, to 115-715A-25R-3, 90 cm), and then to vesicles 1–5 mm in size at base of Unit 9 (115-715A-25R-3, 90–112 cm).
ALTERATION: Moderate to high, varying with color(?).

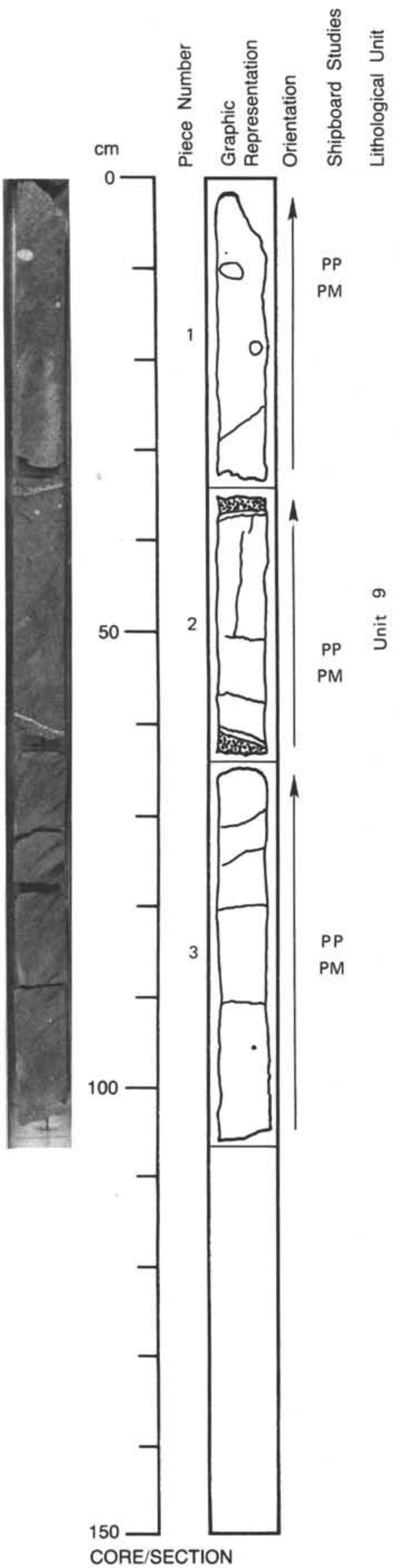

115-715A-25R-2

UNIT 9 (CONTINUED): APHYRIC BASALT

Pieces 1-3

Continuous with 115-715A-25R-1, Unit 9

GROUNDMASS: Massive.
COLOR: Very dark gray (10YR 3/1).
VESICLES: Grading to vesicle-free zone. Piece 1, 10 cm: Calcite-filled vesicles, 1 cm in size.
ALTERATION: Piece 2: At top, 1 cm wide zone of weathering to brown clay minerals. Angular clasts ≤1 cm long occur in weathered zone.
At base of Piece 2, 1 cm wide zone of weathering similar to above.
Piece 3: In center, relatively unaltered portion.
VEINS/FRACTURES: Small, <1 mm wide, calcite veins shown Pieces 1-3 on graphic representation. Piece 2: At top, fine calcite veins run through weathered zone parallel to weathering; however, calcite cuts the brown material.

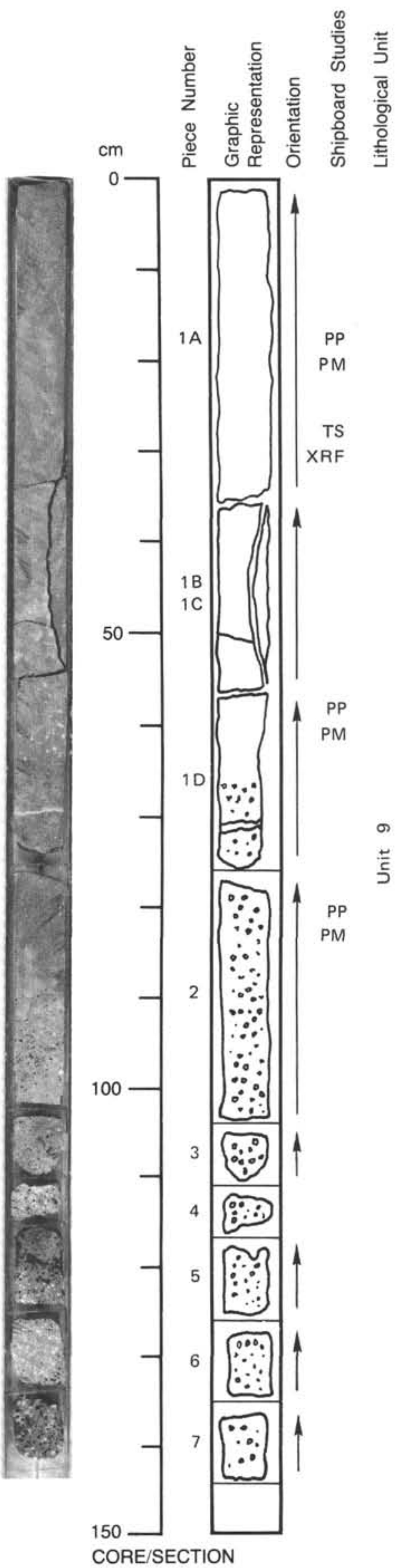

115-715A-25R-3

UNIT 9 (CONTINUED): APHYRIC BASALT

Pieces 1A–7

Continuous with 115-715A-25R-2, Unit 9

GROUNDMASS: Upper half: Aphyric, without vesicles. Lower half: Highly vesicular; lower clinker of the lava flow.
COLOR: Grading downward to very dark gray (5Y 3/1) at 20 cm, dark grayish brown (10YR 4/2) at 100 cm, and reddish and yellowish brown (10YR 5/4) from 100 to 144 cm.
VESICLES: Vesicle-free zone from top to 65 cm. Below 65 cm, vesicles 1–5 mm in size, ≈10%, some filled with carbonate.

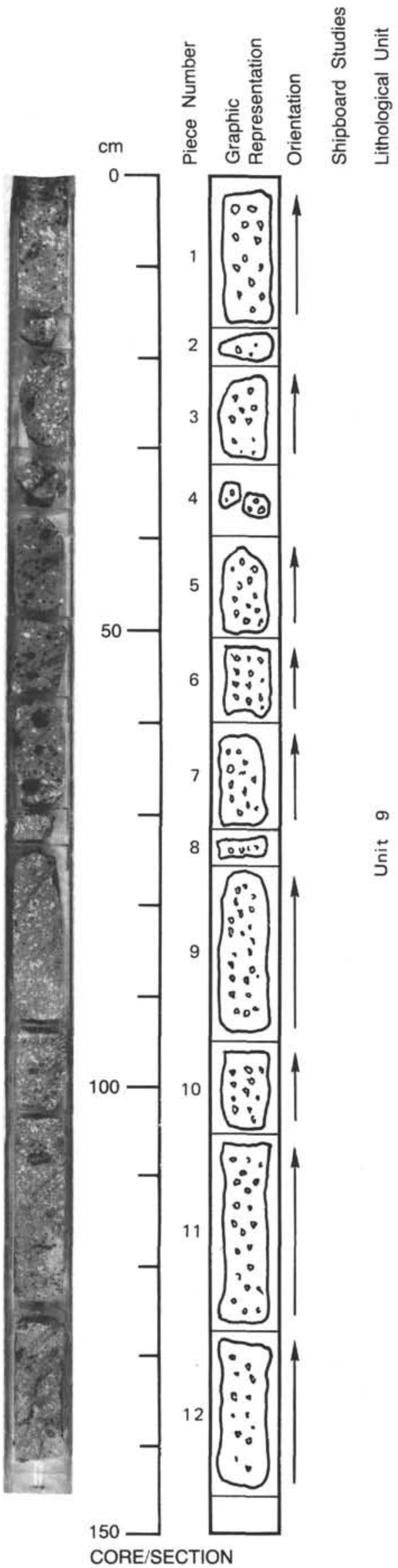

115-715A-25R-4

UNIT 9 (CONTINUED): APHYRIC BASALT

Pieces 1–12

Continuous with 115-715A-25R-3, Unit 9

COLOR: Reddish brown and red (10R 4/6).
VESICLES: Highly vesicular, vesicles as large as 8 mm. Half the vesicles are filled with carbonate.

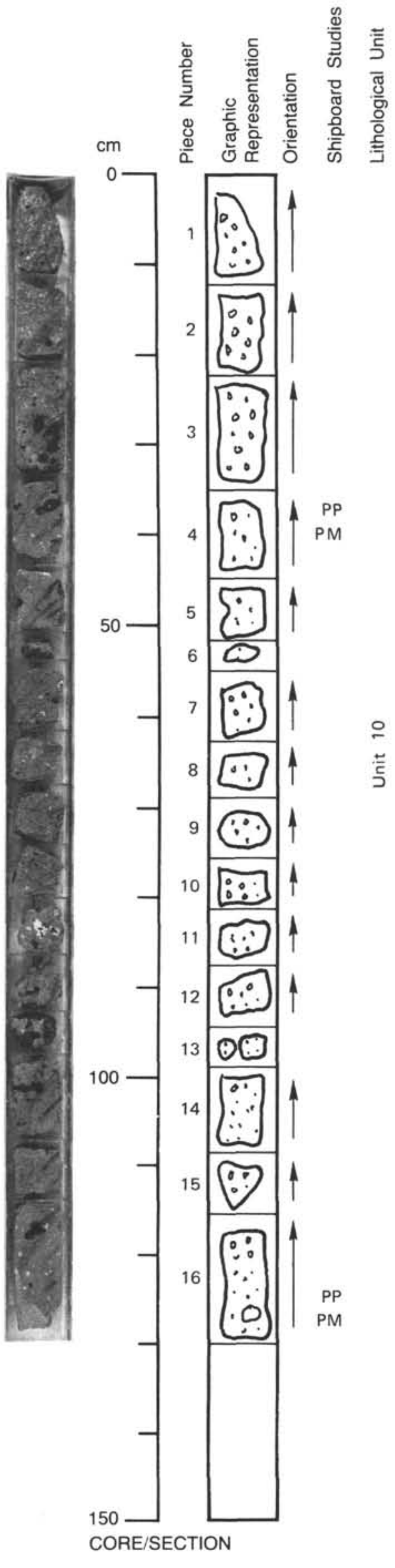

115-715A-25R-5

UNIT 10: APHYRIC BASALT

Pieces 1–16

PHENOCRYSTS: None.
GROUNDMASS: Fine grained.
COLOR: Pieces 1–15: Reddish brown (10YR 5/2).
Piece 16: Dark gray (2.5YR 4/0).
VESICLES: Pieces 1–15: <1 cm in size, ≈10%.
Piece 16: One larger vesicle (≈2 cm in diameter), partly filled with calcite, zeolite; round shape.
ALTERATION: Pieces 1–15: Moderate.
Piece 16: Slight.
VEINS/FRACTURES: None.

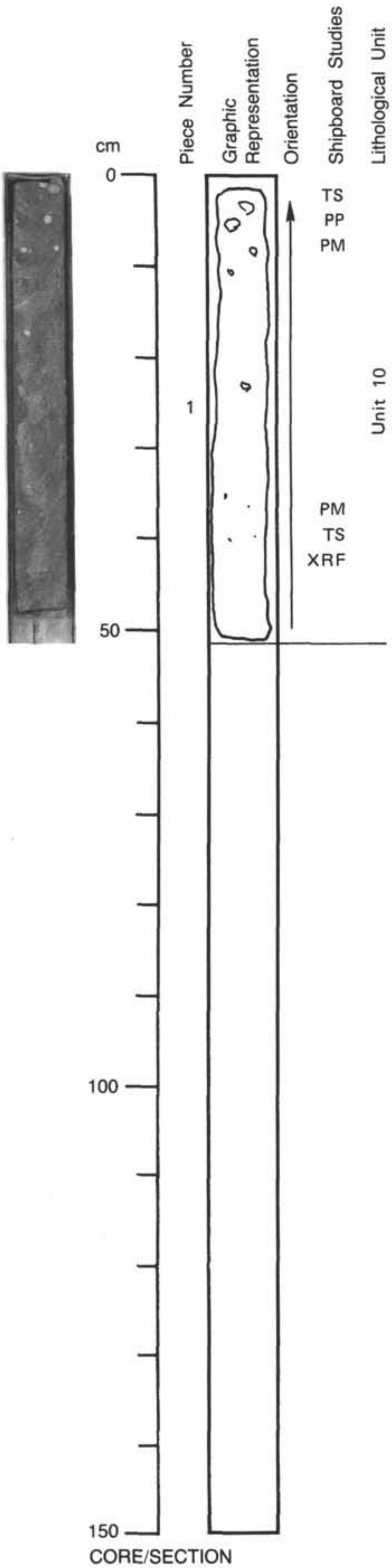

115-715A-25R-6

UNIT 10 (CONTINUED): APHYRIC BASALT

Piece 1

Continuous with 115-715A-25R-5, Unit 10

COLOR: Dark gray (2.5YR 4/0).
VESICLES: Upper part, Piece 1: Vesicle-rich, vesicles <1 cm in size, filled with clay + calcite(?).

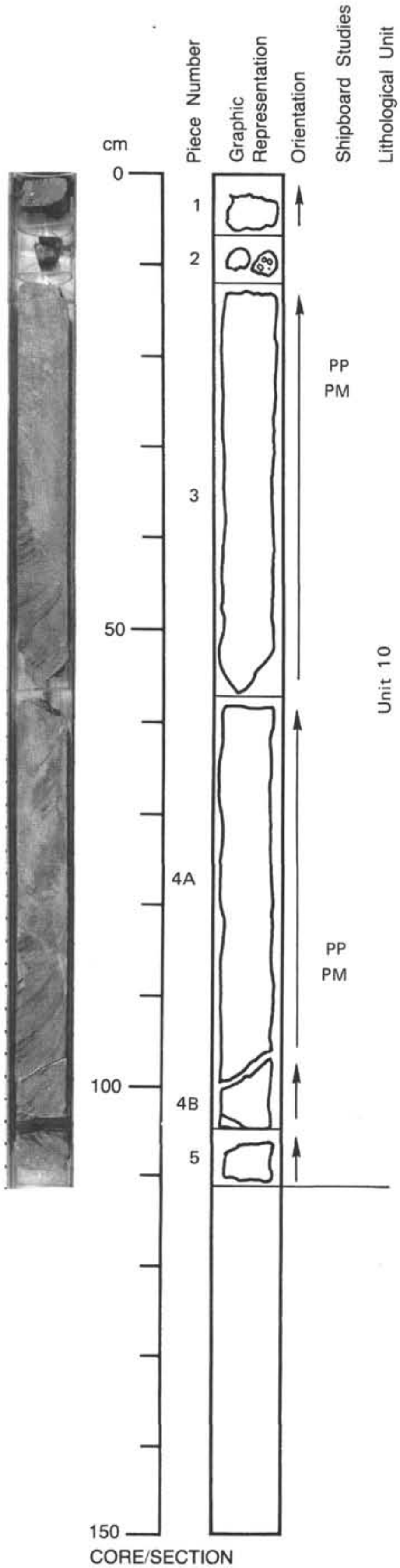

115-715A-26R-1

UNIT 10 (CONTINUED): APHYRIC BASALT

Pieces 1–5

Continuous with 115-715A-25R-6, Unit 10

VESICLES: Generally few vesicles. Piece 2: Highly vesicular.
VEINS/FRACTURES: Calcite-filled veins separate Piece 4A and 4B.

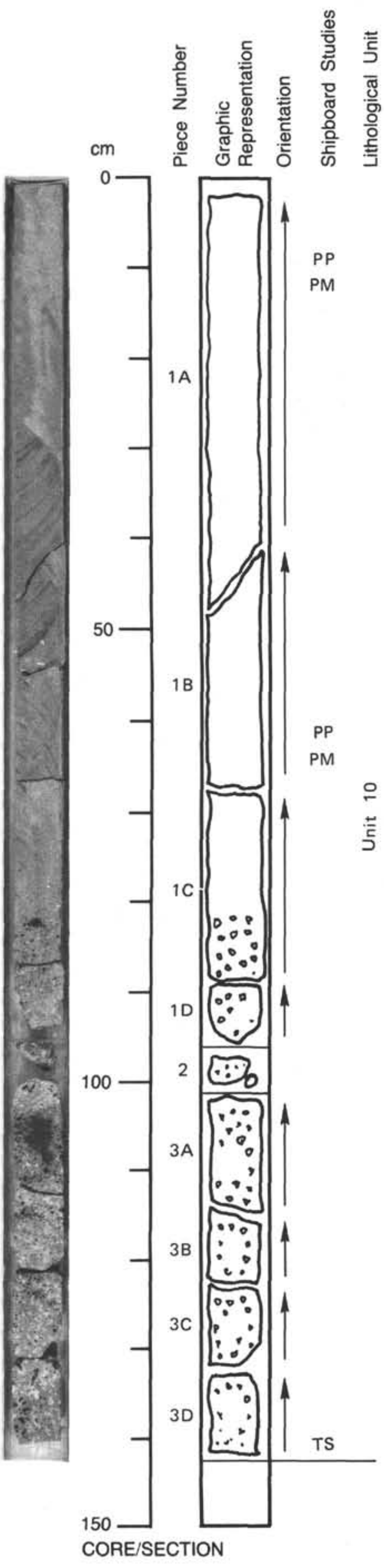

115-715A-26R-2

UNIT 10 (CONTINUED): APHYRIC BASALT

Pieces 1A–3D

Continuous with 115-715A-26R-1, Unit 10

GROUNDMASS: May be lower clinker of lava flow.
COLOR: Vesicular rocks (Piece 1C, lower part, through Piece 3C) are reddish brown.
VESICLES: Pieces 1A, 1B, and upper part of 1C: Generally few vesicles.
Lower part of Piece 1C–Piece 3D: Highly vesicular. Vesicles round to ellipsoidal, <5 mm in size, ≈15%, partly filled with calcite + zeolite(?).

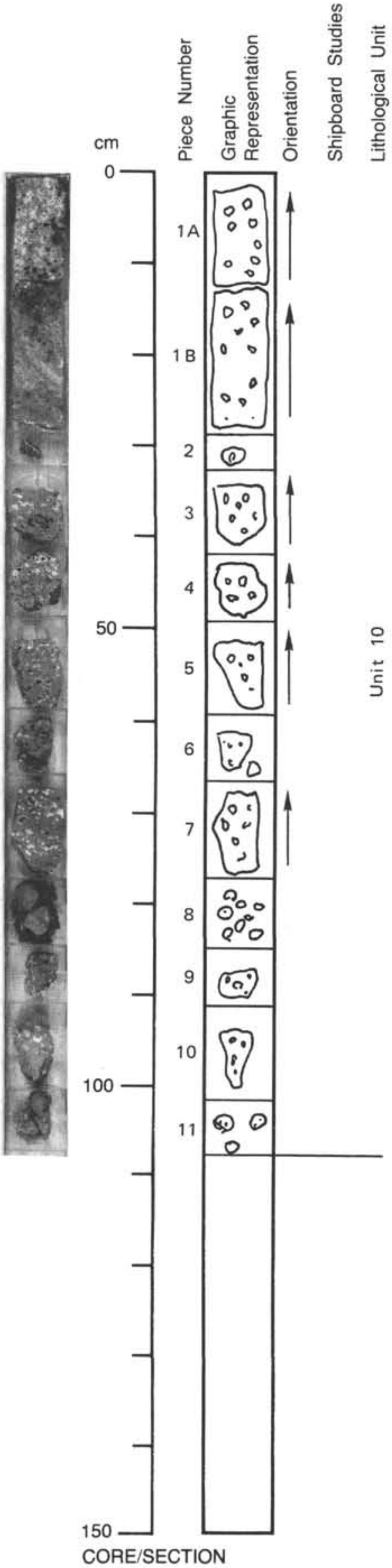

115-715A-26R-3

UNIT 10 (CONTINUED): APHYRIC BASALT

Pieces 1–11

Continuous with 115-715A-26R-2, Unit 10

CONTACTS: Pieces 8–11 are soily or highly altered, indicating the base of clinker.
VESICLES: Highly vesicular. Vesicles as large as 1 cm, filled with calcite + zeolite(?).
ALTERATION: Some parts of Pieces 8–11 are highly altered.

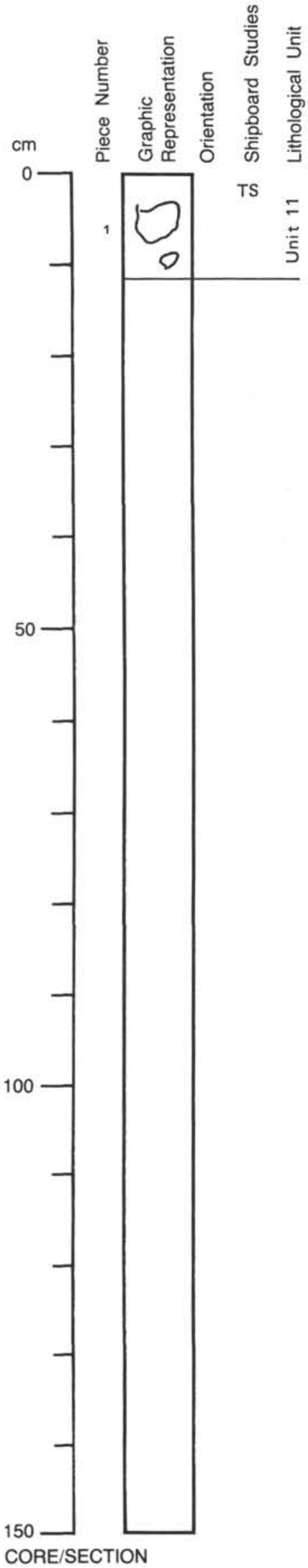

115-715A-27R-CC

UNIT 11: APHYRIC BASALT

Piece 1

PHENOCRYSTS: None.
GROUNDMASS: Fine grained.
COLOR: Dark gray (2.5YR 3/0).
VESICLES: As large as 2 mm, ≈5%, filled with brown clay.
ALTERATION: Moderately to highly altered.

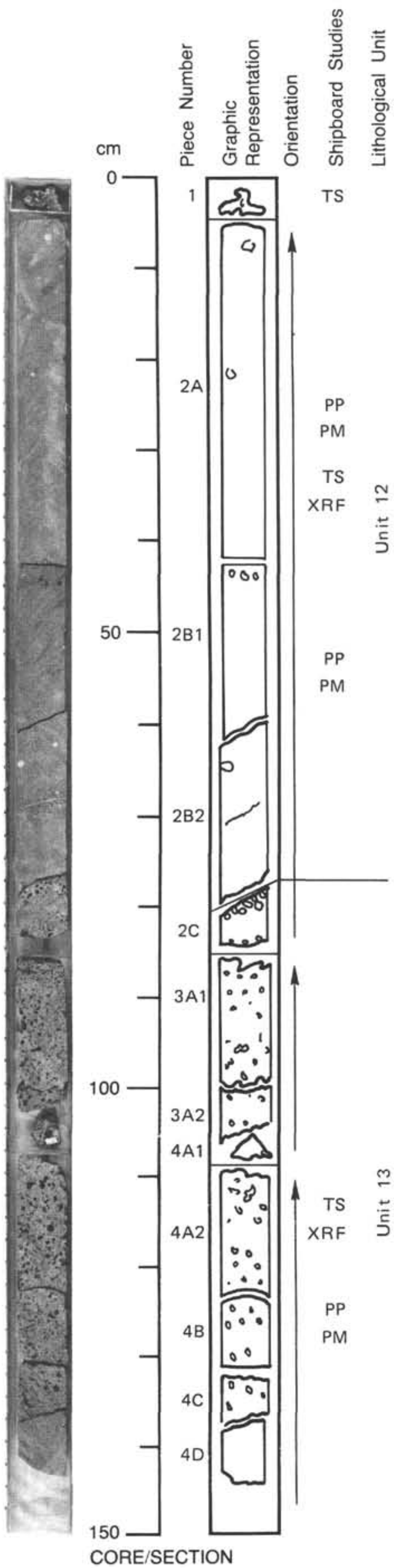

115-715A-29R-1

UNIT 12: PLAGIOCLASE-PHYRIC BASALT

Pieces 2A–2B2

PHENOCRYSTS: Plagioclase, <2 mm long, subhedral, fresh, ≈5%.
GROUNDMASS: Phaneritic, fine-grained plagioclase + clinopyroxene.
VESICLES: Rare, spherical, filled with calcite, <1%.
ALTERATION: Slight, altered to calcite.

UNIT 13: PLAGIOCLASE-PHYRIC BASALT

Pieces 2C–4D

PHENOCRYSTS: Plagioclase, <2 mm long, fresh, 5–10%.
GROUNDMASS: Phaneritic, fine-grained clinopyroxene + plagioclase. Pyrite crystals prominent in parts of matrix.
TEXTURE: Porphyritic, with intersertal groundmass.
VESICLES: Concentrated in upper 60 cm of unit, averaging ≈20% there. Rapid transition to <1% at 133–140 cm.
ALTERATION: Generally slight, but more pronounced in upper vesicular zone.

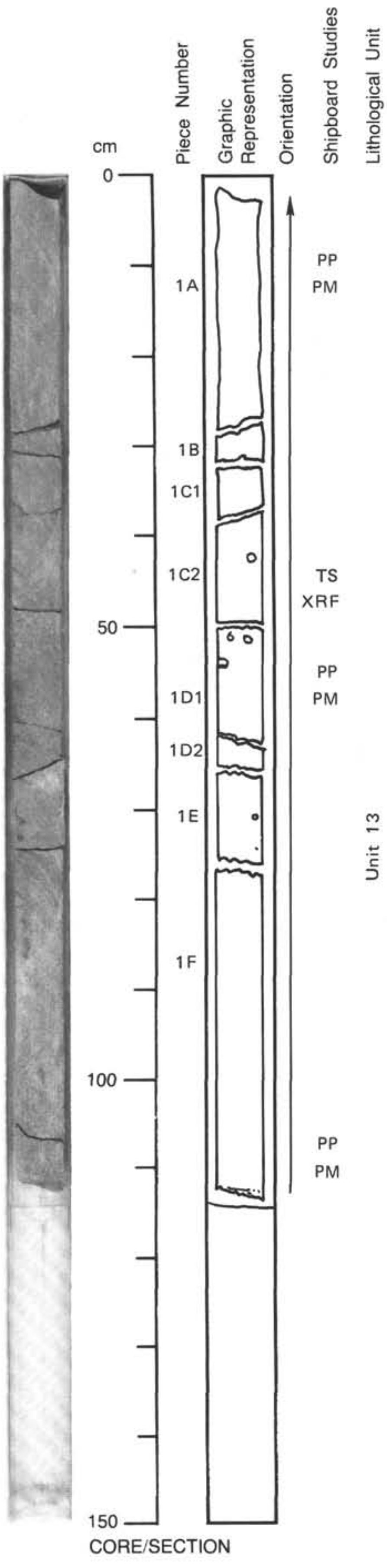

115-715A-29R-2

UNIT 13 (CONTINUED): PLAGIOCLASE-PHYRIC BASALT

Pieces 1A–1F

Continuous with 115-715A-29R-1, Unit 13

VESICLES: Few (similar to 115-715A-29R-1, 133–140 cm). Contains part of flow unit with vesicular top.

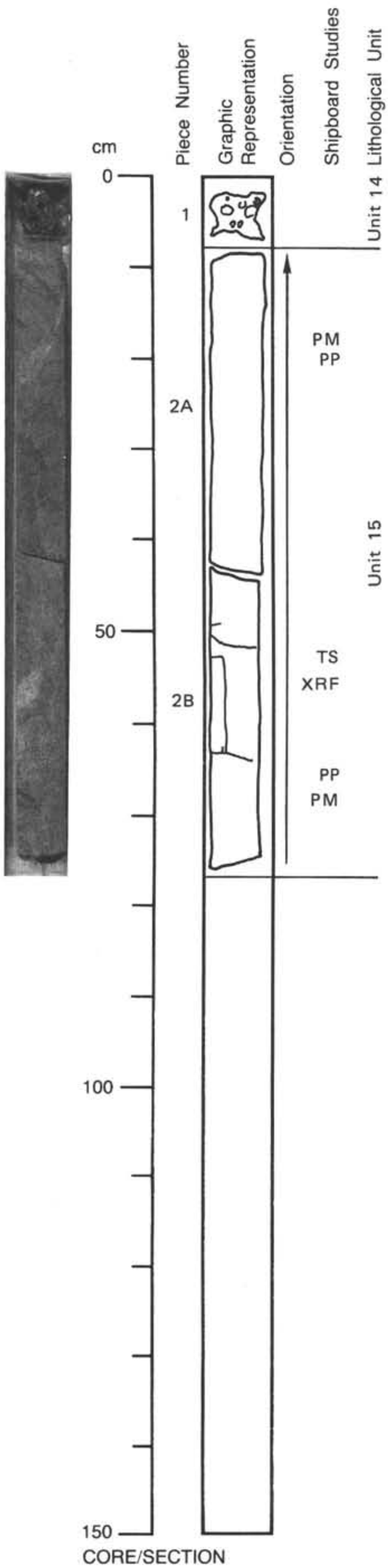

115-715A-30R-1

UNIT 14: HIGHLY ALTERED BASALT FRAGMENT (SOIL HORIZON?)

Piece 1

PHENOCRYSTS: Plagioclase - As large as 5 mm, <5%.
Clinopyroxene - As large as 5 mm, <5%.
GROUNDMASS: Completely altered.
VESICLES: 2-15 mm in size, filled with clay and perfect rhombs of calcite.
ALTERATION: High, to chlorite.

UNIT 15: MASSIVE BASALT

Pieces 2A-2B

CONTACTS: Piece 2A: Upper 5 cm oxidized.
Piece 2A, at 22 cm: Internal boundary shows slight change in mineralogy and texture.
PHENOCRYSTS: Olivine, as large as 1 mm, 5%. Replaced by green clay. In top of unit (Piece 2A, top) and base of unit (115-715A-30R-2, Piece 1, base) the exterior of olivine is oxidized to red clay.
GROUNDMASS: Massive. Fine-grained pyroxene + plagioclase. Partially altered to clay.
COLOR: Oxidized part is red.
VESICLES: None.
ALTERATION: Moderate. Groundmass partially altered to clay.
VEINS/FRACTURES: Piece 2B, base: Low-angle fracture, filled with calcite.
VOIDS: Irregular, <1 mm in size, filled with chlorite.

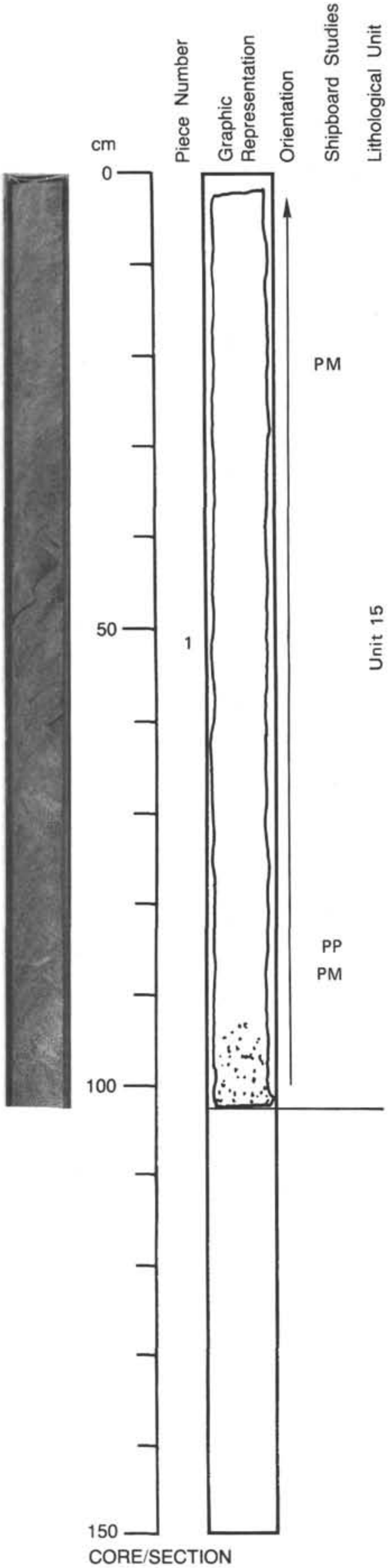

115-715A-30R-2

UNIT 15 (CONTINUED): MASSIVE BASALT UNIT

Piece 1

Continuous with 115-715A-30R-1, Unit 15

CONTACTS: Piece 1: Lower 10 cm oxidized.
PHENOCRYSTS: In base of unit (Piece 1, base) the exterior of olivine is oxidized to red clay.
GROUNDMASS: Massive, fine grained.
COLOR: Oxidized part is red.

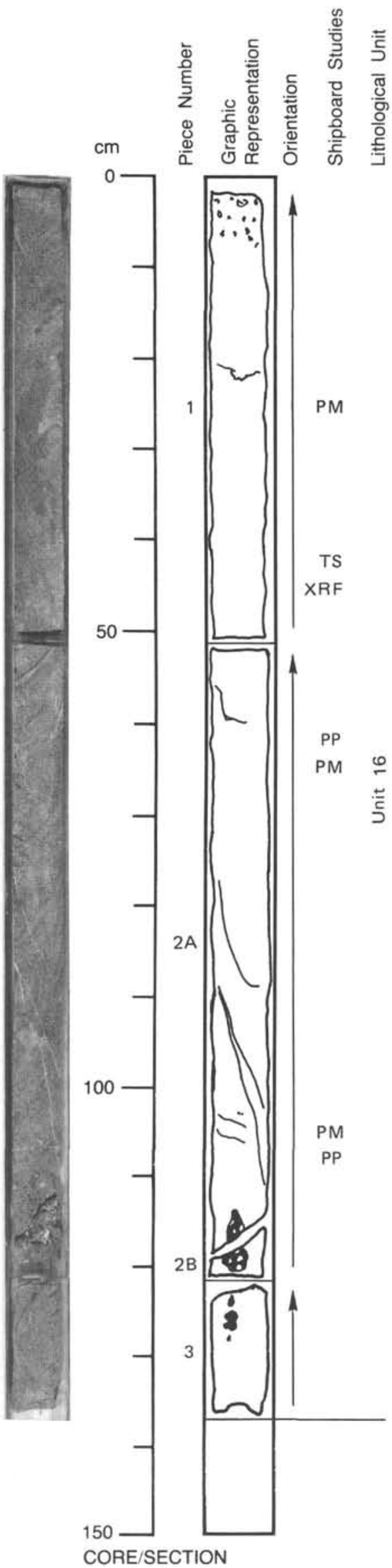

115-715A-30R-3

UNIT 16: OLIVINE-CLINOPYROXENE BASALT

Pieces 1–3

CONTACTS: Piece 1, upper part: Oxidized flow top. Olivine oxidized at top of unit.
PHENOCRYSTS: Olivine - 0.5–1.0 mm, 10% near top of unit, 5% or less in interior of flow.
Clinopyroxene - 0.5–1 mm, <5%.
Plagioclase - Rare, 1 mm.
GROUNDMASS: Fine-grained clinopyroxene and plagioclase partially altered to chlorite.
COLOR: Dark gray.
VESICLES: None.
ALTERATION: Groundmass to clay and olivine to iddingsite. Olivine is oxidized at top and base of unit.
Piece 2A, 110 cm, to Piece 3, 128 cm: Clay- and calcite-rich zone.
VEINS/FRACTURES: High- and low-angle veins, 1–2 mm in size, <1% of unit, filled with calcite.
Piece 2A: High-angle veins filled with calcite.

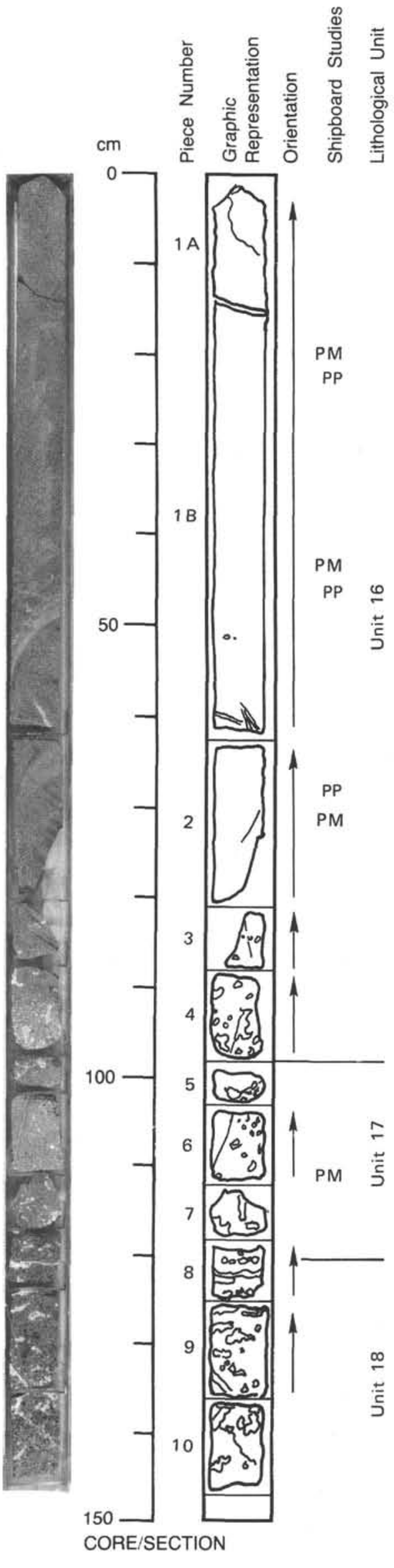

115-715A-30R-4

UNIT 16 (CONTINUED): OLIVINE-CLINOPYROXENE BASALT

Pieces 1A–4

Continuous with 115-715A-30R-3, Unit 16

CONTACTS: Vesicular contact at base of unit.
ALTERATION: Piece 4, lower part: Olivine oxidized at base of unit.
VOIDS: Base of unit, Piece 4, 90–99 cm: 1 cm sized voids, filled with calcite.

UNIT 17: OLIVINE BASALT

Pieces 5–7

PHENOCRYSTS: Olivine, 0.5–1.0 mm, 15%, altered, oxidized.
GROUNDMASS: Fine-grained plagioclase and clinopyroxene. Groundmass oxidized.
VESICLES: Concentrated at top and bottom of unit, 0.5–3.0 mm diameter, 1%. Vesicles >1 mm filled with calcite.
ALTERATION: Olivine altered and oxidized to clay. Oxidized groundmass is dusky red (2.5YR 3/2).
VEINS/FRACTURES: 1–2 mm in size, 1% of rock, filled with calcite.
VOIDS: As large as 2 cm in size, connected to vesicles, 2% of rock, filled with calcite, especially in Piece 4.

UNIT 18: OLIVINE BASALT

Pieces 8–10

VESICLES: Unit 18 is distinguished from Unit 17 by larger number of vesicles and the absence of calcite in many of the larger vesicles.

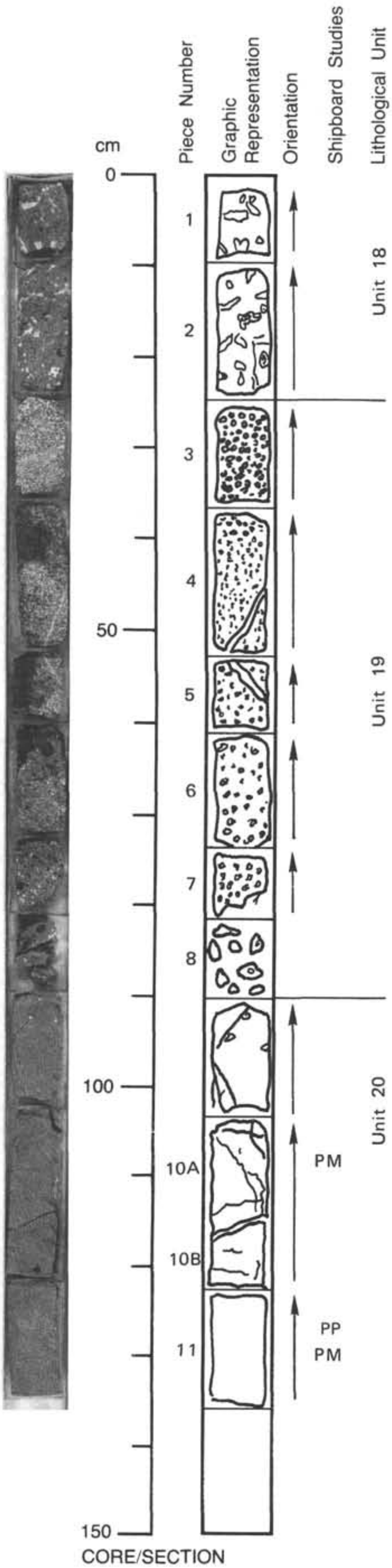

115-715A-30R-5

UNIT 18 (CONTINUED): OLIVINE BASALT

Pieces 1–2

Continuous with 115-715A-30R-4, Unit 18

UNIT 19: OLIVINE BASALT

Pieces 3–8

PHENOCRYSTS: Olivine(?) oxidized to clay, <1 mm in size, 5%.
GROUNDMASS: Fine grained.
VESICLES: 1–5 mm in size, 50% of rock, irregular shapes, filled with calcite.
Piece 3: Vesicles filled with calcite.
Piece 4: Vesicles mostly empty.
ALTERATION: Highly altered, oxidized; mafic phases altered.
VEINS/FRACTURES: 1–3 mm in size, filled with calcite.
Piece 4, lower part: Vein filled with calcite.

UNIT 20: OLIVINE-CLINOPYROXENE-PLAGIOCLASE BASALT

Pieces 9–11

PHENOCRYSTS: Olivine – 0.5 mm in size, 5–10%, altered.
Clinopyroxene – Poikilitic(?).
Plagioclase – 0.5–1.0 mm in size, 1%.
GROUNDMASS: Fine-grained clinopyroxene and plagioclase.
VESICLES: Round, 1–3 mm in size, <5%, clay-filled.
ALTERATION: Moderate, green clay. This section contains freshest rock of Hole 115-715A.
VEINS/FRACTURES: <1%, filled with clay or calcite.

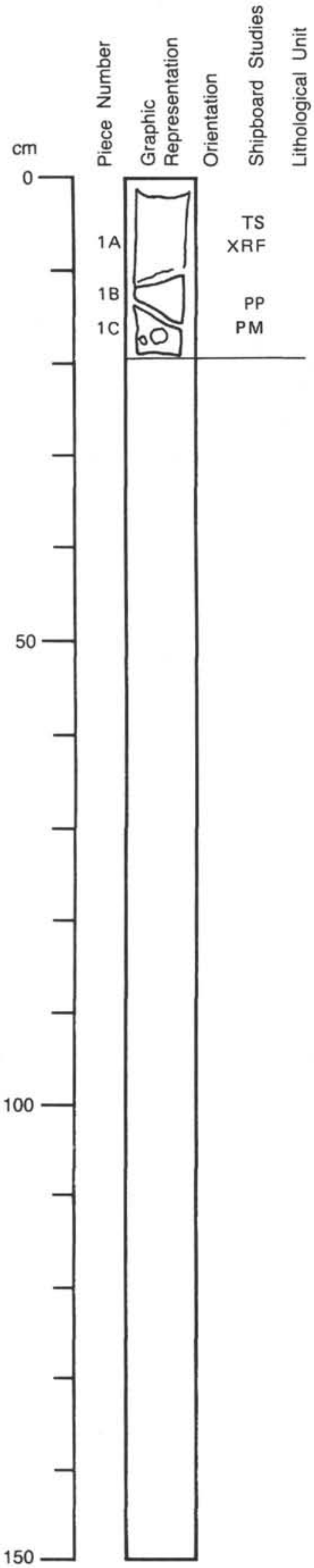

115-715A-30R-6

UNIT 20 (CONTINUED): OLIVINE-CLINOPYROXENE-PLAGIOCLASE BASALT

Pieces 1A–1C

Continuous with 115-715A-30R-5, Unit 20

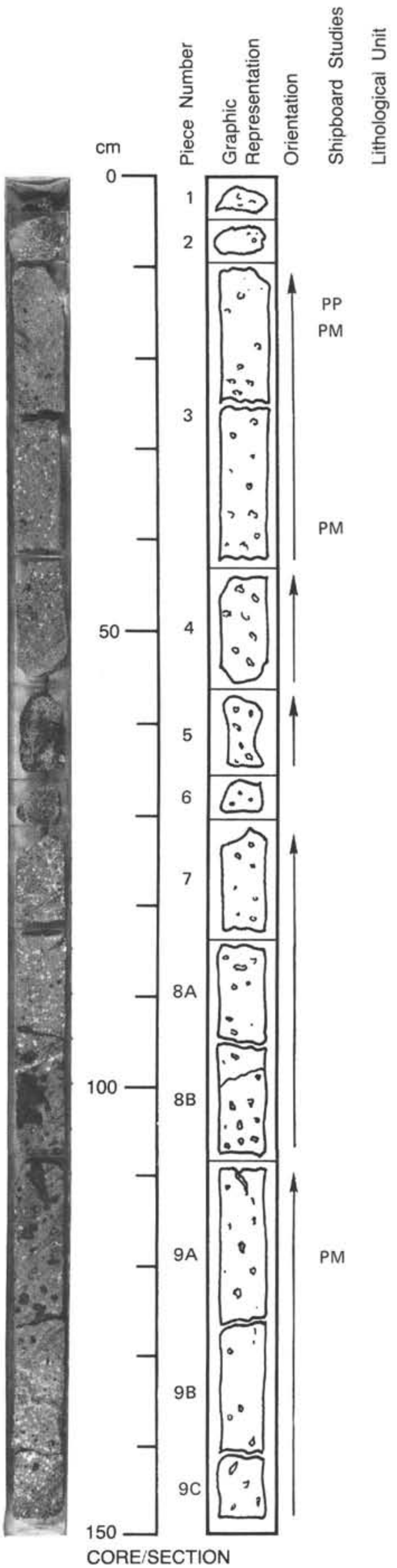

115-715A-31R-1

UNIT 21: MODERATELY ALTERED, VESICULAR PLAGIOCLASE-PHYRIC BASALT

Pieces 1-9C

PHENOCRYSTS: Plagioclase, subhedral, fresh, <2 mm long, $\approx$10% of rock.

GROUNDMASS: Phaneritic, fine grained, with intersertal texture. Possible hyalocrystalline in vesicular zones.

COLOR: Most altered material, e.g., Pieces 5, 6, 7, 9B, and 9C, is weak red (10R 5/4). Freshest vesicular material, e.g., Pieces 3A and 3B, is dark grayish brown (10YR 4/2) and dark brown (10YR 4/3). Freshest massive material (in 115-715A-31R-2, Unit 21) is gray (10YR 5/1) and dark gray (10YR 5/1).

VESICLES: Typically sub-ellipsoidal, as large as 10 mm, uniformly distributed when present, but diminish into a massive zone (see 115-715A-31R-2, Unit 21). Generally partially filled by calcite + limonite.

ALTERATION: Moderate ($\approx$20%), mainly to calcite. Matrix contains $\approx$10% of a reddish alteration phase, possibly(?) iddingsite after olivine.

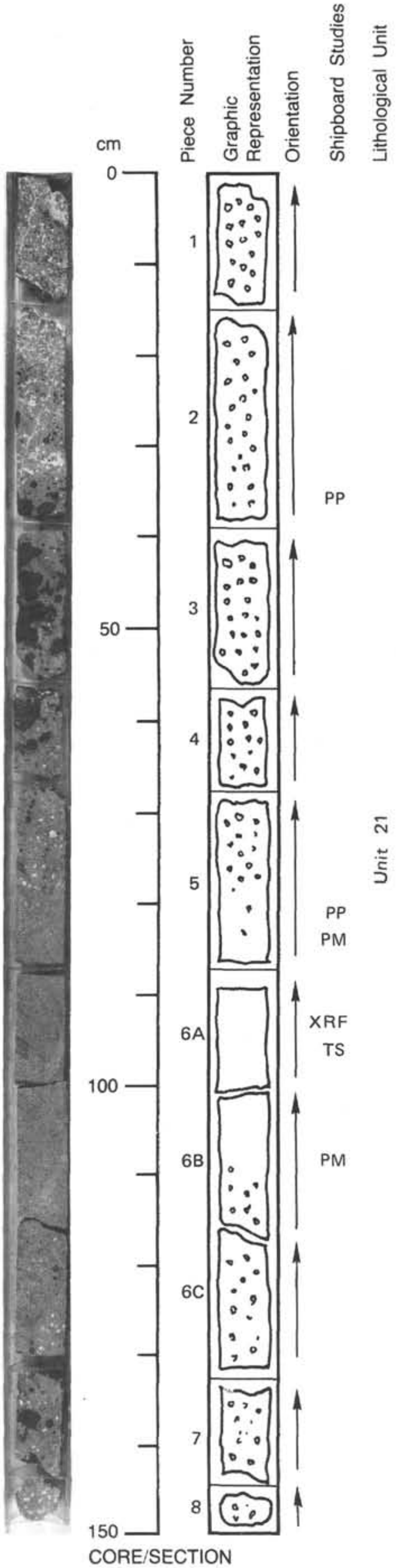

115-715A-31R-2

UNIT 21 (CONTINUED): MODERATELY ALTERED, VESICULAR PLAGIOCLASE-PHYRIC BASALT

Pieces 1-8

Continuous with 115-715A-31R-1, Unit 21

COLOR: Freshest massive material in unit is in 115-715A-31R-2, gray (10YR 5/1) and dark gray (10YR 5/1).
Pieces 1, 2, and 8: Reddish brown (10R 5/6).
Base of Piece 1, top of Piece 2: Yellowish brown (10YR 5/8).
Pieces 3-7: Brownish gray (10YR 3/2).

VESICLES: As large as 3 mm in size, and <10%. Highly vesicular in Pieces 1-4, upper half of Piece 5, lower half of Piece 6B, and Pieces 6B, 6C, 7, and 8. Same as 115-715A-31R-1, Unit 21. Moderately to slightly vesicular in other pieces.

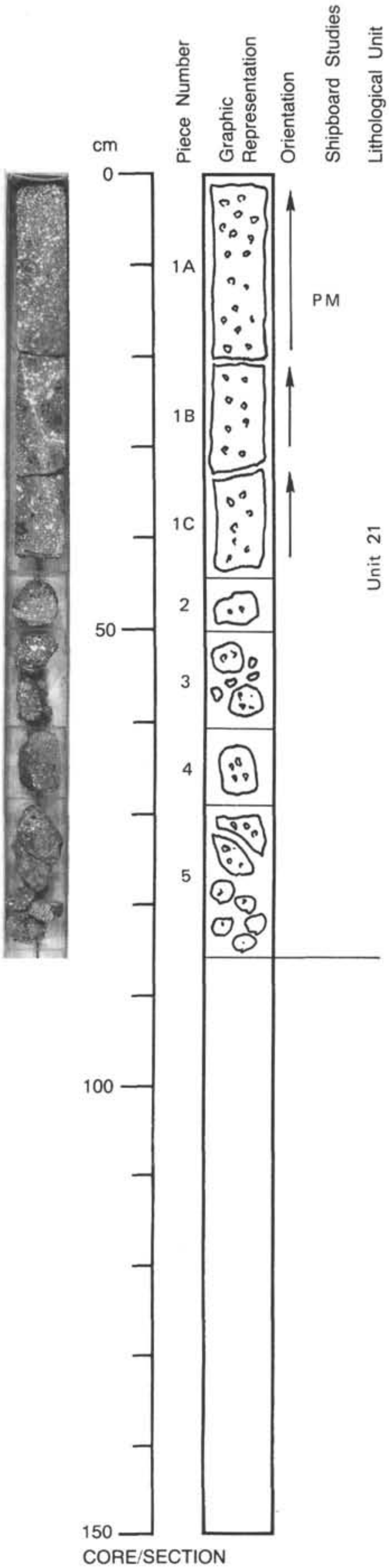

115-715A-31R-3

UNIT 21 (CONTINUED): MODERATELY ALTERED, VESICULAR PLAGIOCLASE-PHYRIC BASALT

Pieces 1-5

Continuous with 115-715A-31R-2, Unit 21

COLOR: Same as upper part of 115-715A-31R-2, Unit 21 (Pieces 1 and 2), reddish brown (10R 5/6).

VESICLES: Same as upper part of 115-715A-31R-2, Unit 21 (Pieces 1 and 2), highly vesicular.

THIN SECTION DESCRIPTION

115-715A-23R-2 (Piece 2A, 26-28 cm)

ROCK NAME: Sparsely plagioclase olivine phyric basalt

WHERE SAMPLED: Center of Unit 4, 212.74 mbsf

TEXTURE: Vesicular, sparsely porphyritic

GRAIN SIZE: Fine

OBSERVER: RBH

PRIMARY MINERALOGY	PERCENT PRESENT	PERCENT ORIGINAL	SIZE RANGE (mm)	APPROX. COMPOSITION	MORPHOLOGY	COMMENTS
PHENOCRYSTS						
Olivine	—	1	<1		Euhedral	Completely altered to red iddingsite.
Plagioclase	3	3	<1.5		Euhedral	Slight oscillatory zoning. Extinction angle = 58 ° (010).
GROUNDMASS						
Olivine(?)	—	<1	0.05			
Plagioclase	46	46	0.5		Laths	Very abundant in groundmass.
Clinopyroxene	10	25	0.1		Subhedral	
Opaques	5	5	0.04	Fe-Ti	Skeletal	Ubiquitous. Very fine skeletal crystals. Possibly somewhat oxidized.

SECONDARY MINERALOGY	PERCENT	REPLACING/ FILLING	COMMENTS
Clays	15	Cpx, ol	Ol is altered to red iddingsite. Groundmass cpx is altered to yellowish opaque clay.
Clays	2	Vesicles	
Carbonate	15	Vesicles	Calcite.
Hematite	1	Cpx, ol	Red pigmentation of clay and altered mafic minerals in groundmass.

VESICLES/ CAVITIES	PERCENT	LOCATION	SIZE RANGE (mm)	FILLING	SHAPE	COMMENTS
Vesicles	20	Even	<5	Calcite, clays	Round, oblate	Some vesicles filled with calcite. Others are completely or partially filled with yellowish cryptocrystalline clays (or other material).

THIN SECTION DESCRIPTION

115-715A-23R-2 (Piece 5, 76-78 cm)

ROCK NAME: Sparsely plagioclase phyric basalt

WHERE SAMPLED: 36 cm below top of Unit 5, 213.30 mbsf

TEXTURE: Fluidal, sparsely porphyritic to aphanitic

GRAIN SIZE: Fine

OBSERVER: YT

PRIMARY MINERALOGY	PERCENT PRESENT	PERCENT ORIGINAL	SIZE RANGE (mm)	APPROX. COMPOSITION	MORPHOLOGY	COMMENTS
PHENOCRYSTS						
Plagioclase	1	1	<0.4		Euhedral	Clear, normally zoned crystals.
GROUNDMASS						
Plagioclase	62	62	<0.2		Subhedral	Fluidal texture.
Clinopyroxene	10	10	<0.2	Augite	Subhedral	Colorless.
Opaques	10	10	<0.2		Subhedral-euhedral	
Glass	—	10				Completely altered to clay.

SECONDARY MINERALOGY	PERCENT	REPLACING/ FILLING	COMMENTS
Clays	10	Glass	Clay + unidentifiable fine-grained minerals.
Carbonate	7	Vesicles	

VESICLES/ CAVITIES	PERCENT	LOCATION	SIZE RANGE (mm)	FILLING	SHAPE	COMMENTS
Vesicles	15	Even	<5	Calcite or none	Round, elliptical	Filled with calcite or empty.

THIN SECTION DESCRIPTION

115–715A–23R–3 (Piece 9, 44–46 cm)

ROCK NAME: Sparsely plagioclase clinopyroxene phyric basalt

WHERE SAMPLED: Interior of Unit 7, 214.23 mbsf

TEXTURE: Sparsely porphyritic

GRAIN SIZE: Fine phaneritic

OBSERVER: ANB

PRIMARY MINERALOGY	PERCENT PRESENT	PERCENT ORIGINAL	SIZE RANGE (mm)	APPROX. COMPOSITION	MORPHOLOGY	COMMENTS
PHENOCRYSTS						
Plagioclase	1	1	<1		Subhedral	Slightly sericitized. Normal zoning on margins.
Clinopyroxene	1	1	<2	Augite	Anhedral	One large rounded colorless augite phenocryst.
GROUNDMASS						
Olivine	—	1	<0.1		Subhedral	Completely altered to iddingsite.
Clinopyroxene	15	15	<0.2	Augite	Subhedral	
Plagioclase	51	51	<0.2		Subhedral	Moderately sericitized.
Spinel	5	5	<0.1	Titano-magnetite	Anhedral	
Glass(?)	—	26				Interstitial. Completely replaced by brown smectite.

SECONDARY MINERALOGY	PERCENT	REPLACING/ FILLING	COMMENTS
Clays	26	Glass(?)	Brown smectite fills interstices.
Iddingsite	1	Ol	—

THIN SECTION DESCRIPTION

115–715A–23R–3 (Piece 14A, 92–94 cm)

ROCK NAME: Sparsely plagioclase phyric basalt

WHERE SAMPLED: Interior of Unit 7, 214.79 mbsf

TEXTURE: Sparsely porphyritic

GRAIN SIZE: Fine

OBSERVER: ANB

PRIMARY MINERALOGY	PERCENT PRESENT	PERCENT ORIGINAL	SIZE RANGE (mm)	APPROX. COMPOSITION	MORPHOLOGY	COMMENTS
PHENOCRYSTS						
Plagioclase	<1	<1	<1		Subhedral	
GROUNDMASS						
Plagioclase	53	53	<0.2		Subhedral	Moderately sericitized.
Clinopyroxene	10	10	<0.1	Augite	Anhedral	Colorless augite.
Olivine	—	4	<0.2		Subhedral–anhedral	Completely replaced by iddingsite + limonite(?).
Spinel	3	3	<0.2	Titano-magnetite	Anhedral	
Glass(?)	—	30				Interstitial. Completely replaced by brown smectites + limonite.

SECONDARY MINERALOGY	PERCENT	REPLACING/ FILLING	COMMENTS
Clays	30	Glass(?)	Brown smectites + limonite in interstices. Also partially stain matrix and plag crystals.
Iddingsite, limonite(?)	4	Ol	

COMMENTS: Oxidized, weathered basalt. Moderately limonite-rich.

THIN SECTION DESCRIPTION

115-715A-23R-3 (Piece 14B, 104-106 cm)

ROCK NAME: Sparsely plagioclase phyric basalt
WHERE SAMPLED: Interior of Unit 7, 214.95 mbsf
TEXTURE: Sparsely porphyritic, fluidal
GRAIN SIZE: Fine, phaneritic
OBSERVER: ANB

PRIMARY MINERALOGY	PERCENT PRESENT	PERCENT ORIGINAL	SIZE RANGE (mm)	APPROX. COMPO-SITION	MORPHOLOGY	COMMENTS
PHENOCRYSTS						
Plagioclase	1	1	<2		Subhedral	Slightly sericitized.
GROUNDMASS						
Plagioclase	65	65	<0.2		Subhedral	Prominent fluidal texture. Moderately sericitized.
Clinopyroxene	15	15	<0.1	Augite	Anhedral	Colorless. Fresh.
Olivine	—	1	<0.1		Subhedral	Completely altered to iddingsite.
Spinel	3	3	<0.1	Titano-magnetite	Anhedral	Completely altered to smectites.
Glass(?)	—	15				

SECONDARY MINERALOGY	PERCENT	REPLACING/ FILLING	COMMENTS
Clays	15	Glass(?)	Yellow-brown smectites.
Iddingsite	1	Ol	

VESICLES/ CAVITIES	PERCENT	LOCATION	SIZE RANGE (mm)	FILLING	SHAPE	COMMENTS
Vesicles	Tr		<2	None	Spherical	Very rare.

THIN SECTION DESCRIPTION

115-715A-24R-1 (Piece 12, 109-111 cm)

ROCK NAME: Sparsely plagioclase phyric basalt
WHERE SAMPLED: Interior of Unit 7, 221.60 mbsf
TEXTURE: Sparsely porphyritic, intersertal
GRAIN SIZE: Fine, phaneritic
OBSERVER: ANB

PRIMARY MINERALOGY	PERCENT PRESENT	PERCENT ORIGINAL	SIZE RANGE (mm)	APPROX. COMPO-SITION	MORPHOLOGY	COMMENTS
PHENOCRYSTS						
Plagioclase	1	1	<2		Subhedral-anhedral	Fresh.
GROUNDMASS						
Olivine	—	4	<0.4		Subhedral-anhedral	Completely altered to iddingsite + limonite.
Plagioclase	50	50	<0.7		Subhedral	Slightly sericitized.
Clinopyroxene	15	15	<0.4	Augite	Anhedral	Colorless crystals.
Spinel	2	2	<0.2	Titano-magnetite	Anhedral	
Glass(?)	—	28				Completely replaced by smectites + limonite.

SECONDARY MINERALOGY	PERCENT	REPLACING/ FILLING	COMMENTS
Clays	28	Glass(?)	Radial growths of brown/yellow smectite + limonite.
Iddingsite	4	Olivine	

VESICLES/ CAVITIES	PERCENT	LOCATION	SIZE RANGE (mm)	FILLING	SHAPE
Vesicles	1	Even	<1	Smectite	Spherical

COMMENTS: Rather oxidized, weathered basalt.

THIN SECTION DESCRIPTION

115-715A-24R-2 (Piece 1, 2-4 cm)

ROCK NAME: Sparsely plagioclase phyric basalt
WHERE SAMPLED: Interior of Unit 7, 222.02 mbsf
TEXTURE: Sparsely porphyritic, fluidal
GRAIN SIZE: Fine, phaneritic
OBSERVER: ANB

PRIMARY MINERALOGY	PERCENT PRESENT	PERCENT ORIGINAL	SIZE RANGE (mm)	APPROX. COMPOSITION	MORPHOLOGY	COMMENTS
PHENOCRYSTS						
Plagioclase	1	1	<1		Subhedral	
GROUNDMASS						
Plagioclase	60	60	<0.5		Subhedral	Strong fluidal texture.
Olivine	—	8	<0.2		Subhedral–anhedral	Completely altered to iddingsite + limonite(?).
Clinopyroxene	20	20	<0.4	Augite	Anhedral	Colorless augite.
Spinel	3	3	<0.3	Titano-magnetite	Subhedral	
Glass(?)	—	8				Interstitial. Completely replaced by smectites.

SECONDARY MINERALOGY	PERCENT	REPLACING/ FILLING	COMMENTS
Clays	8	Glass(?)	Yellow-brown smectite clays, possibly after glass.
Iddingsite, limonite(?)	8	Ol	

COMMENTS: Oxidized, weathered basalt.
Transversed by thin fracture, discontinuously filled by calcite.

THIN SECTION DESCRIPTION

115-715A-24R-2 (Piece 3, 27-30 cm)

ROCK NAME: Sparsely plagioclase phyric basalt
WHERE SAMPLED: Interior of Unit 7, 222.27 mbsf
TEXTURE: Sparsely porphyritic, subophitic
GRAIN SIZE: Aphanitic, hyalocrystalline
OBSERVER: ANB

PRIMARY MINERALOGY	PERCENT PRESENT	PERCENT ORIGINAL	SIZE RANGE (mm)	APPROX. COMPOSITION	MORPHOLOGY	COMMENTS
PHENOCRYSTS						
Plagioclase	1	1	<2		Subhedral	Fresh. Strong normal zoning.
GROUNDMASS						
Plagioclase	40	40	<0.3		Subhedral	Fresh. Normal zoning. Subophitic, intergrown with augite.
Clinopyroxene	30	30	<0.2	Augite	Anhedral	Colorless augite.
Spinel	3	3	<0.2	Titano-magnetite	Anhedral	
Olivine	—	2	<0.1		Subhedral	Completely altered to brown smectites.
Glass	—	24				Interstitial. Altered at least partially to brown smectites.

SECONDARY MINERALOGY	PERCENT	REPLACING/ FILLING	COMMENTS
Clays	26	Glass, ol	Brown smectites. Replacement of interstitial glass.

VESICLES/ CAVITIES	PERCENT	LOCATION	SIZE RANGE (mm)	FILLING	SHAPE	COMMENTS
Vesicles	Tr		<1	Smectite	Spherical	Filled by brown smectite + limonite(?).

THIN SECTION DESCRIPTION

115-715A-25R-3 (Piece 1A, 25-27 cm)

ROCK NAME: Highly olivine phyric basalt

WHERE SAMPLED: Interior of Unit 9, 233.25 mbsf

TEXTURE: Highly phyric, subophitic

GRAIN SIZE: Fine, phaneritic

OBSERVER: JDG

PRIMARY MINERALOGY	PERCENT PRESENT	PERCENT ORIGINAL	SIZE RANGE (mm)	APPROX. COMPO-SITION	MORPHOLOGY	COMMENTS
PHENOCRYSTS						
Olivine	—	10	<1.5		Euhedral	Completely altered to clays.
GROUNDMASS						
Plagioclase	39	39	<0.4		Subhedral	Appears quite fresh.
Clinopyroxene	39	39	0.2	Augite	Anhedral	Some grains could be altered.
Opaques	2	2	<0.04	Fe-Ti	Subhedral	
Glass(?)	—	10				Completely altered.

SECONDARY MINERALOGY	PERCENT	REPLACING/ FILLING	COMMENTS
Clays	20	Glass(?), ol	Replacing glass or some augite. Hard to tell for sure what is being replaced.

VESICLES/ CAVITIES	PERCENT	LOCATION	SIZE RANGE (mm)	FILLING	SHAPE
Vesicles	<1		<2.5	Clays	Round

THIN SECTION DESCRIPTION

115-715A-25R-6 (Piece 1, 2-4 cm)

ROCK NAME: Aphyric basalt

WHERE SAMPLED: Interior of Unit 10, 237.52 mbsf

TEXTURE: Aphyric, subophitic

GRAIN SIZE: Fine,

OBSERVER: ANB

PRIMARY MINERALOGY	PERCENT PRESENT	PERCENT ORIGINAL	SIZE RANGE (mm)	APPROX. COMPO-SITION	MORPHOLOGY	COMMENTS
GROUNDMASS						
Plagioclase	60	60	<1		Subhedral	Moderately sericitized.
Clinopyroxene	20	20	<2	Augite		Ophitic to subophitic intergrowths with plag. Colorless.
Spinel	1	1	<0.5	Titano-magnetite	Anhedral	Ilmenite laths also possibly present.
Olivine	—	Tr	<0.5		Anhedral	Completely altered to serpentine.
Glass(?)	—	19				Interstitial. Completely altered.

SECONDARY MINERALOGY	PERCENT	REPLACING/ FILLING	COMMENTS
Clays	19	Glass(?)	Radially disposed pale green interstitial clays (possibly chlorite group).
Serpentine	Tr	Ol	

THIN SECTION DESCRIPTION

115–715A–25R–6 (Piece 1, 37–38 cm)

ROCK NAME: Moderately olivine phyric basalt
WHERE SAMPLED: Interior of Unit 10, 237.87 mbsf
TEXTURE: Subophitic, moderately porphyritic
GRAIN SIZE: Medium, phaneritic
OBSERVER: JDG

PRIMARY MINERALOGY	PERCENT PRESENT	PERCENT ORIGINAL	SIZE RANGE (mm)	APPROX. COMPO-SITION	MORPHOLOGY	COMMENTS
PHENOCRYSTS						
Olivine	—	5	<2.5		Euhedral	Completely altered to chlorite.
GROUNDMASS						
Plagioclase	44	45	<0.8	An 70	Subhedral–euhedral	Looks very fresh.
Clinopyroxene	46	50	<0.8	Augite	Anhedral	Some grains altered to chlorite(?).
Oxides	1	1	0.1	Fe-Ti	Euhedral	

SECONDARY MINERALOGY	PERCENT	REPLACING/ FILLING	COMMENTS
Chlorite	10	Ol, cpx, plag	Irregular masses in matrix.

VESICLES/ CAVITIES	PERCENT	LOCATION	SIZE RANGE (mm)	FILLING	SHAPE	COMMENTS
Vesicles	1		5	Carbonate	Round	One large vesicle.

THIN SECTION DESCRIPTION

115–715A–26R–2 (Piece 3D, 139–140 cm)

ROCK NAME: Sparsely olivine phyric basalt
WHERE SAMPLED: Vesicular bottom of Unit 10, 242.39 mbsf
TEXTURE: Sparsely porphyritic, intersertal
GRAIN SIZE: Fine, phaneritic
OBSERVER: ANB

PRIMARY MINERALOGY	PERCENT PRESENT	PERCENT ORIGINAL	SIZE RANGE (mm)	APPROX. COMPO-SITION	MORPHOLOGY	COMMENTS
PHENOCRYSTS						
Olivine	—	2	<1		Anhedral	Completely altered to red iddingsite.
GROUNDMASS						
Olivine	—	20	<0.2		Anhedral	Completely altered to red iddingsite.
Clinopyroxene	10	10	<0.2	Augite	Anhedral	Colorless.
Plagioclase	67	67	<0.9		Subhedral	Slightly sericitized.
Spinel	1	1	<0.2	Titano-magnetite	Anhedral	

SECONDARY MINERALOGY	PERCENT	REPLACING/ FILLING	COMMENTS
Iddingsite	22	Ol	Red.

VESICLES/ CAVITIES	PERCENT	LOCATION	SIZE RANGE (mm)	FILLING	SHAPE	COMMENTS
Vesicles	25	Even	<1.5	Calcite	Irregular	Calcite infills vesicles. Interstices are empty.

COMMENTS: Slightly oxidized, weathered basalt. Rock is vesicular (25%) with irregular, calcite-filled cavities and abundant angular, inter-crystalline cavities in matrix (25%).
N.B. Ol phenocrysts were heavily plucked out in manufacture of slide.

THIN SECTION DESCRIPTION

115-715A-27R-1 (Piece 1, 1-2 cm)

ROCK NAME: Highly olivine phyric basalt
WHERE SAMPLED: Bottom of Unit 11, 248.91 mbsf
TEXTURE: Ophitic, highly porphyritic
GRAIN SIZE: Fine, phaneritic
OBSERVER: JDG

PRIMARY MINERALOGY	PERCENT PRESENT	PERCENT ORIGINAL	SIZE RANGE (mm)	APPROX. COMPO-SITION	MORPHOLOGY	COMMENTS
PHENOCRYSTS						
Olivine	—	15	3		Euhedral	Completely altered to chlorite + hematite.
GROUNDMASS						
Plagioclase	42	42	<0.6		Subhedral	
Clinopyroxene	42	42	<1.2	Augite	Anhedral	
Opaques	1	1	<0.15	Fe-Ti	Anhedral	

SECONDARY MINERALOGY	PERCENT	REPLACING/ FILLING	COMMENTS
Clays	15	Ol	Chlorite + hematite. Possible minor replacement of augite.

VESICLES/ CAVITIES	PERCENT	LOCATION	SIZE RANGE (mm)	FILLING	SHAPE
Vesicles	<1		53	Clays	Round

COMMENTS: Beautiful ophitic texture.
Hematite may be a weathering product.

THIN SECTION DESCRIPTION

115-715A-29R-1 (Piece 1, 1-2 cm)

ROCK NAME: Highly clinopyroxene olivine plagioclase phyric basalt
WHERE SAMPLED: Piece above Unit 12, 267.71 mbsf
TEXTURE: Highly porphyritic oxidized
GRAIN SIZE: Hyaline
OBSERVER: ANB

PRIMARY MINERALOGY	PERCENT PRESENT	PERCENT ORIGINAL	SIZE RANGE (mm)	APPROX. COMPO-SITION	MORPHOLOGY	COMMENTS
PHENOCRYSTS						
Olivine	—	10	<2		Subhedral	Completely altered to red iddingsite.
Plagioclase	20	20	<2	An 66	Euhedral	Complex oscillatory zoning.
Clinopyroxene	<1	<1	<0.2	Augite	Subhedral	Colorless. Microphenocrysts.
GROUNDMASS						
Glass	—	69				Completely altered to yellow-brown smectite.

SECONDARY MINERALOGY	PERCENT	REPLACING/ FILLING	COMMENTS
Clays	69	Glass	Yellow-brown smectite (+ limonite).
Iddingsite	10	Ol	Red.

VESICLES/ CAVITIES	PERCENT	LOCATION	SIZE RANGE (mm)	FILLING	SHAPE	COMMENTS
Vesicles	15	Even	<10	Carbonate, zeolite	Irregular	Filled by carbonate + zeolite.

COMMENTS: Strongly weathered, oxidized basalt. Glass completely altered to smectite.

THIN SECTION DESCRIPTION

115-715A-29R-1 (Piece 2A, 33-35 cm)

ROCK NAME: Aphyric basalt
WHERE SAMPLED: Center of Unit 12, 268.03 mbsf
TEXTURE: Intersertal, subophitic
GRAIN SIZE: Fine
OBSERVER: YT

PRIMARY MINERALOGY	PERCENT PRESENT	PERCENT ORIGINAL	SIZE RANGE (mm)	APPROX. COMPO-SITION	MORPHOLOGY	COMMENTS
GROUNDMASS						
Plagioclase	42	42	<0.5	An 50-60	Subhedral	Clear. Unzoned.
Clinopyroxene	20	20	<0.2	Augite	Subhedral	Colorless to slightly brownish.
Opaque	3	3	<0.1	Magnetite(?), ilmenite(?)	Euhedral-subhedral	Completely altered.
Olivine	—	<1	<0.1			Completely altered to clay.
Glass	—	30				

SECONDARY MINERALOGY	PERCENT	REPLACING/ FILLING	COMMENTS
Clays	35	Glass, ol, vesicles	Brownish green-gray clays.
Carbonate	<1	Vesicles	

VESICLES/ CAVITIES	PERCENT	LOCATION	SIZE RANGE (mm)	FILLING	SHAPE	COMMENTS
Vesicles	5	Even	<1	Clay	Irregular	Clay ± carbonate fills vesicles.

THIN SECTION DESCRIPTION

115-715A-29R-1 (Piece 4A2, 116-118 cm)

ROCK NAME: Aphyric basalt
WHERE SAMPLED: Top of Unit 13, 268.86 mbsf
TEXTURE: Subophitic, aphyric
GRAIN SIZE: Phaneritic
OBSERVER: JDG

PRIMARY MINERALOGY	PERCENT PRESENT	PERCENT ORIGINAL	SIZE RANGE (mm)	APPROX. COMPO-SITION	MORPHOLOGY	COMMENTS
GROUNDMASS						
Plagioclase	50	50		An 74	Subhedral	Some normal zoning. Fresh.
Clinopyroxene	7	43	<0.4	Augite	Anhedral	Distinctly brown colored.
Opaques	2	2				
Olivine	—	Tr				

SECONDARY MINERALOGY	PERCENT	REPLACING/ FILLING	COMMENTS
Chlorite	1	Cpx(?), ol(?)	May replace cpx and/or ol.
Clay	36	Cpx	

VESICLES/ CAVITIES	PERCENT	LOCATION	SIZE RANGE (mm)	FILLING	SHAPE	COMMENTS
Vesicles	15		<6	Celadonite	Oval, irregular	Vesicles lined with celadonite.

THIN SECTION DESCRIPTION

115-715A-29R-2 (Piece 1C2, 41-42 cm)

ROCK NAME: Highly olivine phyric basalt

WHERE SAMPLED: Interior of Unit 13, 269.62 mbsf

TEXTURE: Subophitic, highly porphyritic

GRAIN SIZE: Fine, phaneritic

OBSERVER: JDG

PRIMARY MINERALOGY	PERCENT PRESENT	PERCENT ORIGINAL	SIZE RANGE (mm)	APPROX. COMPOSITION	MORPHOLOGY	COMMENTS
PHENOCRYSTS						
Olivine	—	10	1.2		Euhedral	Completely altered.
GROUNDMASS						
Plagioclase	45	45	<0.8	An 78	Subhedral	Slightly zoned.
Clinopyroxene	38	43	<0.8	Augite	Anhedral	Brownish color.
Opaques	2	2	<0.2	Fe-Ti	Subhedral	

SECONDARY MINERALOGY	PERCENT	REPLACING/FILLING	COMMENTS
Chlorite	15	Ol, cpx	May be mostly altered ol.

COMMENTS: Rock appears very fresh except for minor ol + cpx alteration.

THIN SECTION DESCRIPTION

115-715A-30R-1 (Piece 2B, 50-53 cm)

ROCK NAME: Aphyric basalt

WHERE SAMPLED: Interior of Unit 15, 271.20 mbsf

TEXTURE: Intersertal, subophitic

GRAIN SIZE: Fine

OBSERVER: YT

PRIMARY MINERALOGY	PERCENT PRESENT	PERCENT ORIGINAL	SIZE RANGE (mm)	APPROX. COMPOSITION	MORPHOLOGY	COMMENTS
GROUNDMASS						
Plagioclase	57	57	<0.6	An 60	Subhedral	Rarely zoned. Clear crystals.
Clinopyroxene	20	20	<0.3	Augite	Subhedral	Colorless to pale brown.
Olivine	—	15	<0.4		Euhedral-subhedral	Completely altered.
Opaque	3	3	<0.2	Magnetite(?)	Euhedral-subhedral	Completely altered.
Glass	—	5				

SECONDARY MINERALOGY	PERCENT	REPLACING/FILLING	COMMENTS
Clays	20	Ol, glass	Green clay + brown clay + reddish brown clay.

THIN SECTION DESCRIPTION

115-715A-30R-3 (Piece 1, 40-41 cm)

ROCK NAME: Aphyric basalt
WHERE SAMPLED: Interior of Unit 16, 274.10 mbsf
TEXTURE: Intersertal, subophitic
GRAIN SIZE: Fine
OBSERVER: YT

PRIMARY MINERALOGY	PERCENT PRESENT	PERCENT ORIGINAL	SIZE RANGE (mm)	APPROX. COMPOSITION	MORPHOLOGY	COMMENTS
GROUNDMASS						
Plagioclase	46	61	<0.5	An 60	Subhedral	Unzoned. Clear. Altered to zeolite(?).
Clinopyroxene	15	15	<0.3	Augite	Subhedral	Colorless to slightly brownish.
Olivine	15	16	<0.5	Fo 80(?)	Euhedral–subhedral	Rim altered to iddingsite. Zoned.
Opaques	3	3	<0.1	Magnetite(?)	Euhedral–subhedral	Completely altered.
Glass	—	5(?)				

SECONDARY MINERALOGY	PERCENT	REPLACING/ FILLING	COMMENTS
Clays	1	Ol	Iddingsite.
Carbonate	5	Plag, glass	
Zeolites	15	Plag(?)	

VESICLES/ CAVITIES	PERCENT	LOCATION	SIZE RANGE (mm)	FILLING	SHAPE
Vesicles	<1	Even	<0.5	Calcite	Irregular

COMMENTS: Lots of fresh ol.

THIN SECTION DESCRIPTION

115-715A-30R-6 (Piece 1A, 4-5 cm)

ROCK NAME: Aphyric basalt
WHERE SAMPLED: Bottom of Unit 20, 278.24 mbsf
TEXTURE: Intersertal, subophitic
GRAIN SIZE: Fine
OBSERVER: YT

PRIMARY MINERALOGY	PERCENT PRESENT	PERCENT ORIGINAL	SIZE RANGE (mm)	APPROX. COMPOSITION	MORPHOLOGY	COMMENTS
GROUNDMASS						
Plagioclase	45	45	<0.5	An 50-60	Subhedral	Clear, unzoned crystals.
Clinopyroxene	20	20	<0.2	Augite	Subhedral	Colorless. Occasionally slightly brownish.
Olivine	—	7	<0.2		Subhedral	Completely altered to clays.
Glass	—	25				Completely altered to clays.
Opaques	3	3	<0.1	Magnetite(?)	Euhedral–subhedral	

SECONDARY MINERALOGY	PERCENT	REPLACING/ FILLING	COMMENTS
Clays	32	Ol, glass	Serpentine(?), chlorite(?).

VESICLES/ CAVITIES	PERCENT	LOCATION	SIZE RANGE (mm)	FILLING	SHAPE
Vesicles	5	Even	<1	Clay	Irregular

THIN SECTION DESCRIPTION

115-715A-31R-2 (Piece 6A, 94-95 cm)

ROCK NAME: Aphyric basalt

WHERE SAMPLED: Interior of Unit 21, 280.64 mbsf

TEXTURE: Intersertal, subophitic

GRAIN SIZE: Fine

OBSERVER: YT

PRIMARY MINERALOGY	PERCENT PRESENT	PERCENT ORIGINAL	SIZE RANGE (mm)	APPROX. COMPO-SITION	MORPHOLOGY	COMMENTS
GROUNDMASS						
Plagioclase	35	47	<0.5	An 50-60	Subhedral	Unzoned, clear crystals.
Clinopyroxene	20	20	<0.3	Augite	Subhedral	Slightly brownish.
Opaque	3	3	<0.1	Magnetite (?)	Euhedral-subhedral	
Glass	—	20				Completely altered to clays.
Olivine	—	10	<0.3		Subhedral	Completely altered.

SECONDARY MINERALOGY	PERCENT	REPLACING/ FILLING	COMMENTS
Clays	42	Glass, ol, plag, vesicles	Brownish to reddish clay.

VESICLES/ CAVITIES	PERCENT	LOCATION	SIZE RANGE (mm)	FILLING	SHAPE
Vesicles	1	Even	<1	Clay	Round

COMMENTS: Calcite vein.